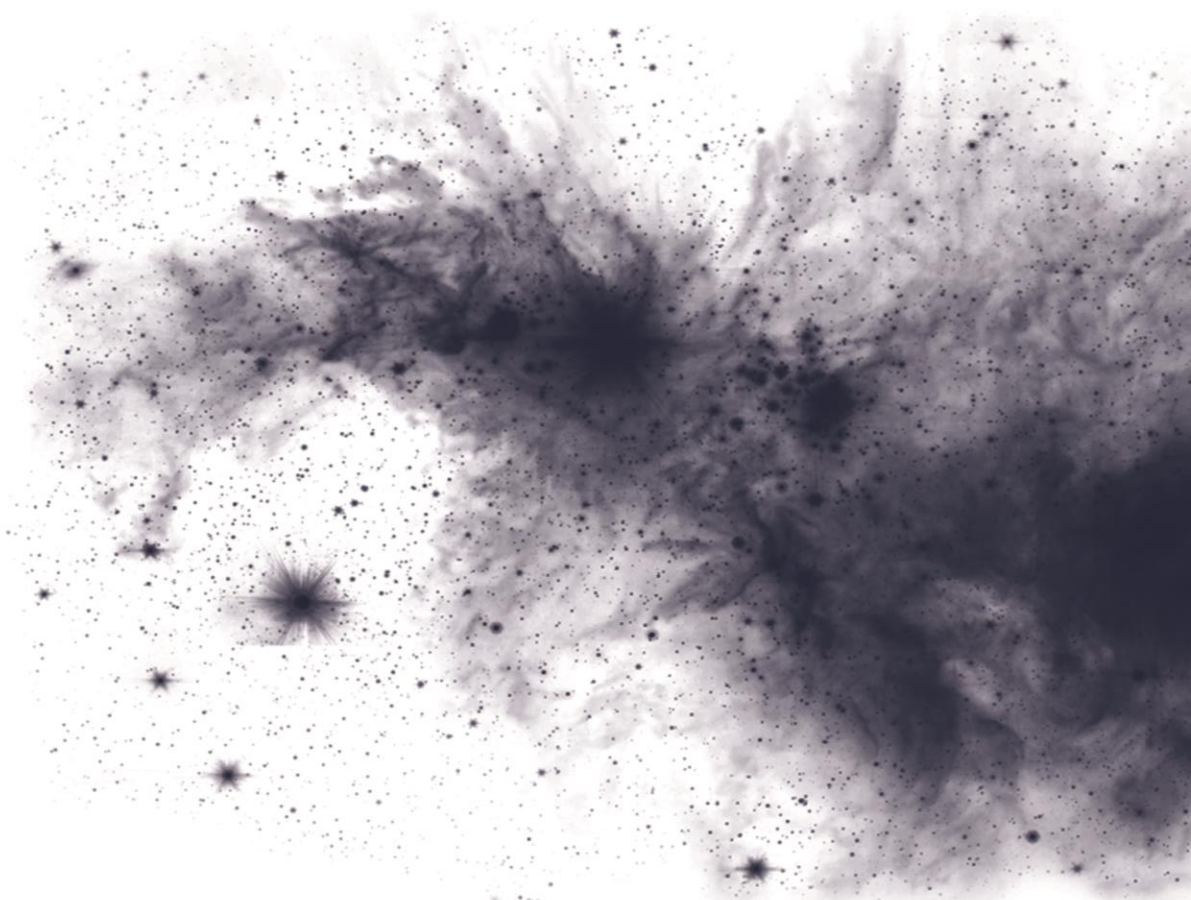
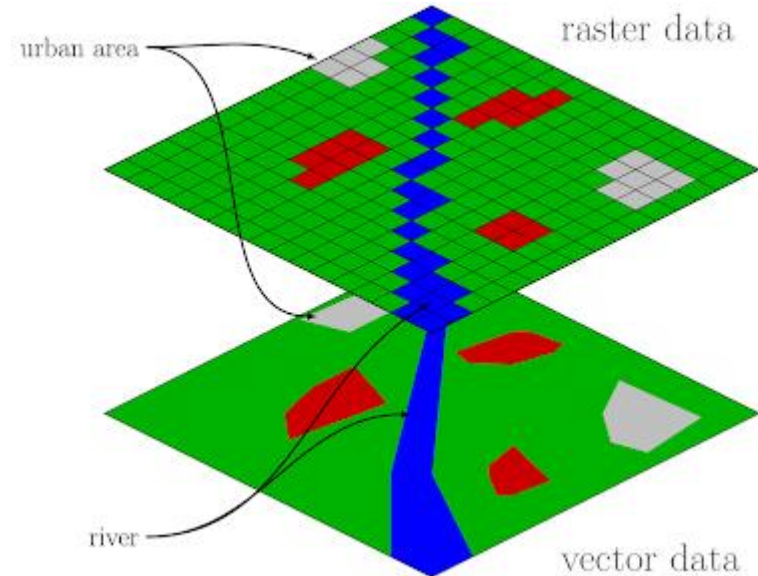
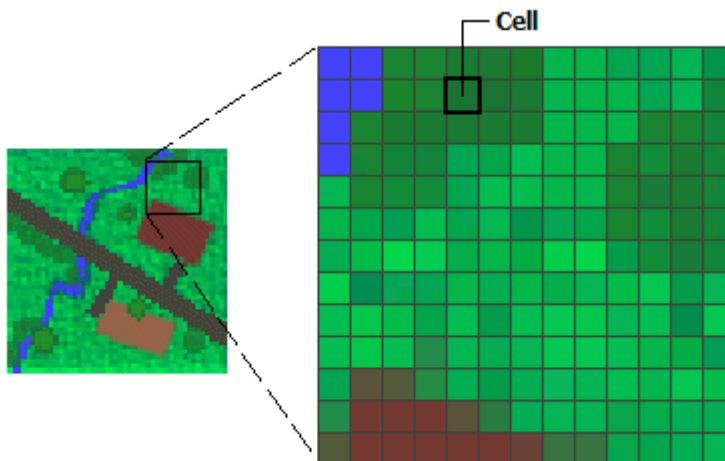


# Raster measurement systems

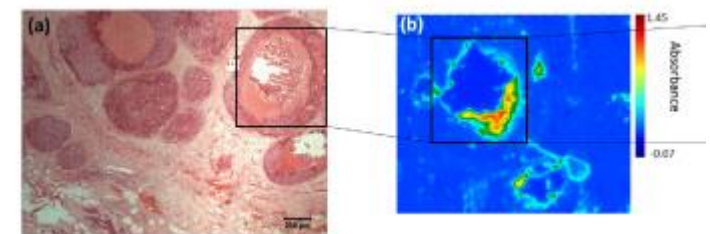
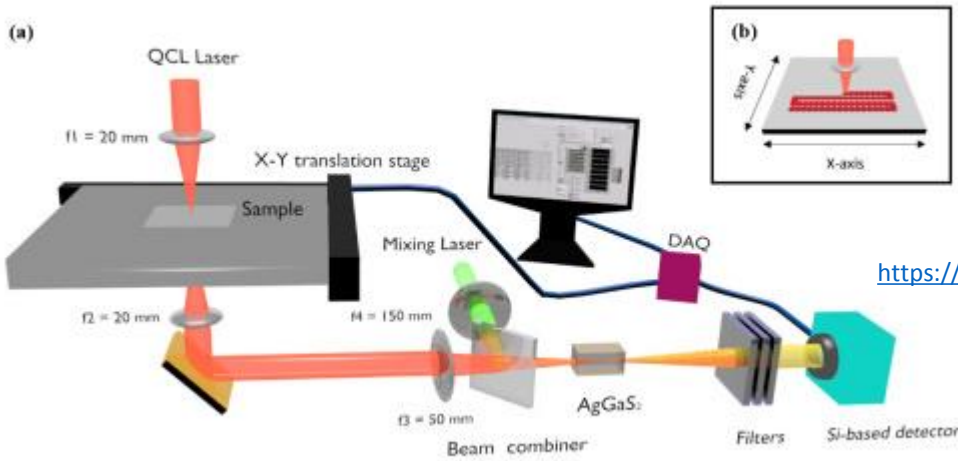
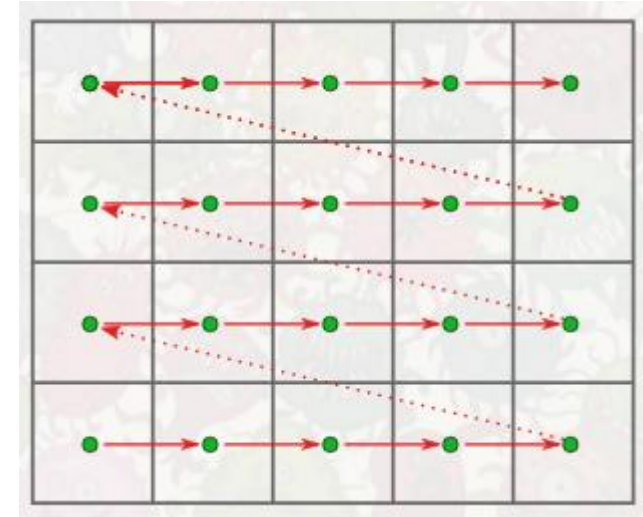
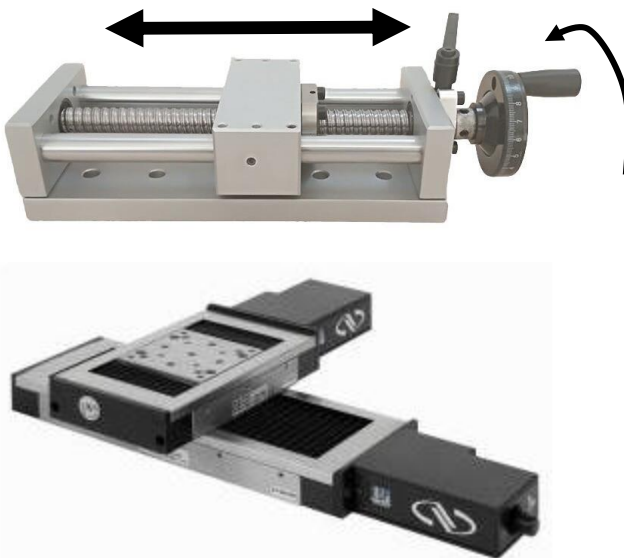


**Prof. L. Svilainis**

# Raster measurement / scanning systems

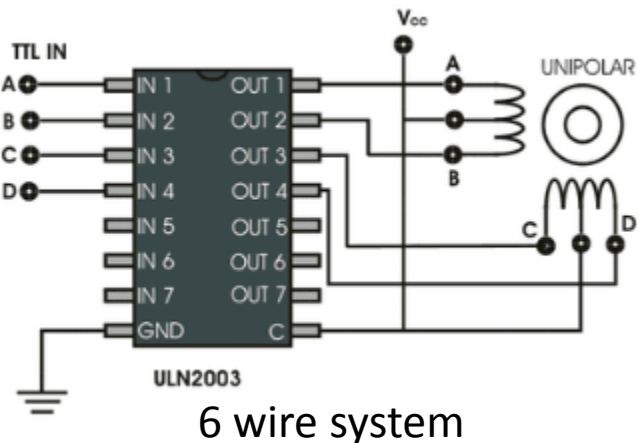
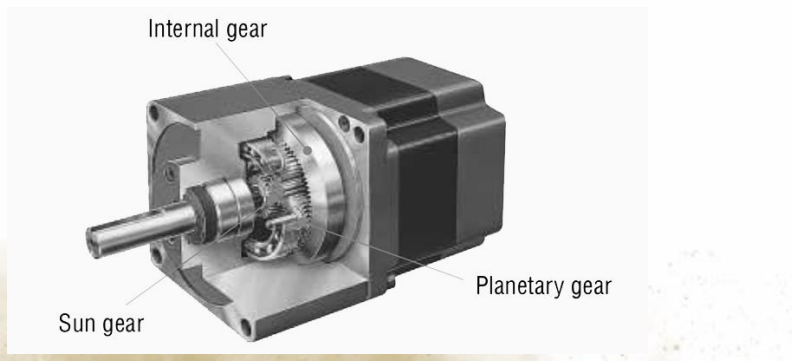
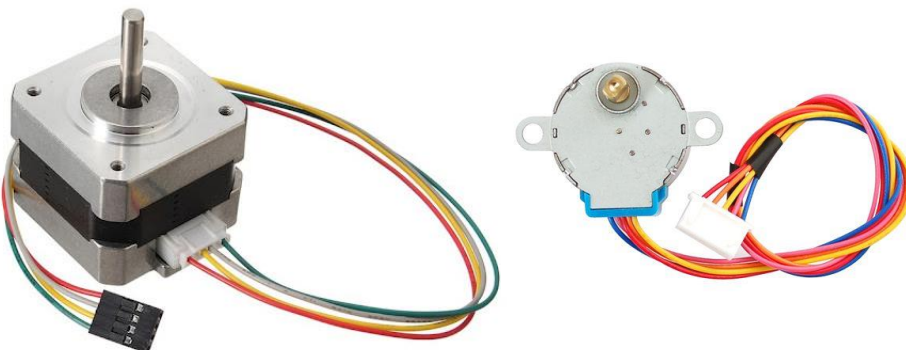
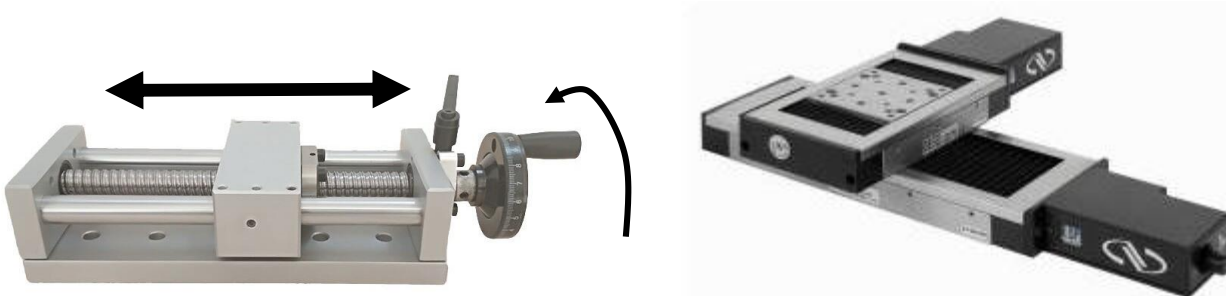


# Raster measurement / scanning systems



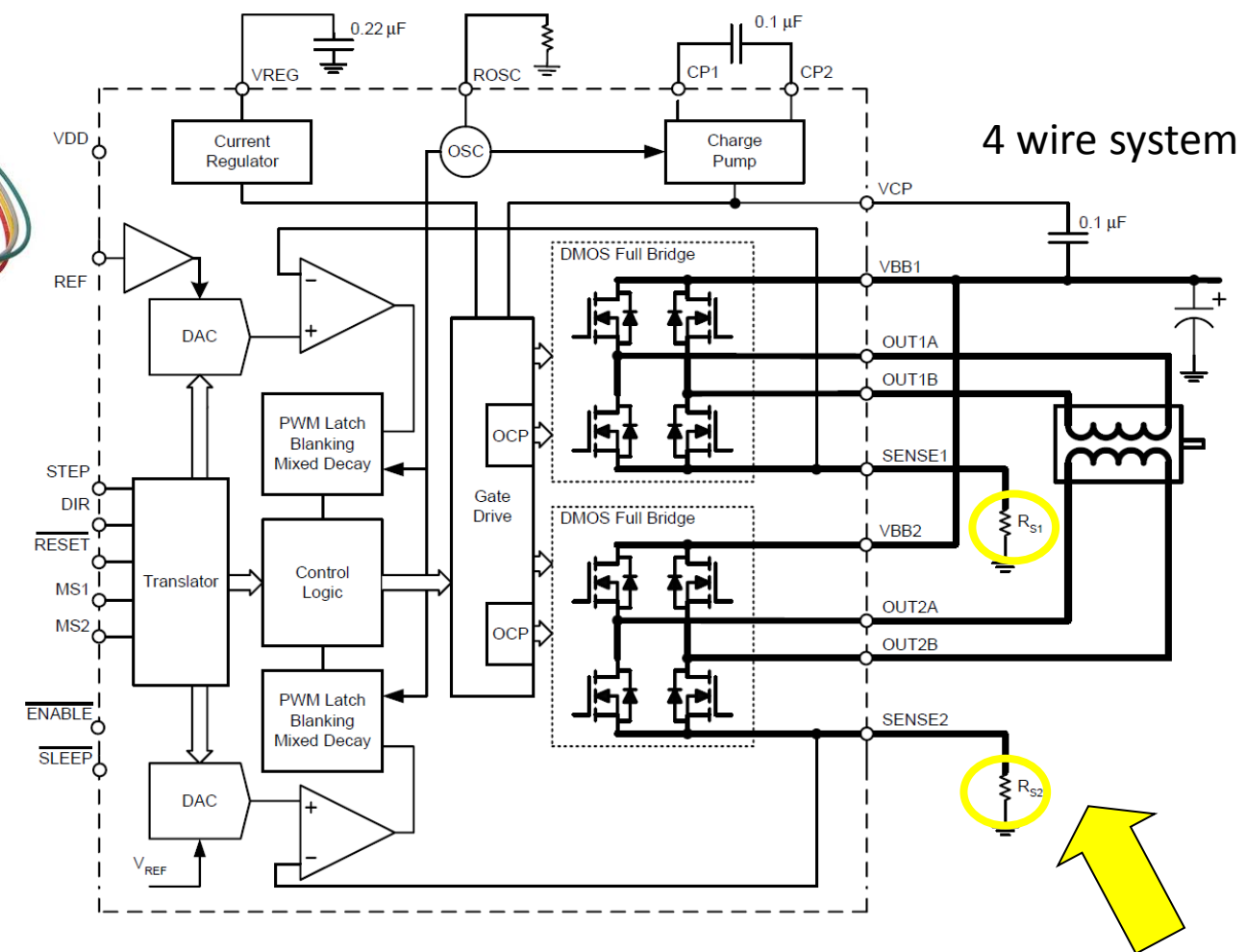
<https://www.osapublishing.org/boe/fulltext.cfm?uri=boe-9-10-4979&id=398562>

# Scanning: step motor



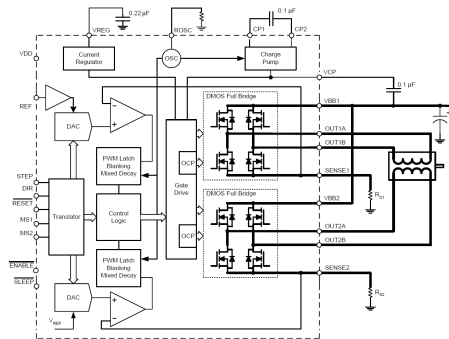
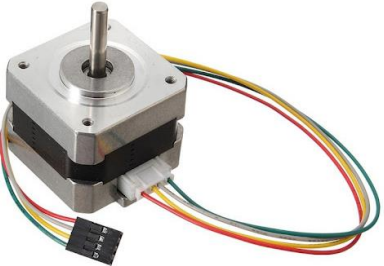
<https://youtu.be/eyqwLiowZiU>  
<https://youtu.be/Ew6eVGnj7r0>

# Scanning : step motor

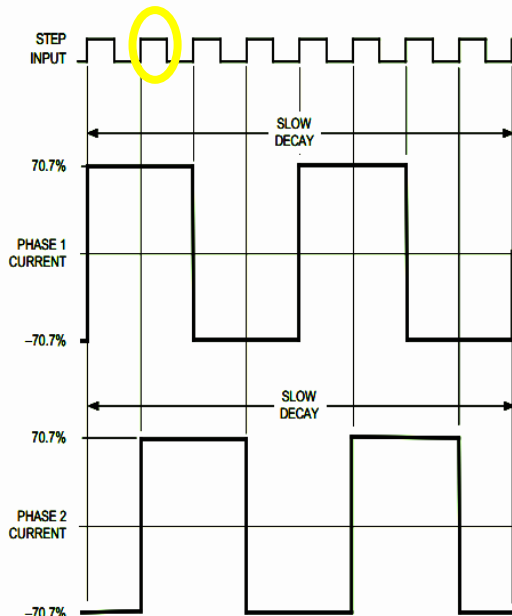


# Scanning : step motor microstepping

1922

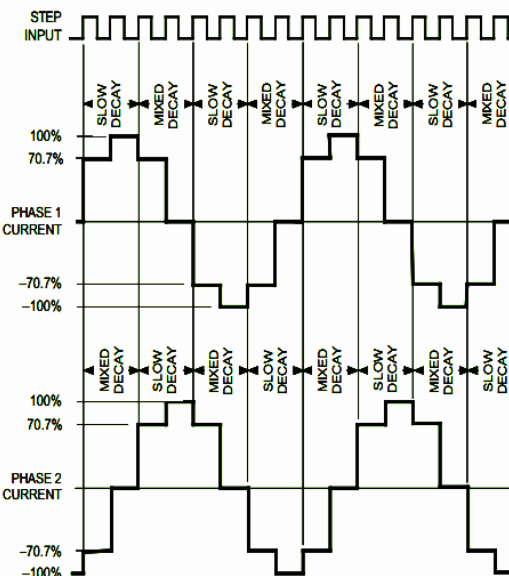


Full Step Operation

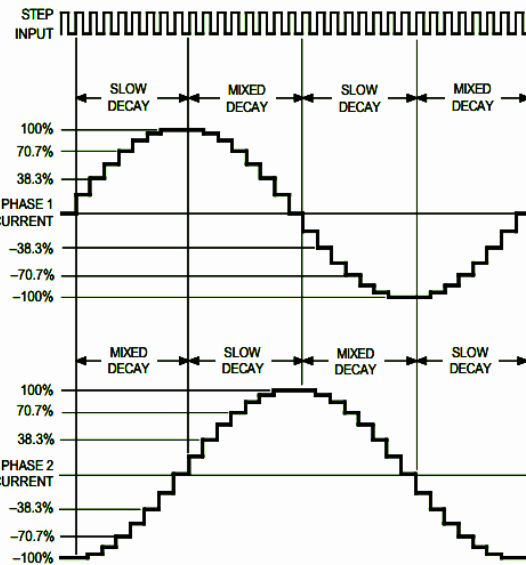


Full step = 1.8deg

Half Step Operation



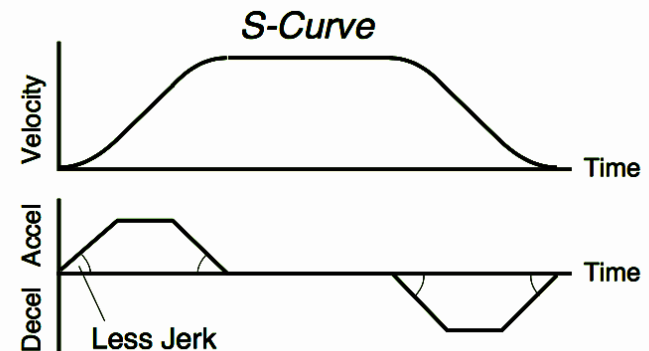
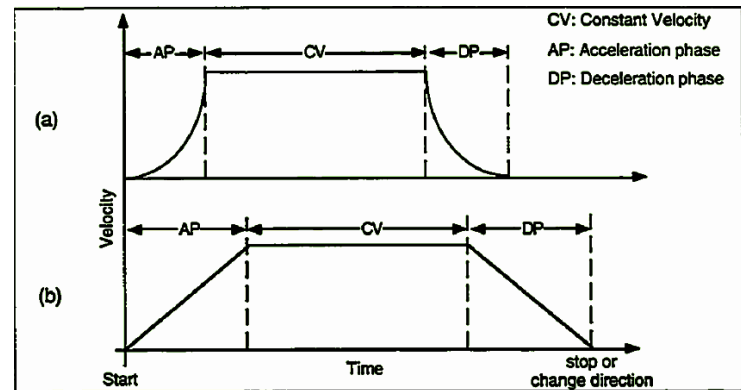
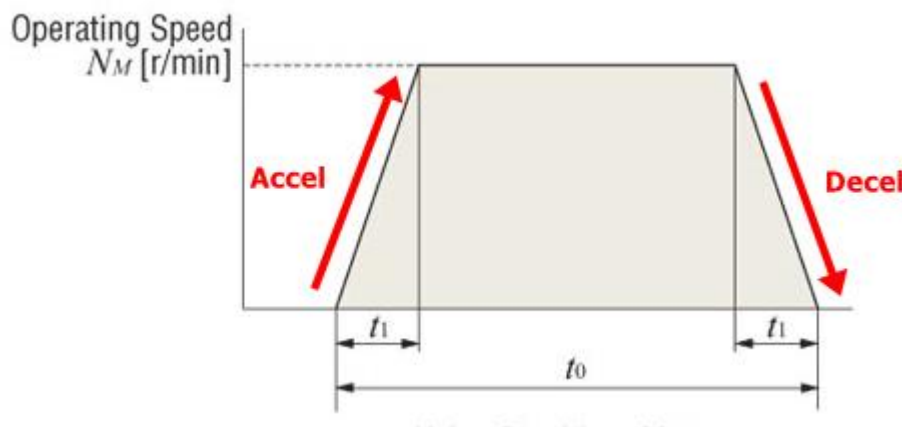
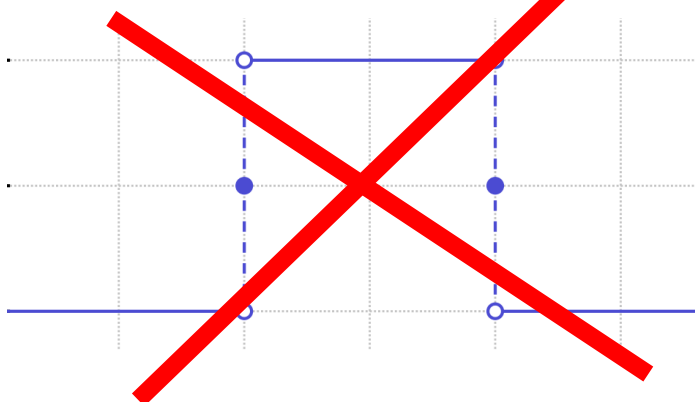
8 Microstep/Step Operation



Microstepping advantage: not only increased resolution, but increased stability (dead speed), less noise

# Scanning : speed profile

Rectangular speed profile=stall



# Scanning : DC motor



## DC motor:

- +Much faster response time
  - +much wider range of speed
  - +less torque dependency on speed
  - +can run continuously
  - +efficiency ~85%
  - +just 2 wires
  - +brushless versions exist

## Step motor:

- +can operate in open loop

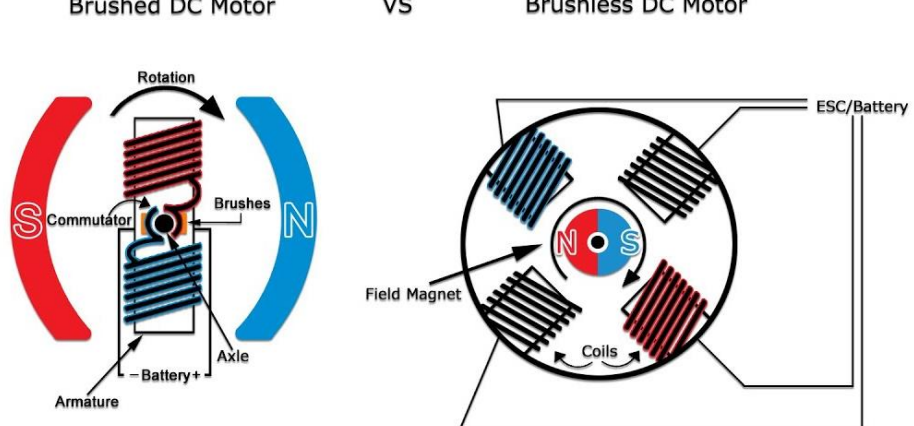
+no need for encoder

+brushless

-can slip

- speed range of stepper motors is <2000 RPM,
- max torque at low speed, decreases as speed increases.

-not intended for continuous operation  
(efficiency=heat)

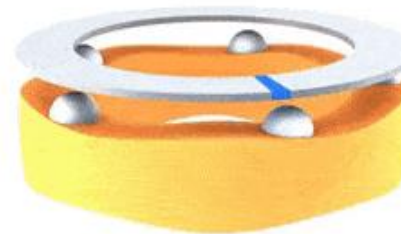


# Scanning : piezo motor

PI Piezo Motor Precision Positioning Solutions



- up to 1000 N
- sub-nm Resolution
- Self-Locking



Inertia Motors

PiezoWalk®

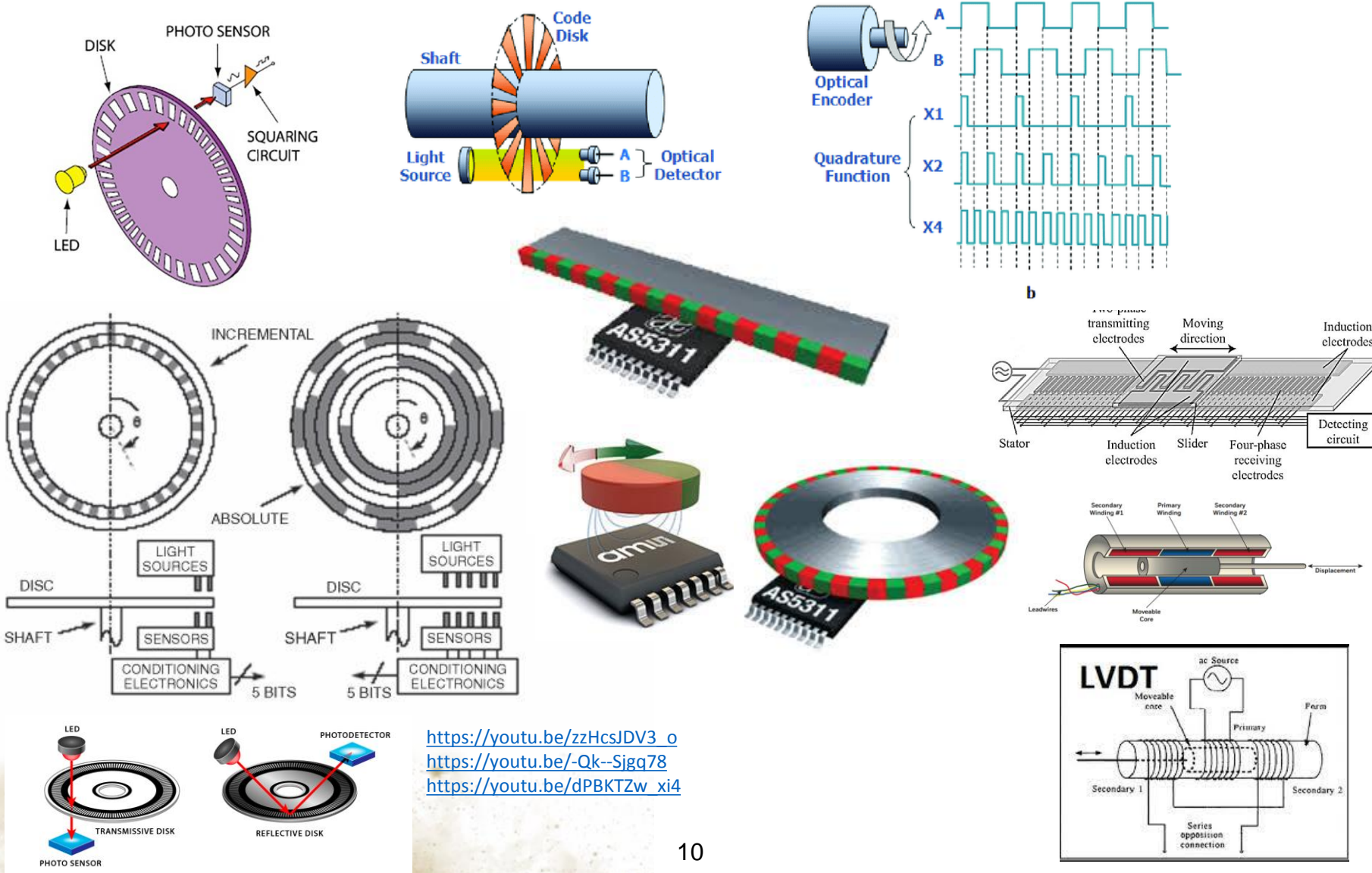
Ultrasonic

Piezomike

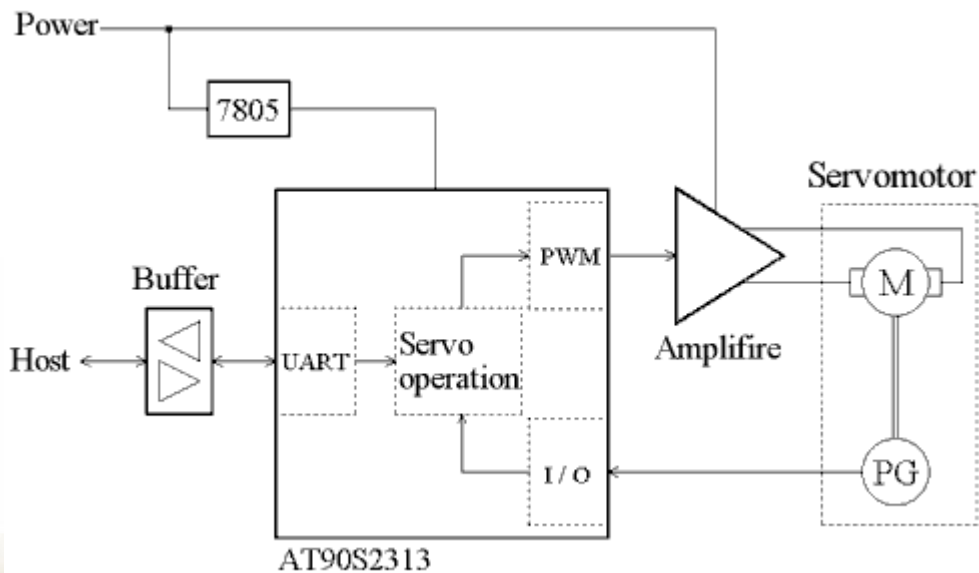
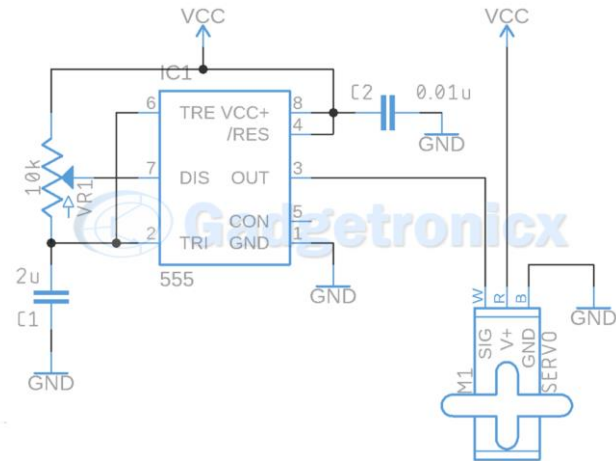
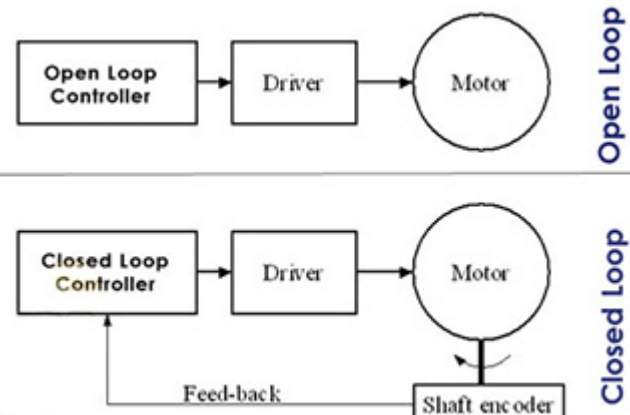
Mini-Rod

- +very small step
- +no power consumption in static position
- +can be micron size
- complex control electronics
- short life
- can slip

# Scanning : position encoding

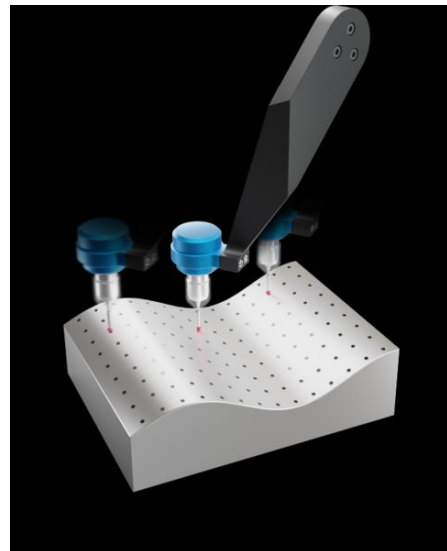


# Scanning : servo motor/closed loop

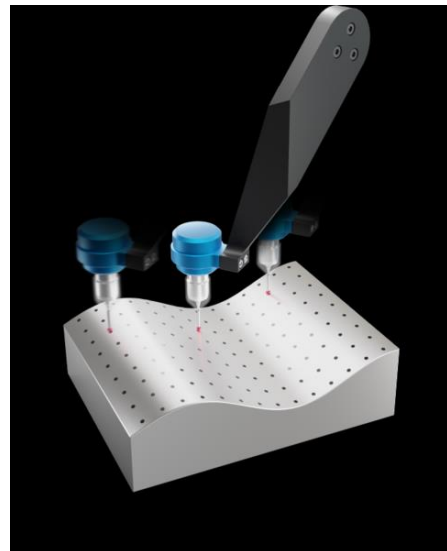


<https://youtu.be/zFe2JwP2NLw>  
<https://youtu.be/Gzo9m0tMD0A>  
<https://youtu.be/hg3TIFlxWCo>

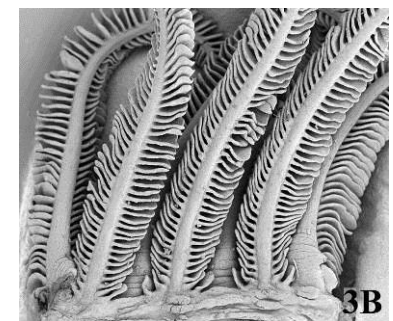
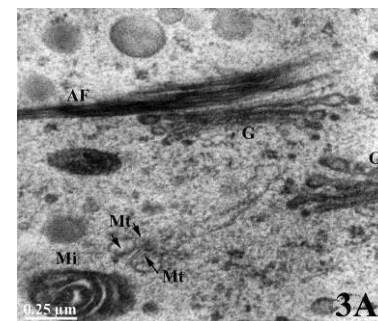
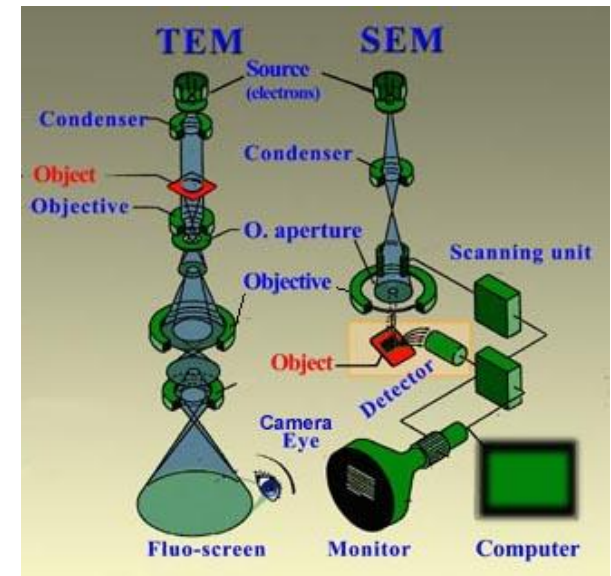
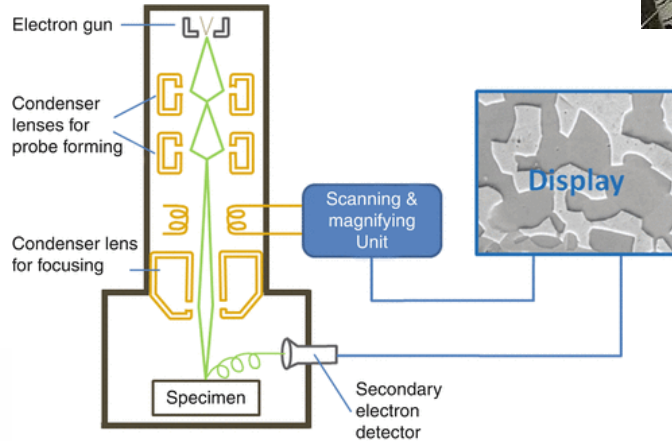
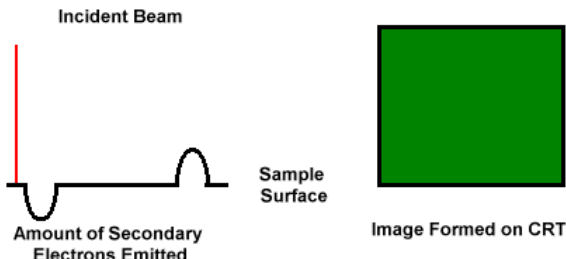
# Raster measurement: coordinate machine



# Raster measurement: coordinate machine

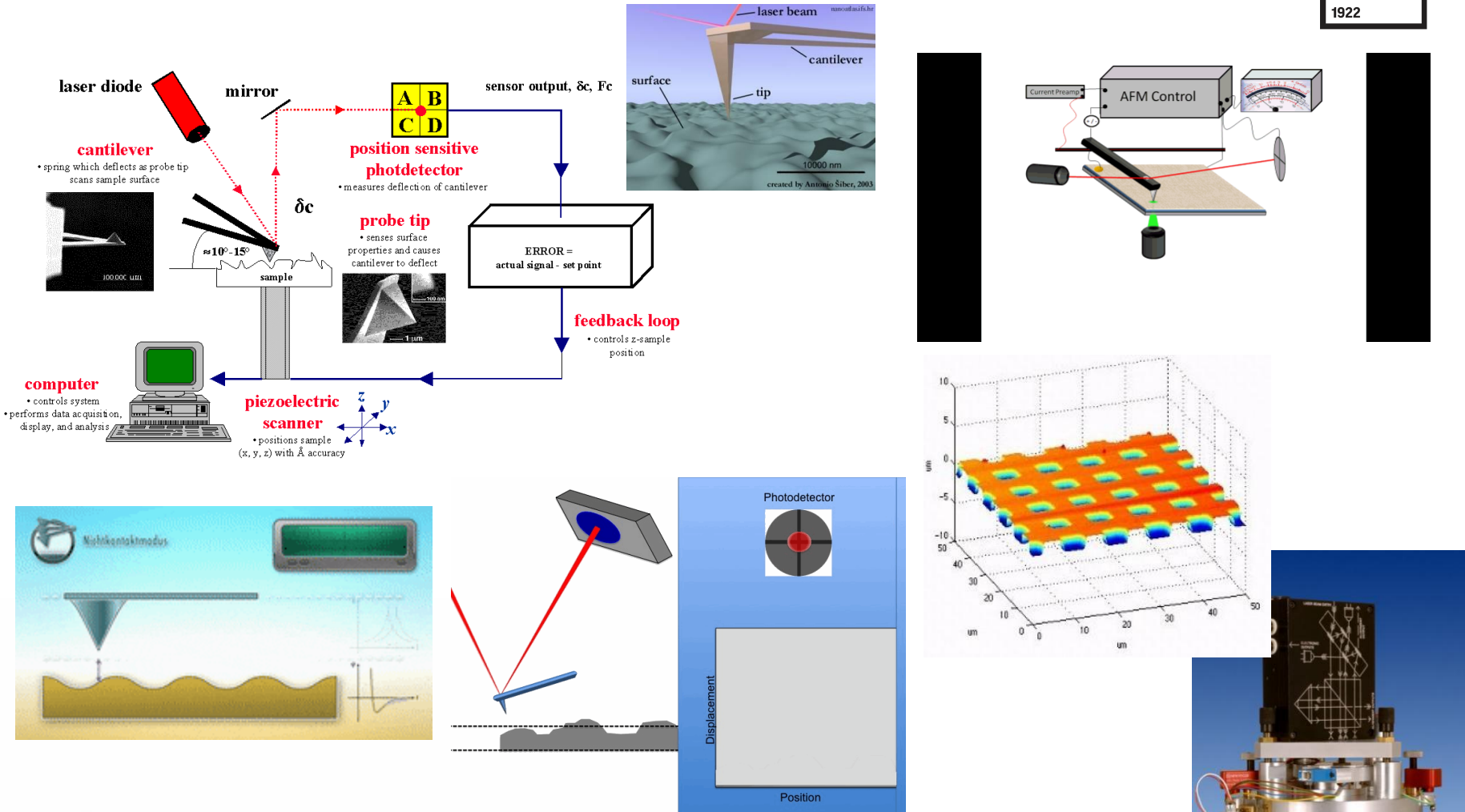


# SEM : scanning electron microscopy



<https://youtu.be/uQ1gClkBbIQ>  
<https://youtu.be/QJYuTpK8Fs>  
[https://youtu.be/385n7o\\_dats](https://youtu.be/385n7o_dats)  
<https://gfycat.com/gifs/search/scanning+electron+microscope>  
<http://www.seallabs.com/hiw4.htm>  
<http://www.vcbio.science.ru.nl/en/image-gallery/electron/>  
<http://www.lms.caltech.edu/research/uem.html>  
<http://www.biologie.uni-hamburg.de/b-online/e03/03e.htm>  
<http://www.uiowa.edu/~cemrf/methodology/tem/index.htm>

# AFM : atomic force microscopy

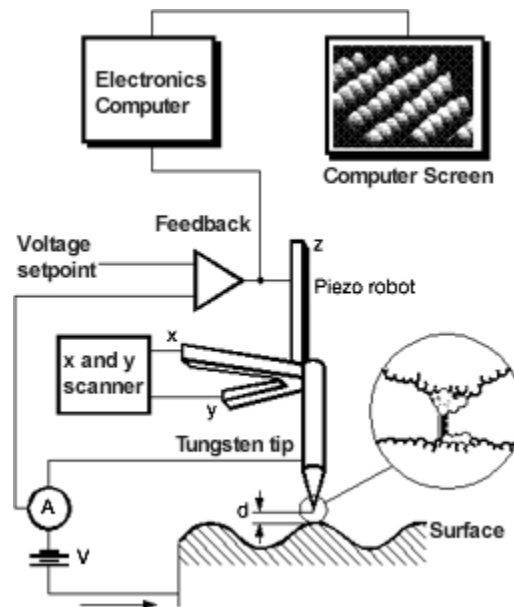
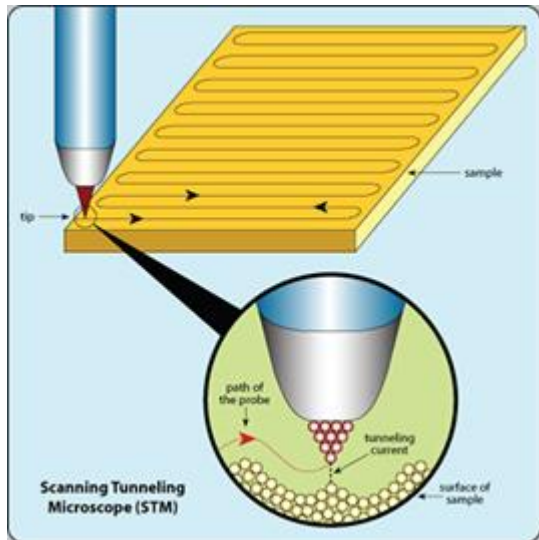


[http://www.nanotech-now.com/Art\\_Gallery/antonio-siber.htm](http://www.nanotech-now.com/Art_Gallery/antonio-siber.htm)

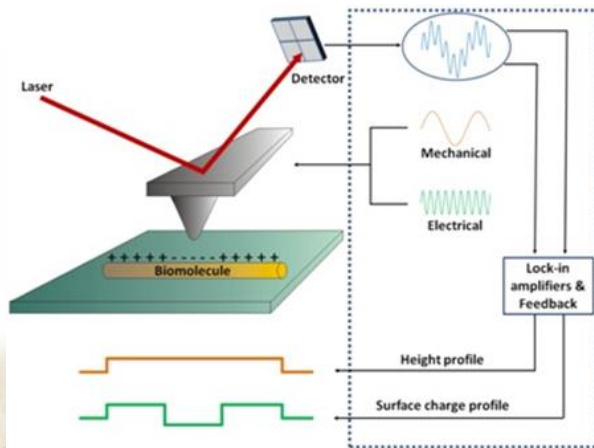
<http://web.mit.edu/cortiz/www/nanomechanics.html>

<http://www.npl.co.uk/engineering-measurements/dimensional/nano-dimensional/products-and-services/metrological-atomic-force-microscope>

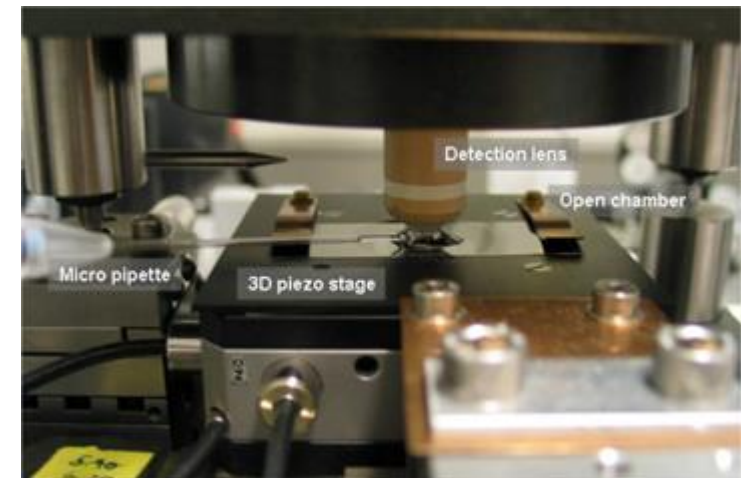
# Other raster measurement systems



STM : scanning tunnel microscope



MFM: molecular force microscope

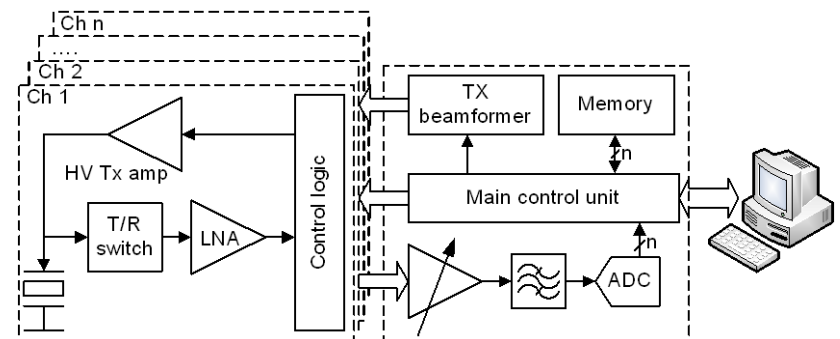
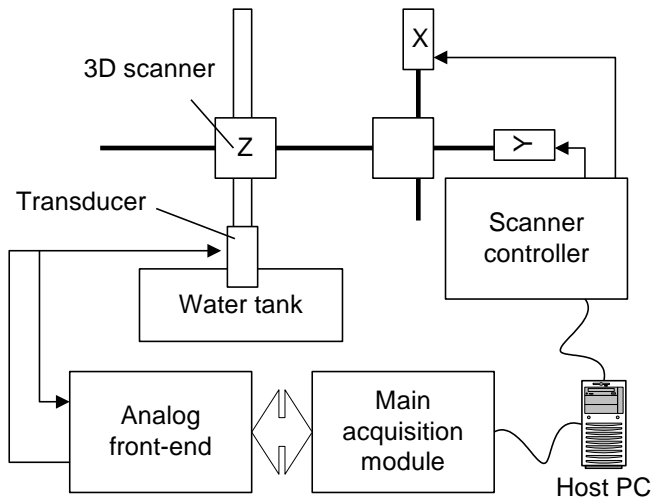


Piezoelectric Force Microscopy (PFM)

# Image measurement machine



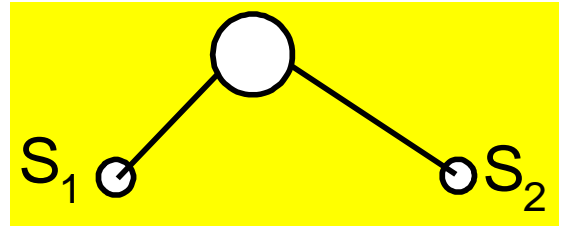
# Ultrasonic system



# Coordinates estimation

Two distinct techniques:

- Using reference points;
- Using trajectory (dead reckoning);



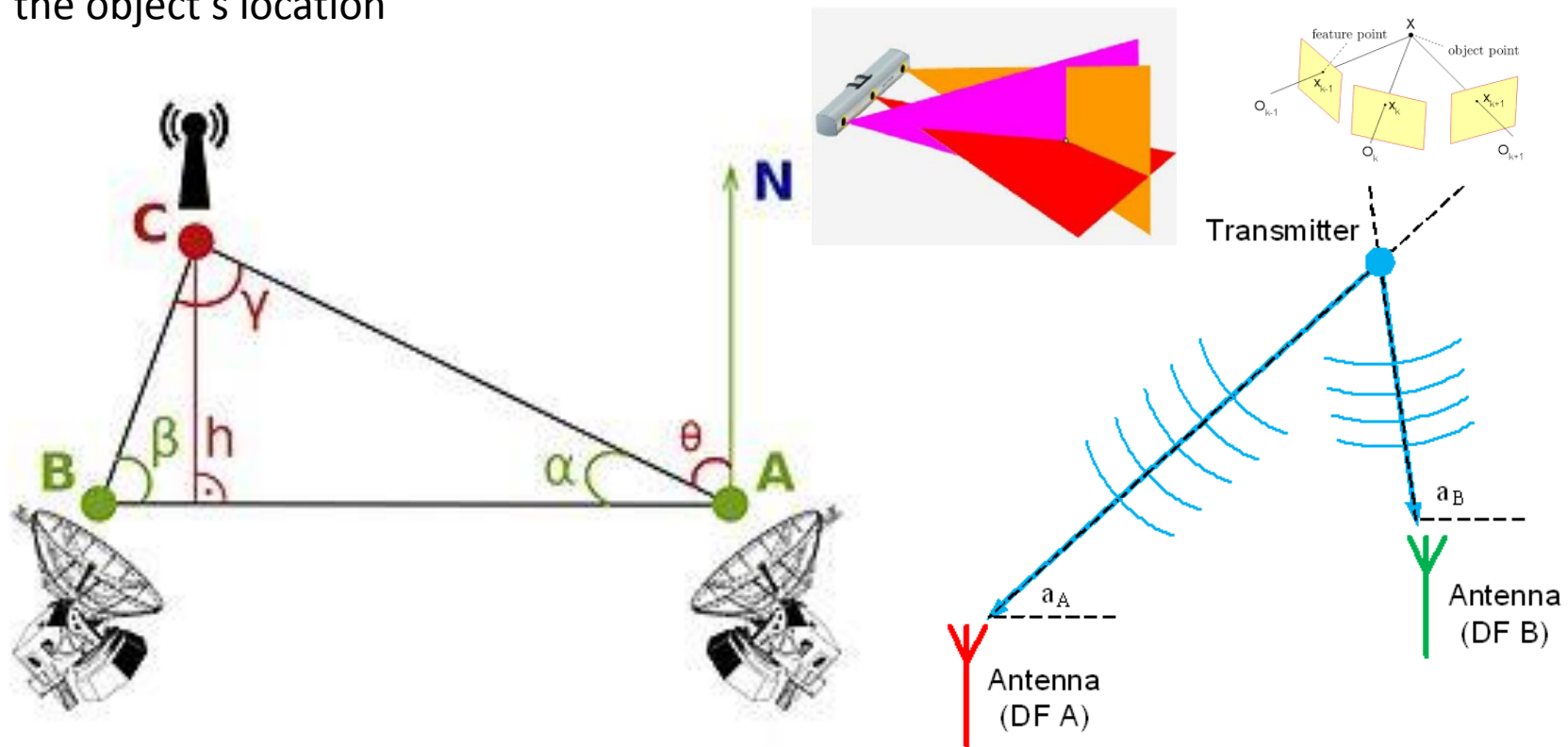
Using reference points :

- Angle of arrival (AOA), rather angles to target, *triangulation*;
- Time of arrival (TOA), rather distances to target, *trilateration*;
- Time difference of arrival (TDOA), rather difference of distances to target, *hyperbolic/multilateration*;
- Time sum of arrival (TSOA), rather sum of distances from reference point to target and to another point, *elliptic*;
- Combined / hybrids: e.g. distance and direction;

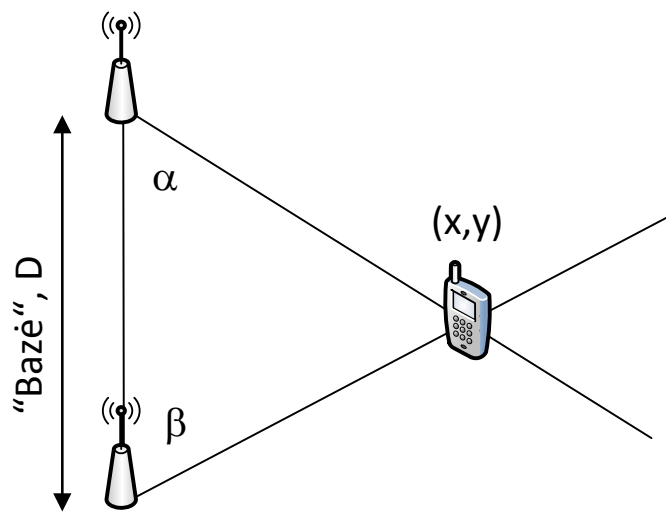
# Triangulation

Triangulation principle is using angle of arrival (AOA) or direction of arrival (DOA) in estimation:

intersection of the lines angles towards the object from reference points reveal the object's location

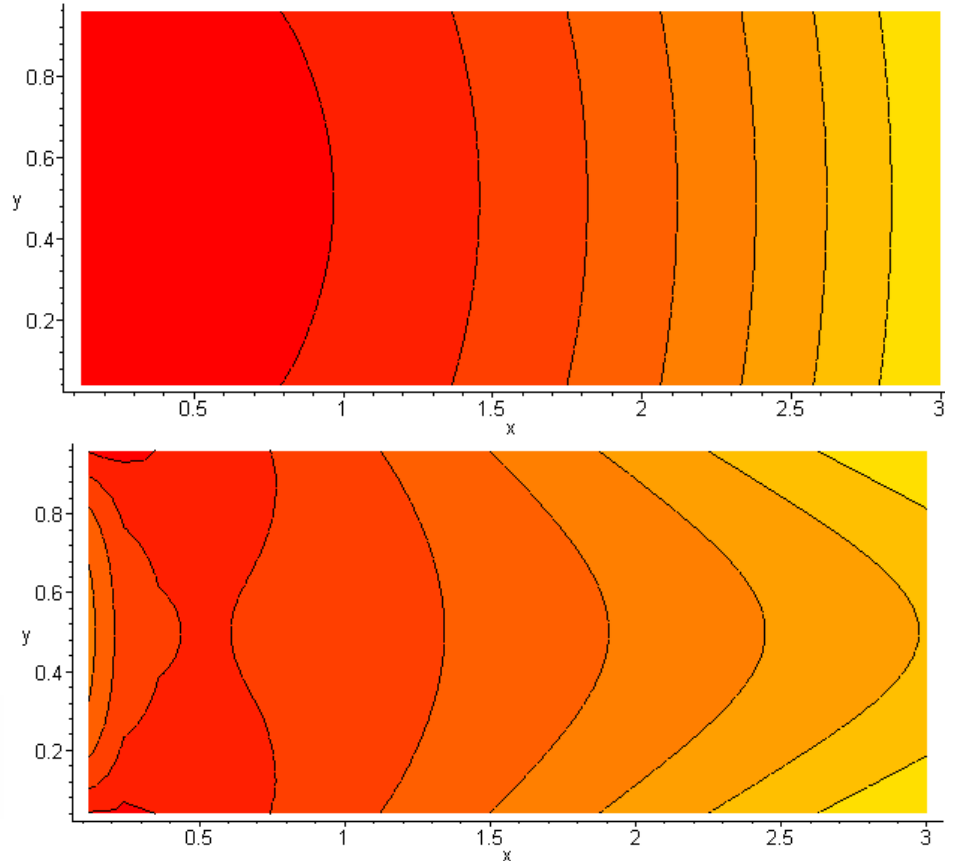


# Triangulation



$$x := \frac{D}{\frac{1}{\tan(\alpha)} + \frac{1}{\tan(\beta)}}$$

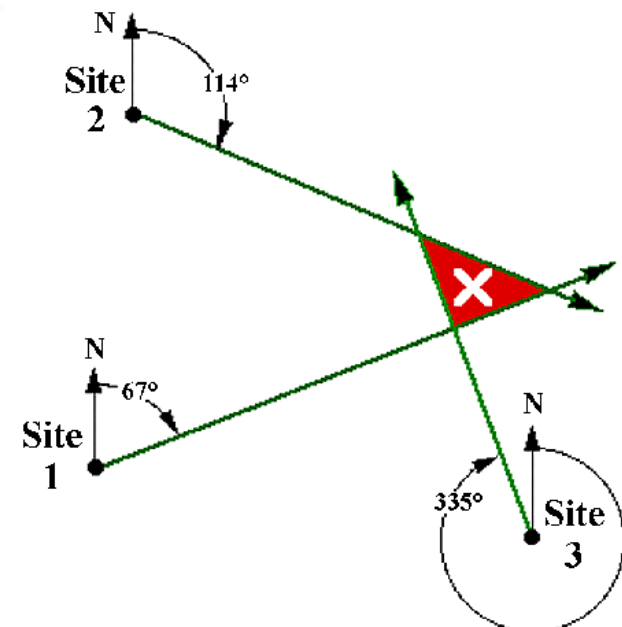
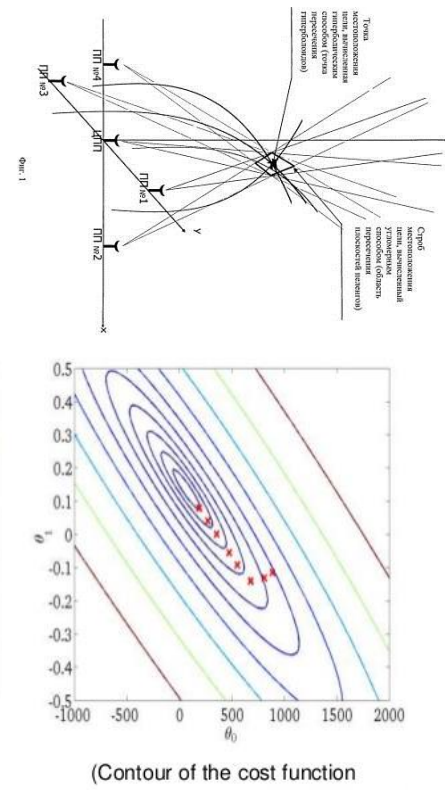
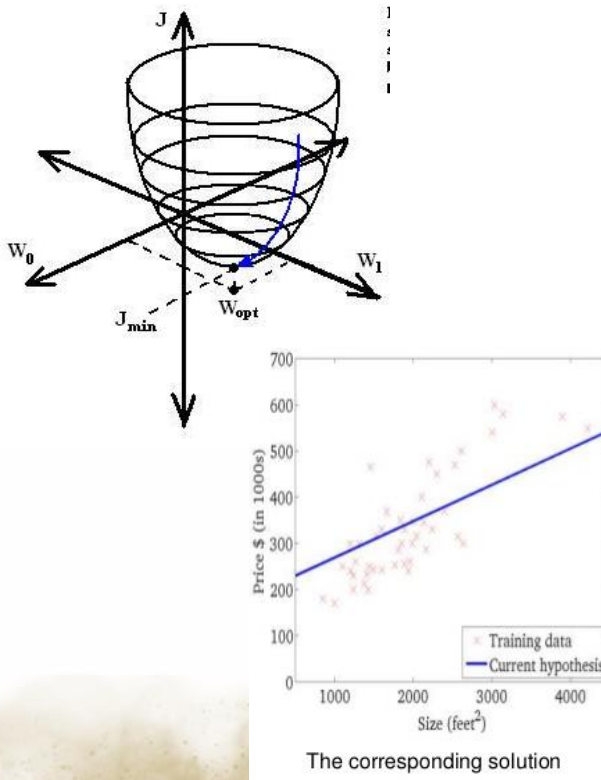
$$y := \frac{D}{\left( \frac{1}{\tan(\alpha)} + \frac{1}{\tan(\beta)} \right) \tan(\beta)}$$



# Triangulation

1922

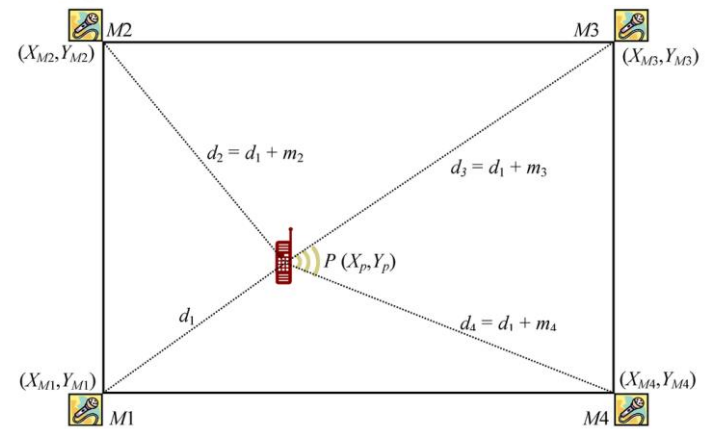
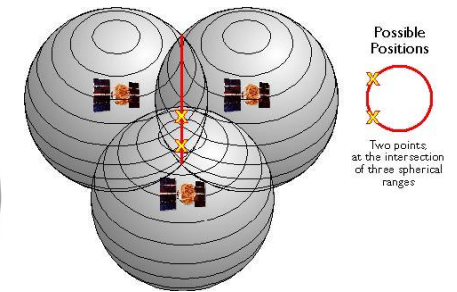
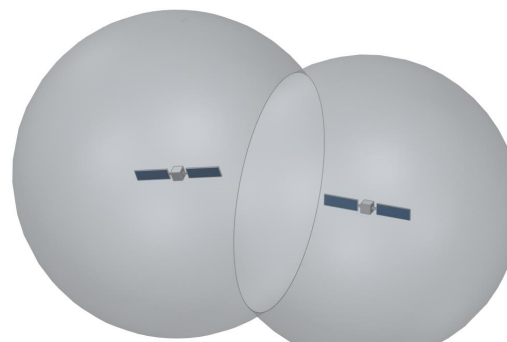
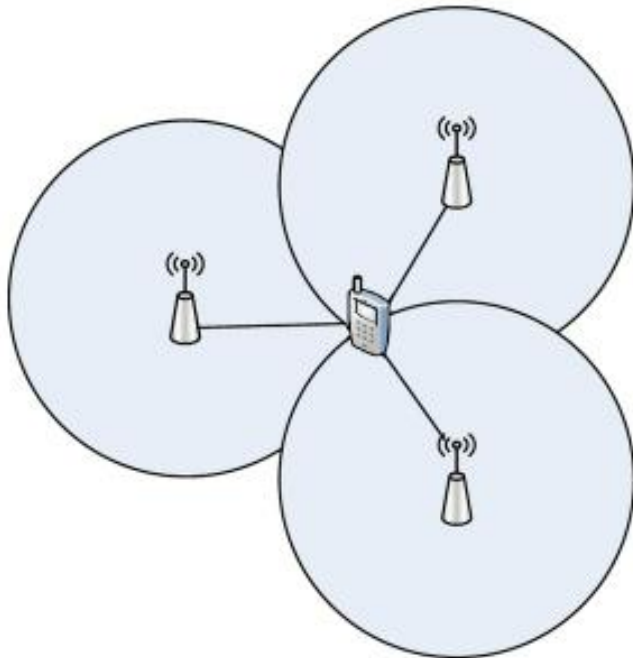
Exact (analytical) solution cannot be used under real circumstances: random noise degrades the of angle estimation accuracy;  
No single intersection point.  
Approximate (e.g. least mean squares) solution is usually used.



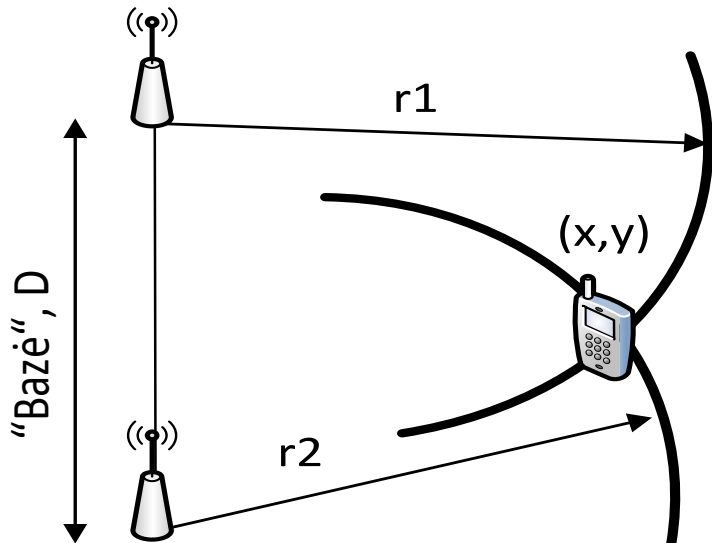
# Trilateration

Trilateration is using time of arrival (TOA) or Time of Flight (TOF) to calculate the actual distances from the reference points (using EM wave speed).

Intersection of circles (2D space) or spheres (3D space) with their centers located at the reference points reveal the coordinates of the object

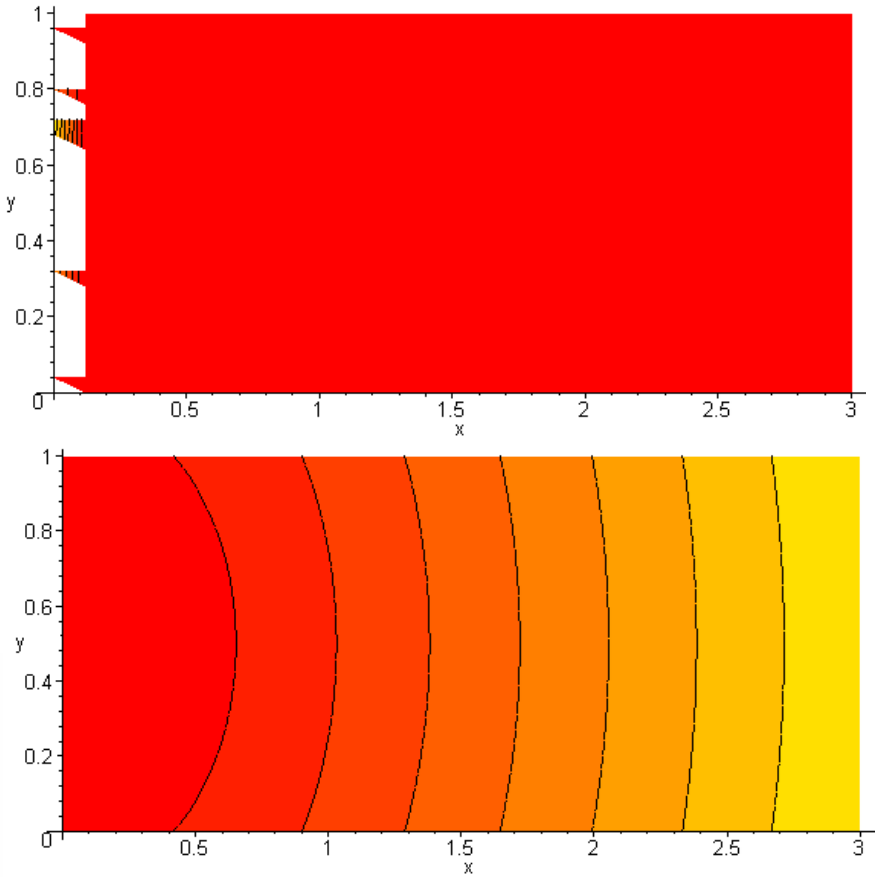


# Trilateration



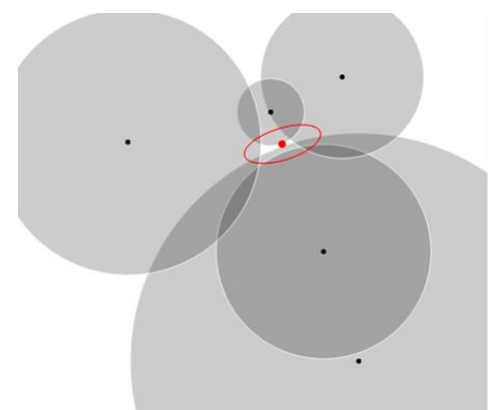
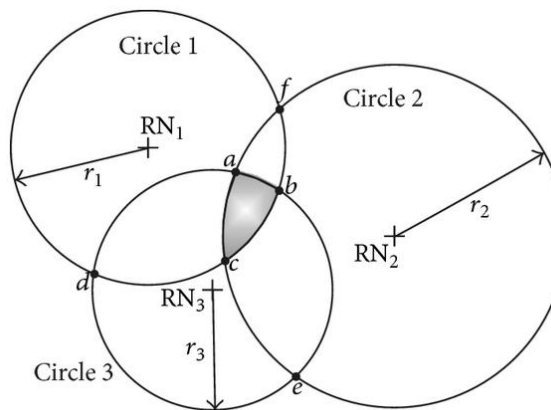
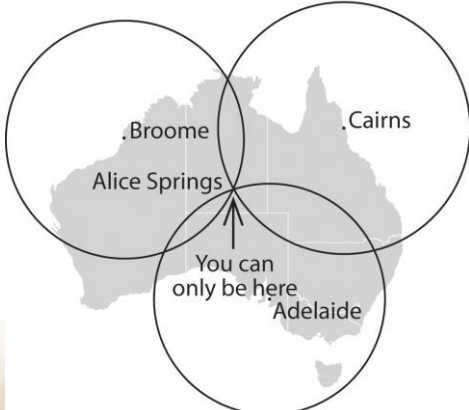
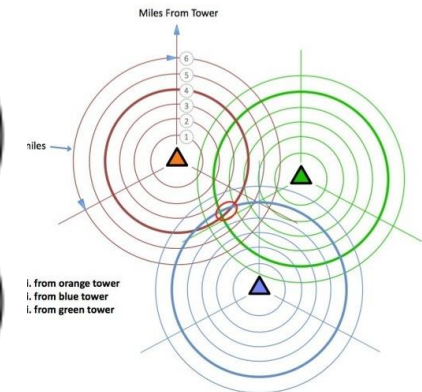
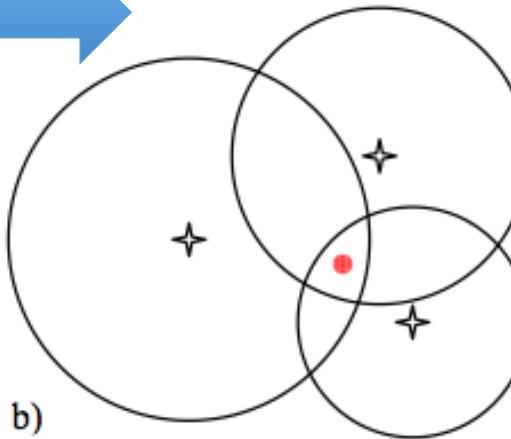
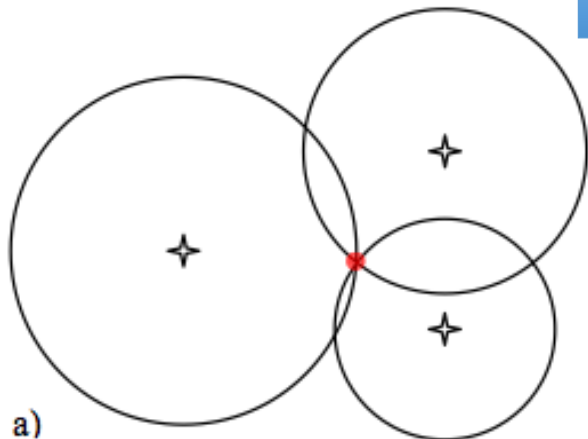
$$x := \frac{1}{2} r_1 \sqrt{4 - \frac{(-D^2 - r_1^2 + r_2^2)^2}{r_1^2 D^2}}$$

$$y := \frac{1}{2} \frac{-D^2 - r_1^2 + r_2^2}{D}$$



# Trilateration

Random errors dilute the precision so approximate solutions are used instead

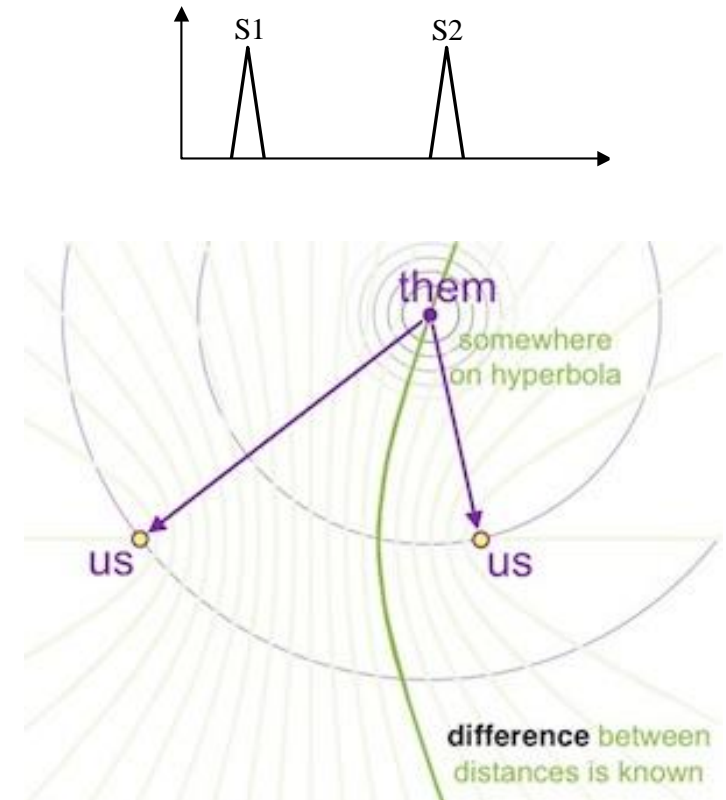
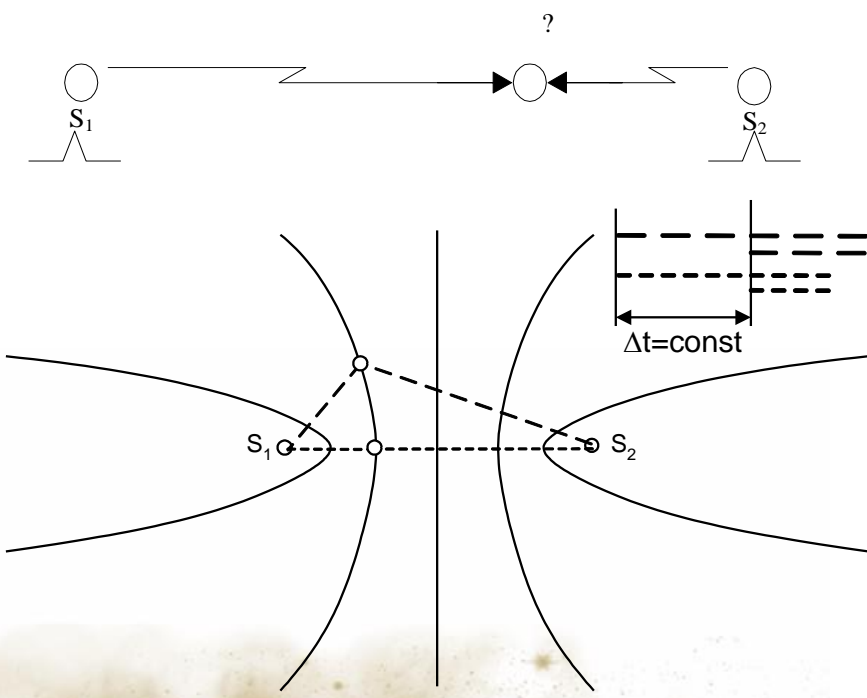


# Hyperbolic / Multilateration

Hyperbolic or multilateration technique is using distance differences.

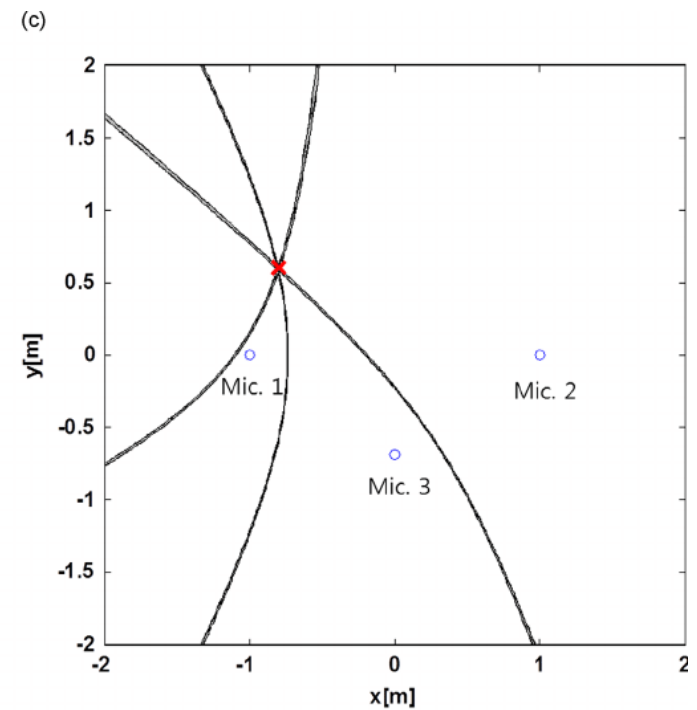
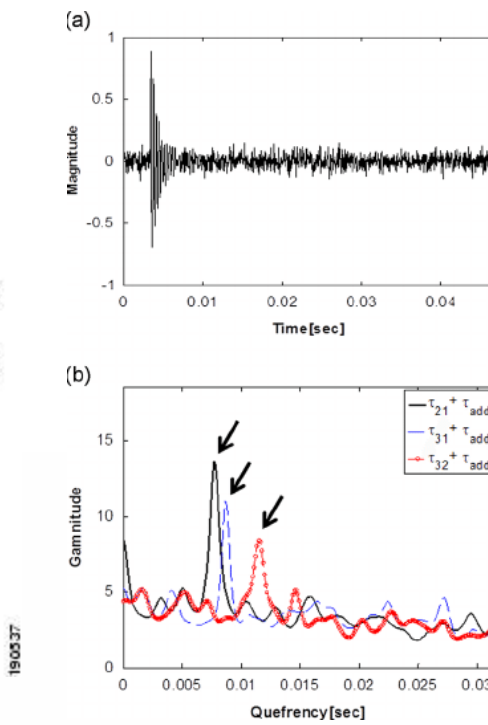
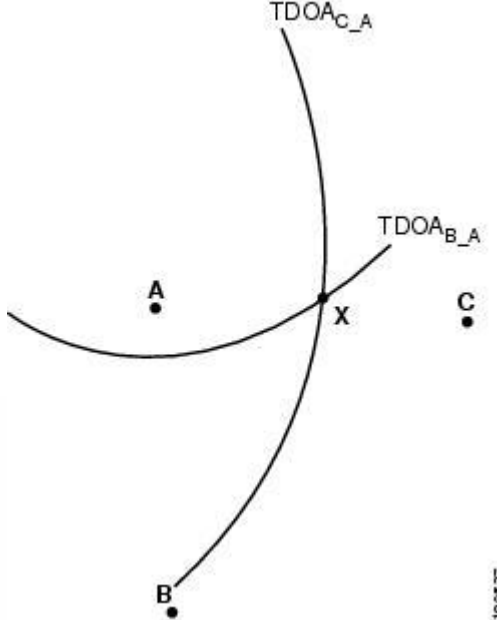
Time difference of arrival (TDOA) -> distance (using EM wave speed)

Pair of the reference points -> equal difference curve (hyperbolae).



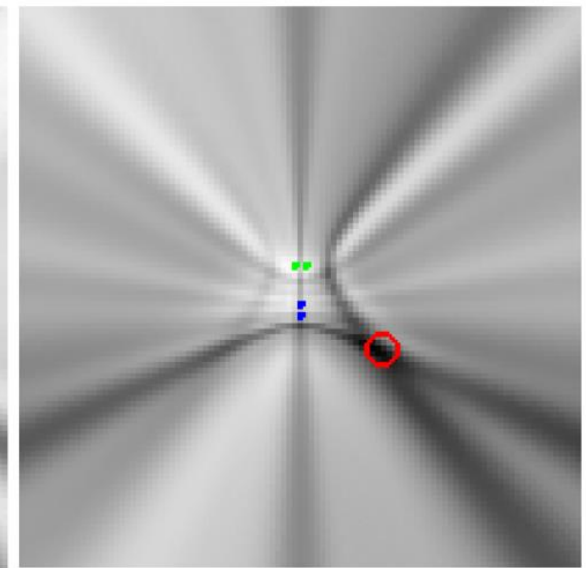
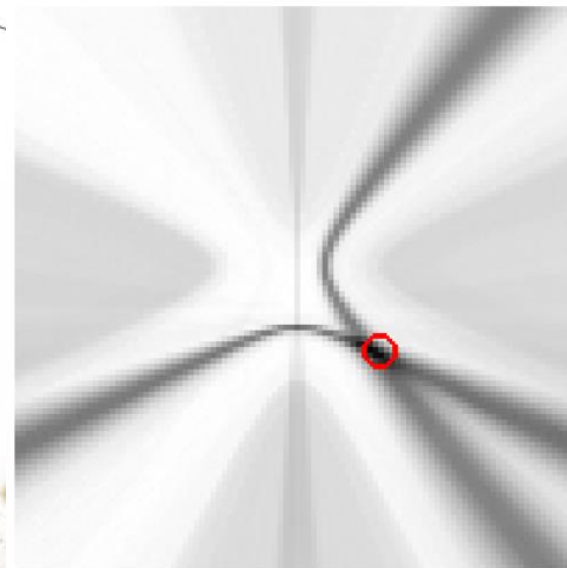
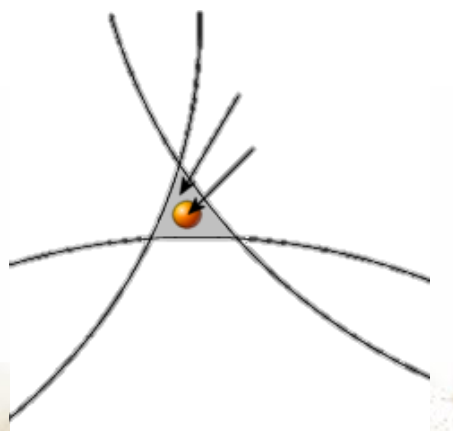
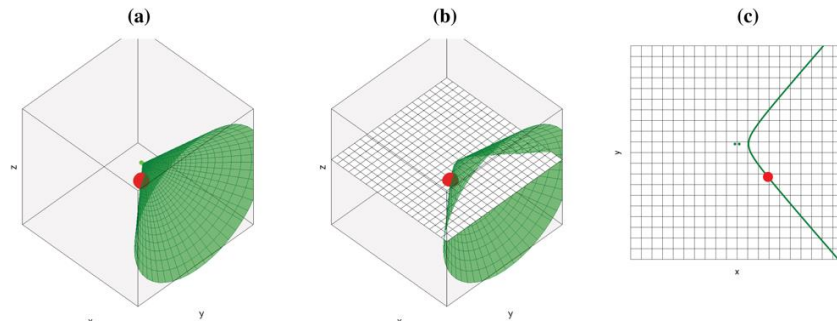
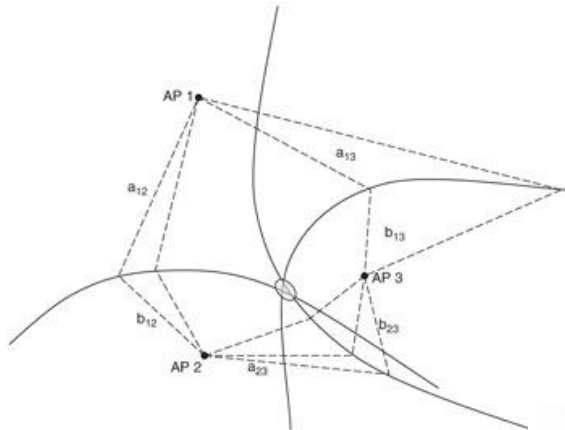
# Hyperbolic / Multilateration

Pair of the reference points -> equal difference curve (hyperbolae). Intersection of hyperbolae = object coordinates.  
At least three reference points are required.



# Hyperbolic / Multilateration

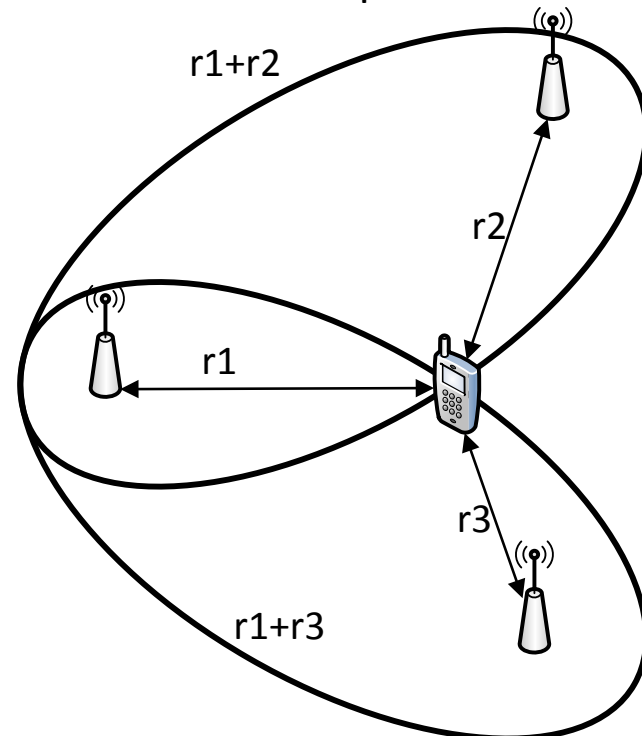
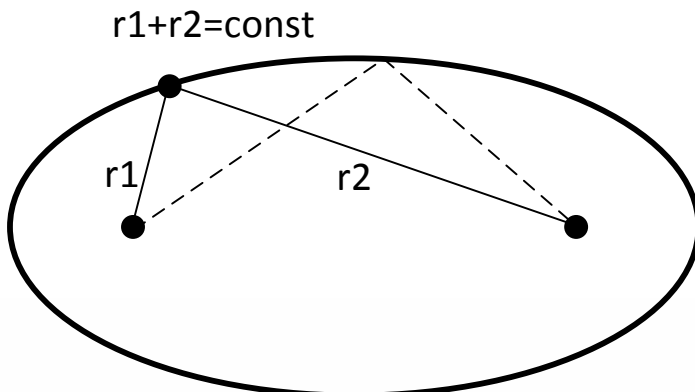
Random errors dilute the precision so approximate solutions are used instead



# Elliptic

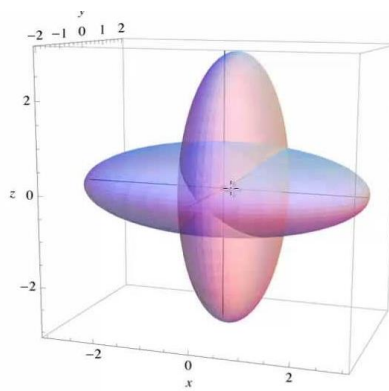
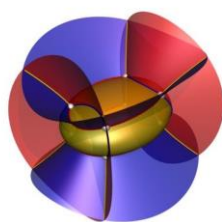
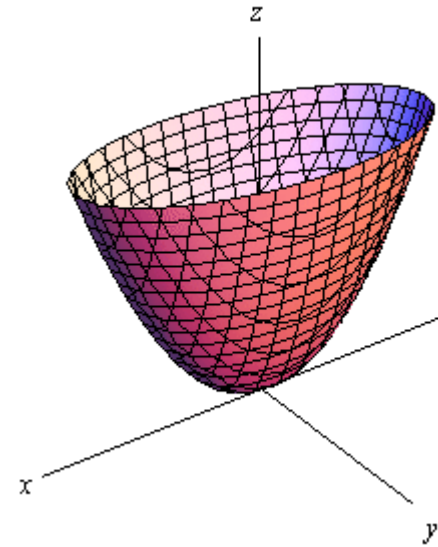
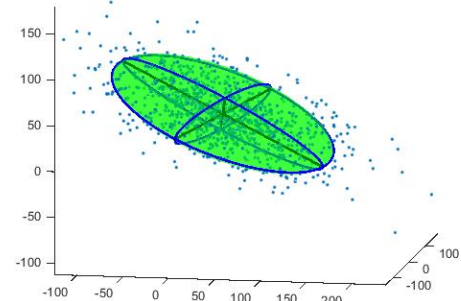
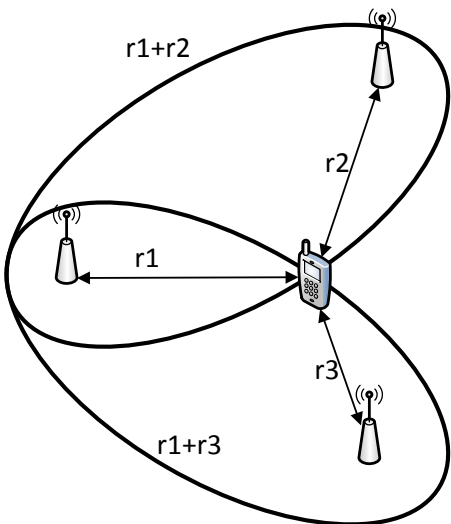
Elliptic position estimation technique is using time sum of arrival (TSOA). Every pair of reference points is exchanging the signals using the object. Equal TSOA positions give an ellipse in 2D space and ellipsoid in 3D space. The intersection of the ellipsoids reveal the object coordinates.

At least three reference points are required to establish the 2D position fix



# Elliptic

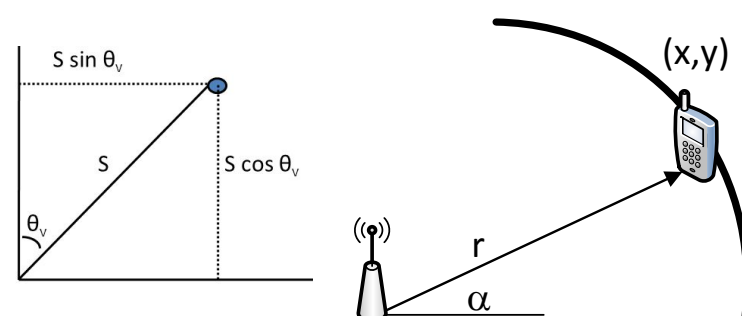
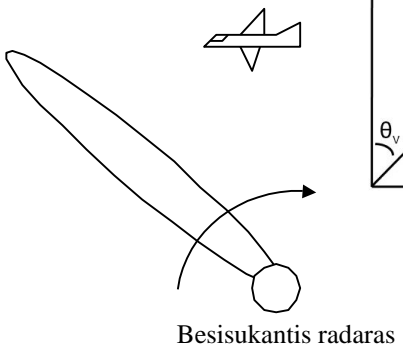
Random errors dilute the precision -> approximate solutions are used



# Hybrids

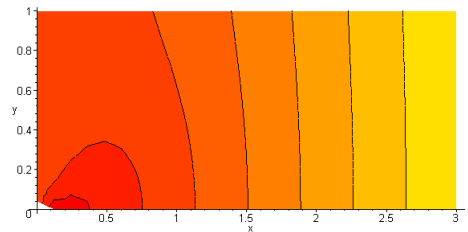
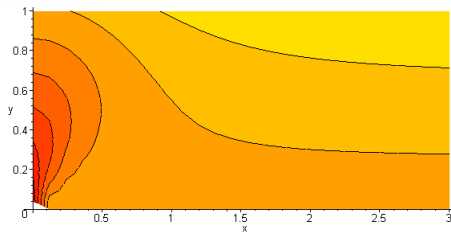
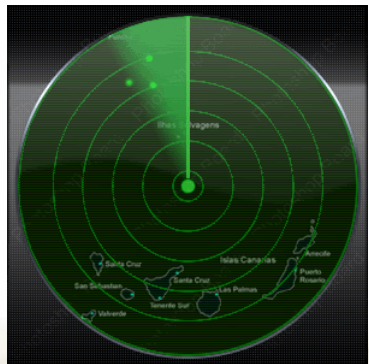
Techniques mentioned above can be combined to produce any hybrid.

E.g. : combining the distance and angle of arrival (triangulation):  
this technique is used by radar

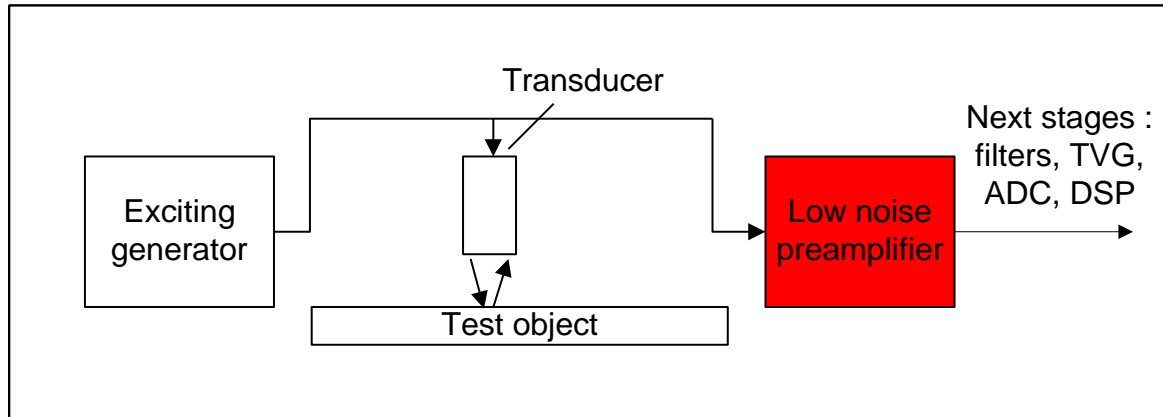


$$x := \cos(\alpha) r$$

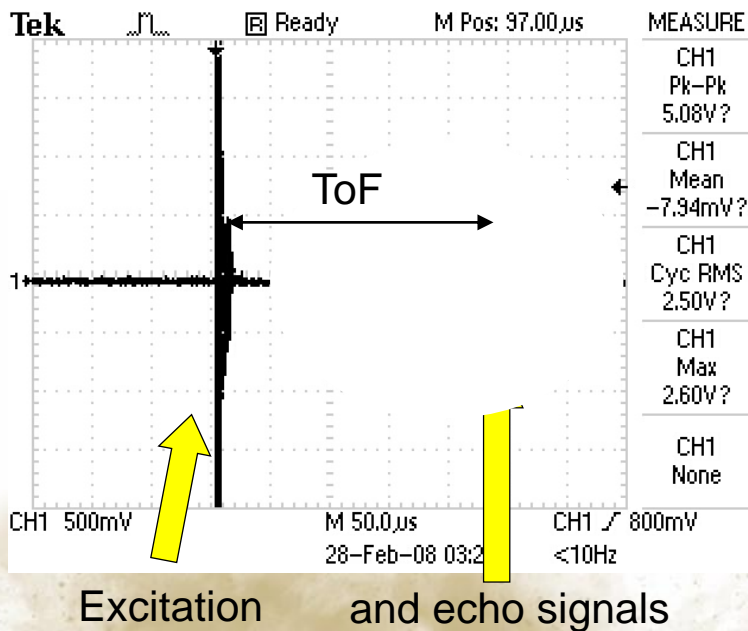
$$y := \sin(\alpha) r$$



# What is Time of Flight (ToF)?



General ultrasonic inspection system structure

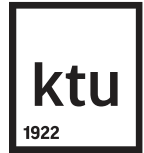


Time of Flight (ToF)

Or Time delay estimate (TDE):

1. Time for signal to travel in media
2. Distance in time between the transmitted and received signals

# TOF Applications



NDT:

- defect location and sizing, thickness measurement, load, density



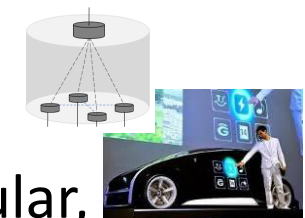
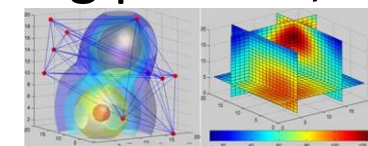
Technical and scientific measurements:

- temperature, load, mechanical properties, curing process, chemical composition, air and liquid velocity



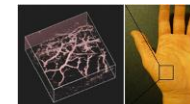
Navigation and robotics:

- trilateration, distance to obstacle, surface profiling



Medicine:

- blood diagnostics, glucose level; tissue, cardiovascular, skeletal diagnostics, internal temperature distribution or elastography imaging

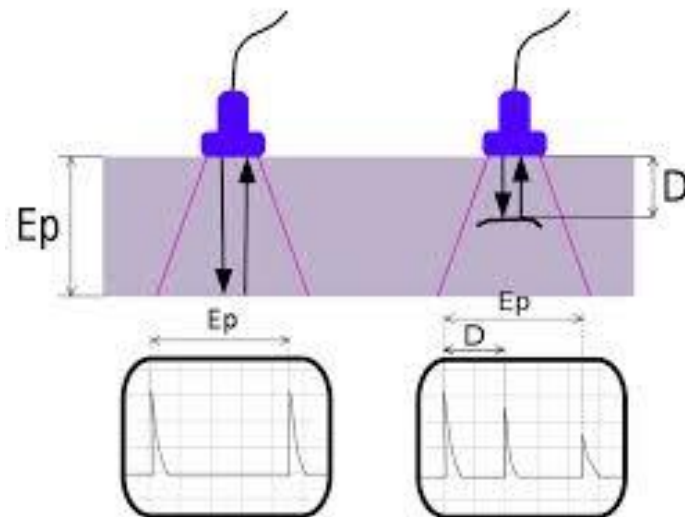
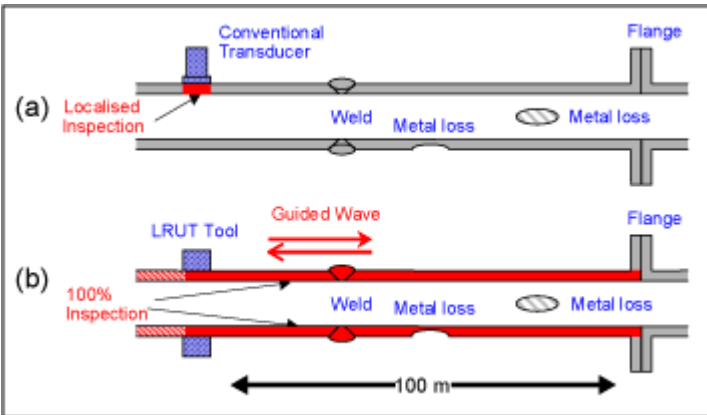


Food industry:

- sugar content, fruit ripeness, meat or milk products quality.



# Distance, Thickness



$$D = ct \quad , \text{one directional}$$

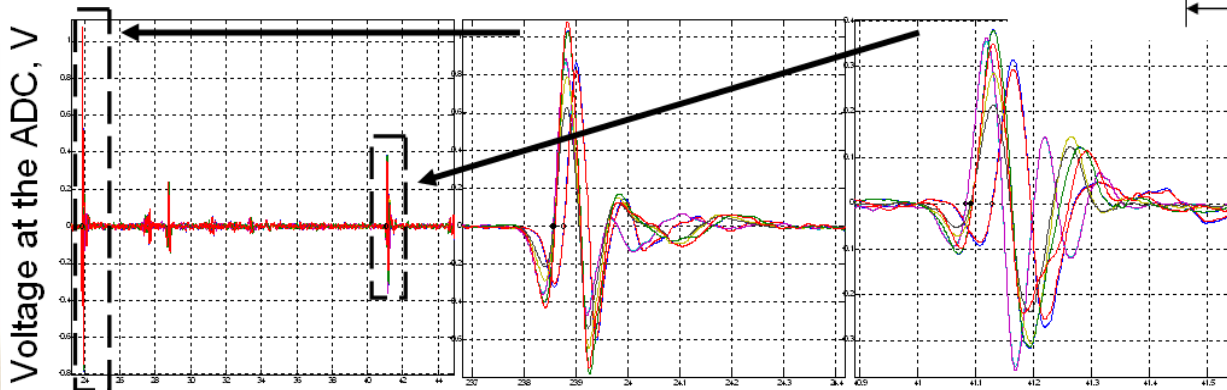
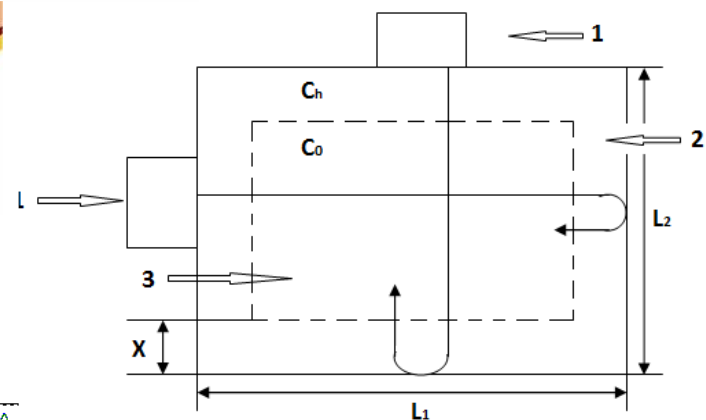
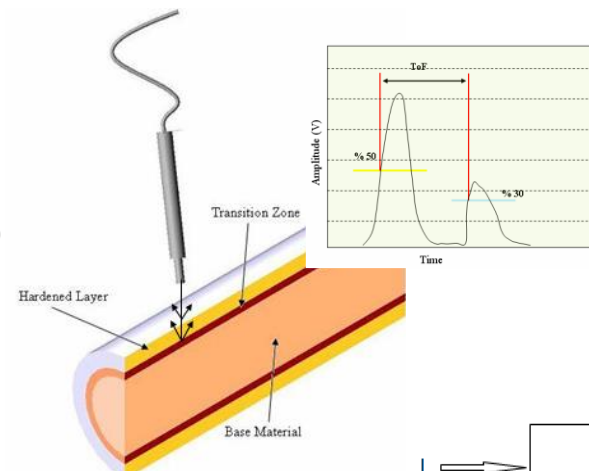
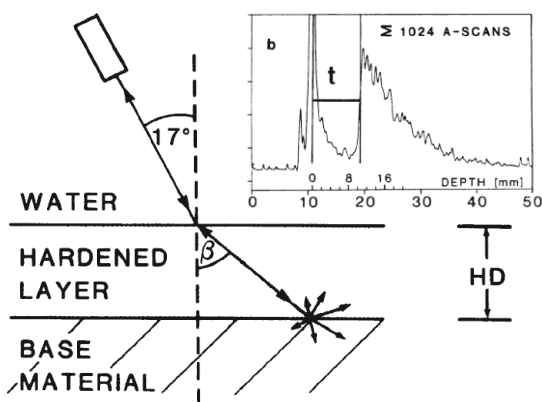
$$D = \frac{ct}{2} \quad , \text{reflection}$$

$$Z = \frac{p}{v} \qquad T_p = \frac{2Z_2}{Z_1 + Z_2}$$

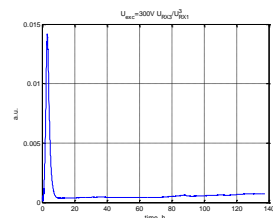
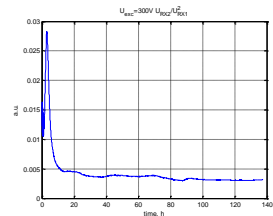
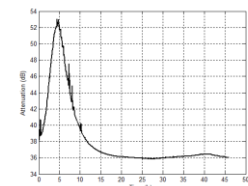
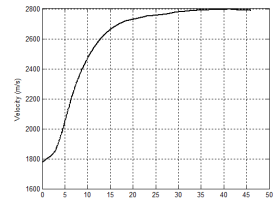
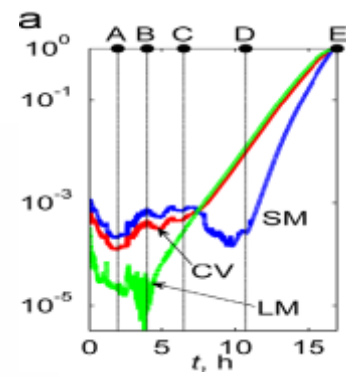
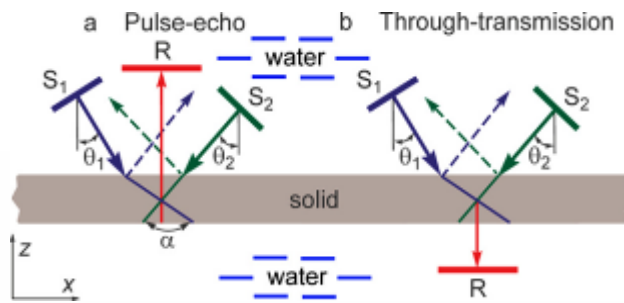
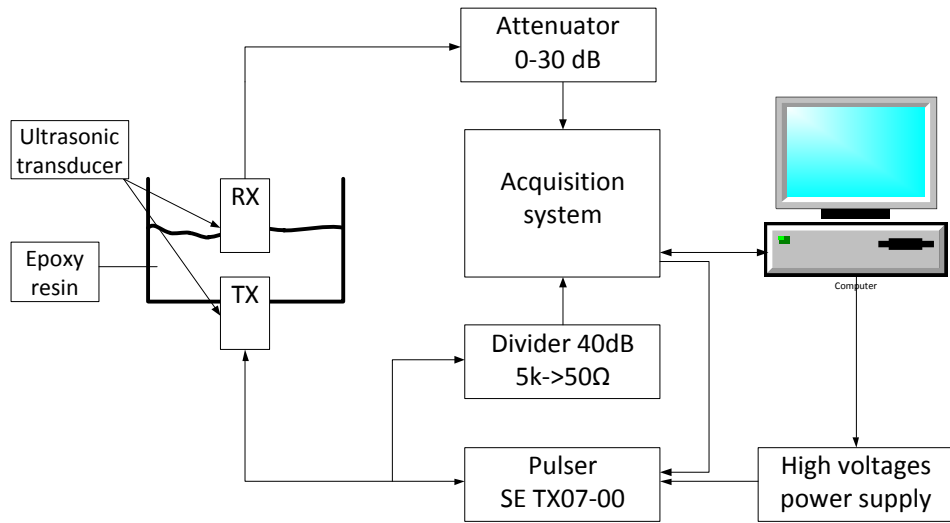
$$R_p + 1 = T_p \qquad R_p = \frac{Z_2 - Z_1}{Z_1 + Z_2}$$

# Hardening, Tempering Depth

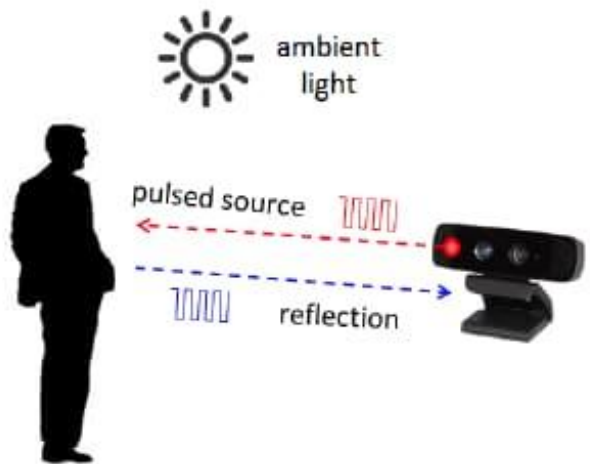
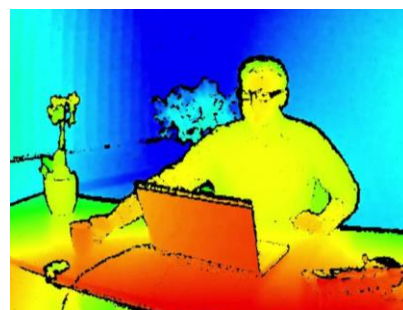
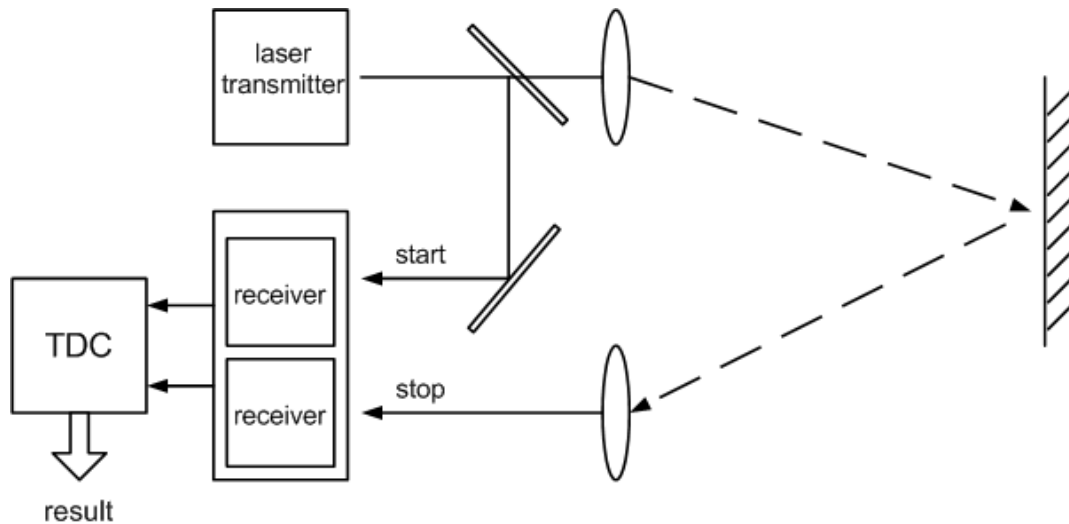
US-TRANSDUCER



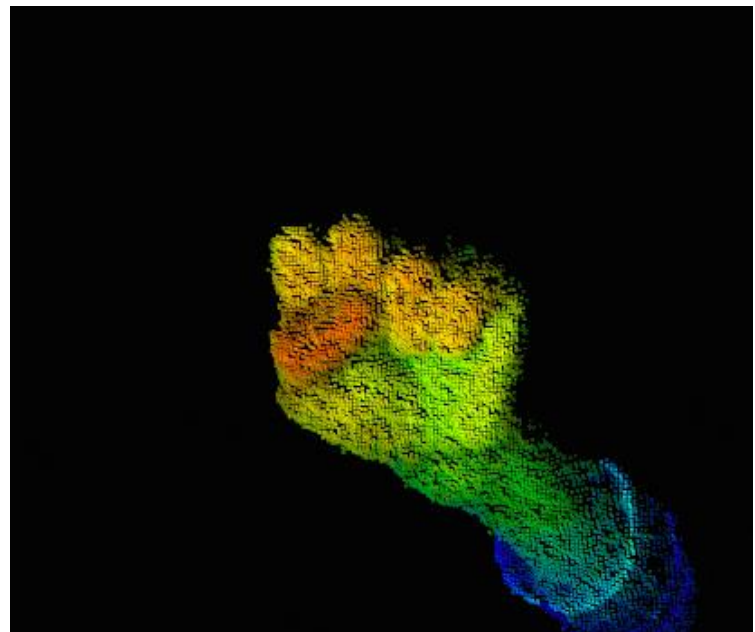
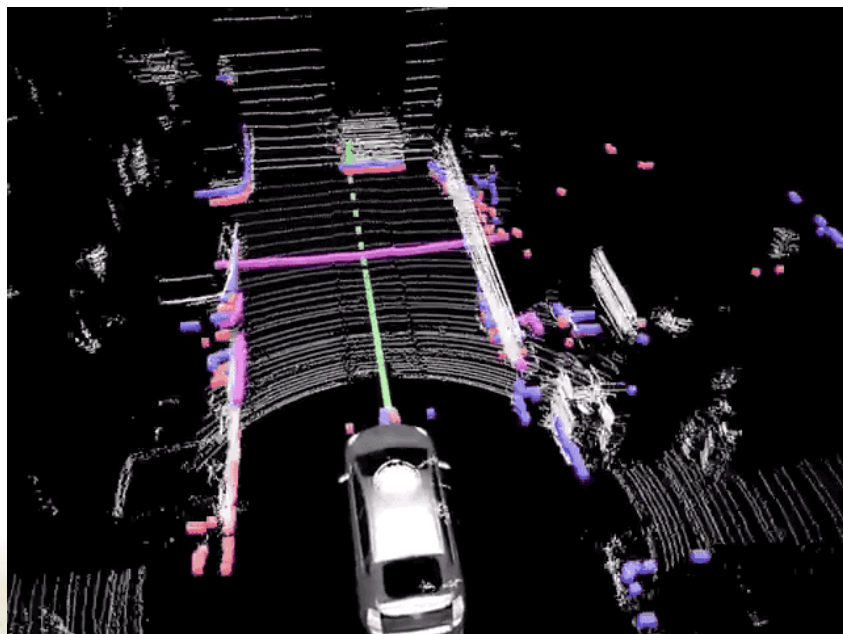
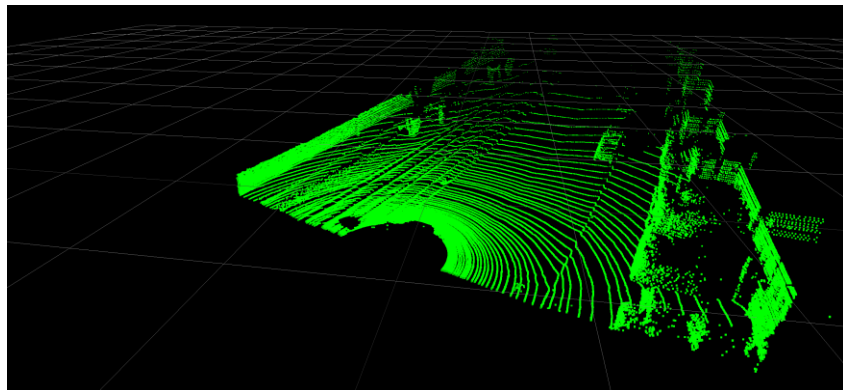
# Curing State Monitoring



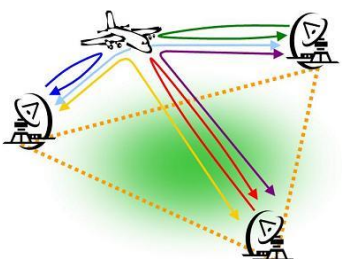
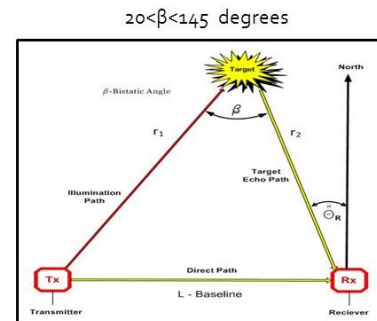
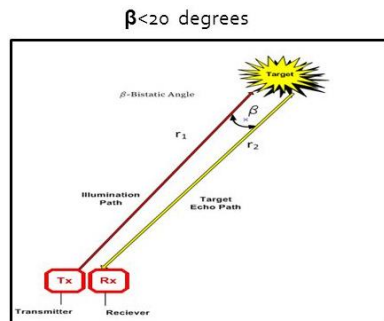
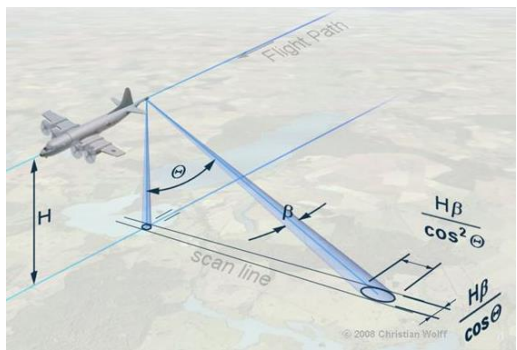
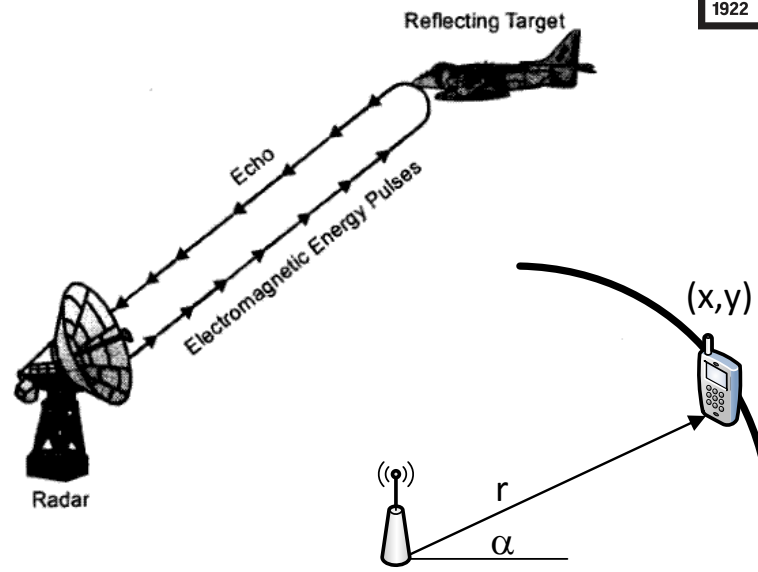
# Time Of Flight (TOF) - Lidar



# Time Of Flight (TOF) Camera



# RADAR

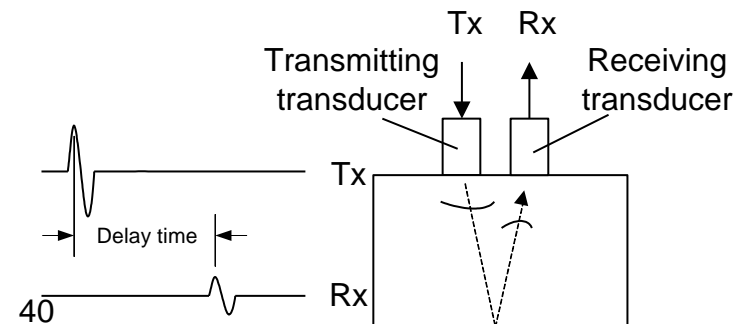
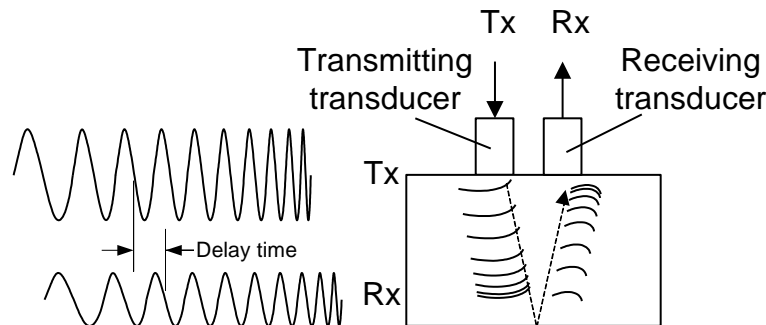
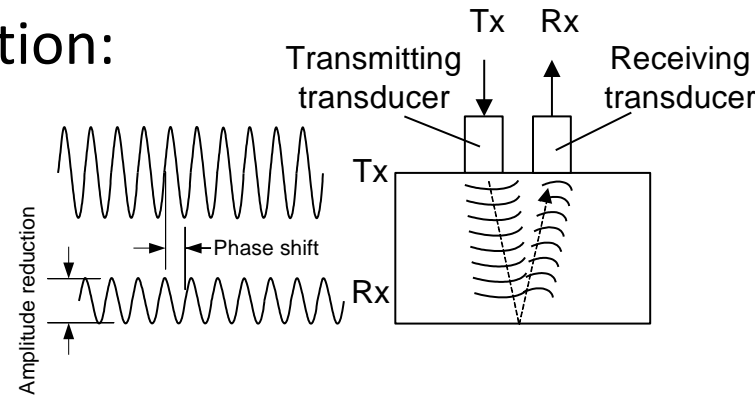
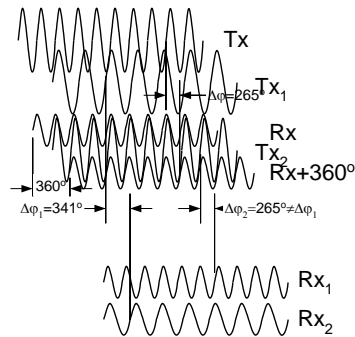


# Tof estimation vs. signal parameter

1922

Signal parameter used for estimation:

- Amplitude;
- Phase;
- Frequency;
- Group delay (pulsed).

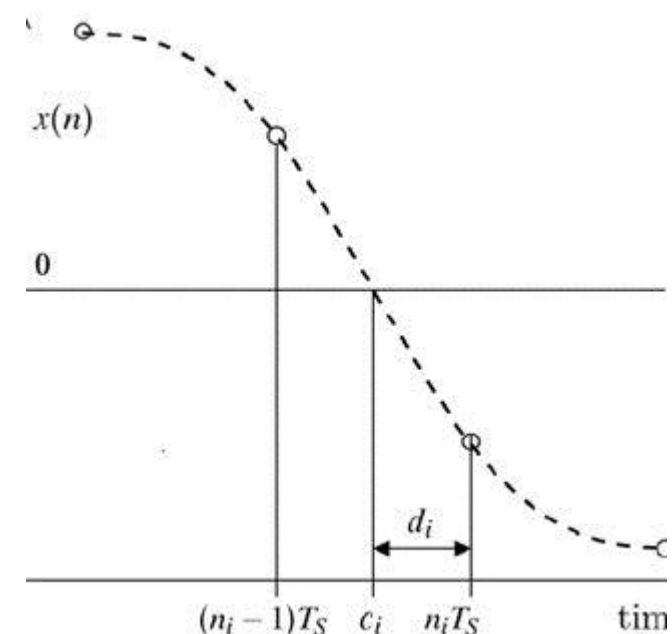
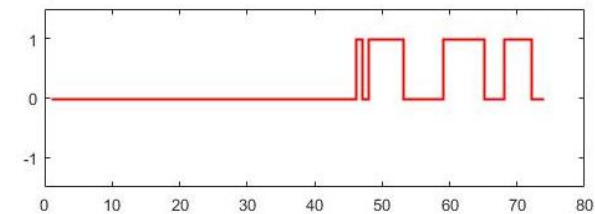
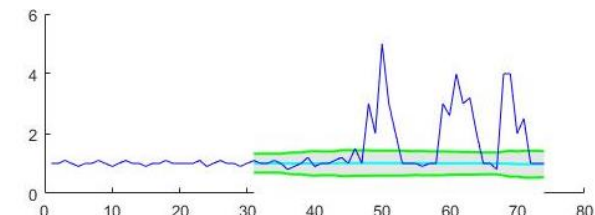
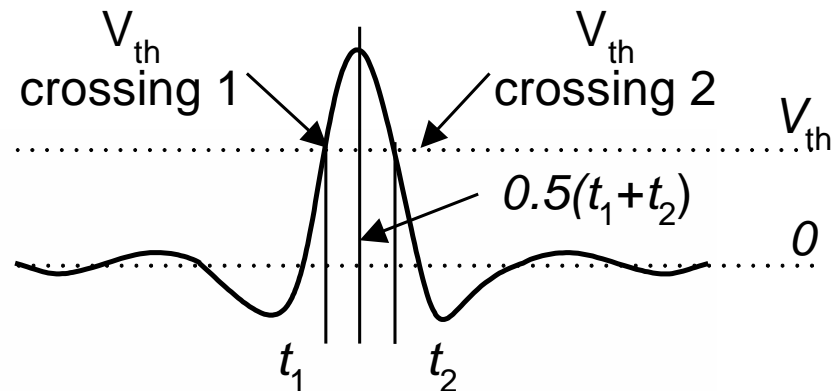


# Tof by level crossing: thresholding

- Start counter
- Stop when level crossing detected

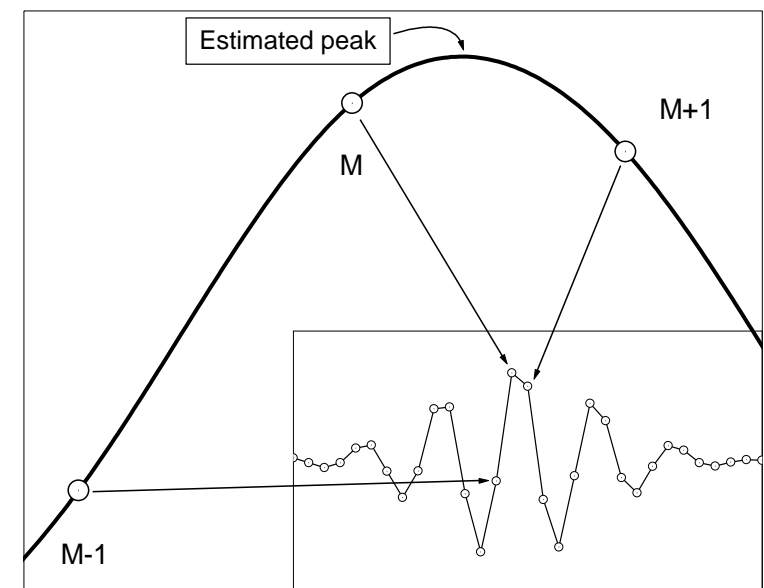
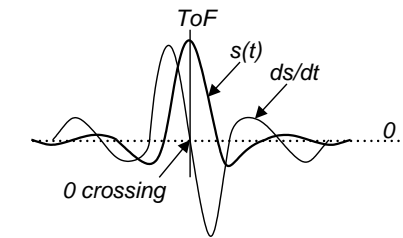
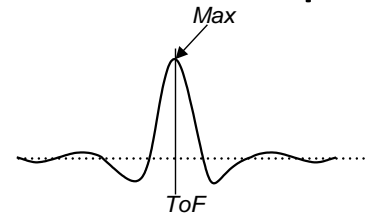
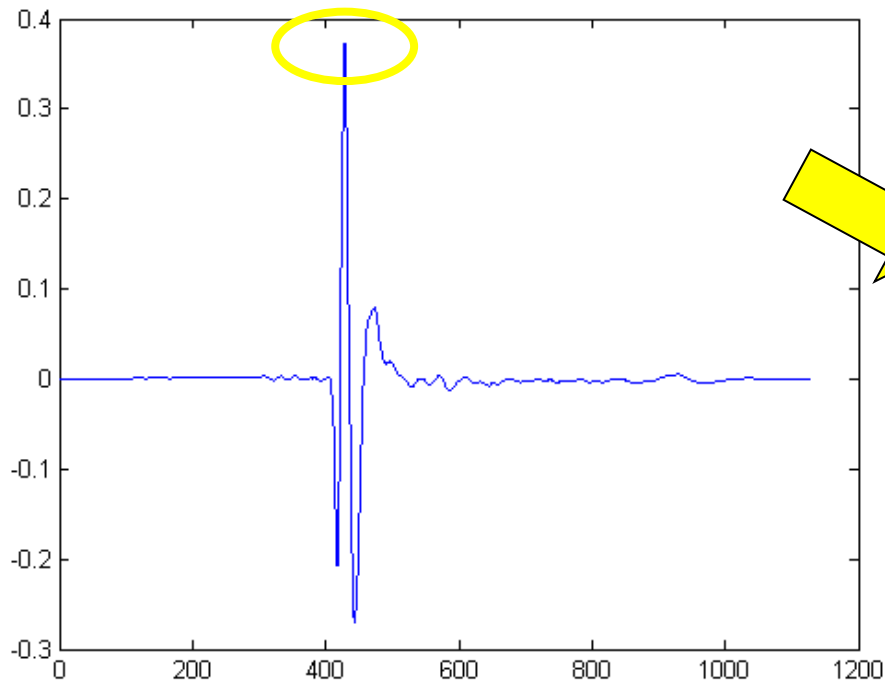


- Find the level crossing
- Interpolate ZC using linear interpolation
- Can be augmented for several crossings



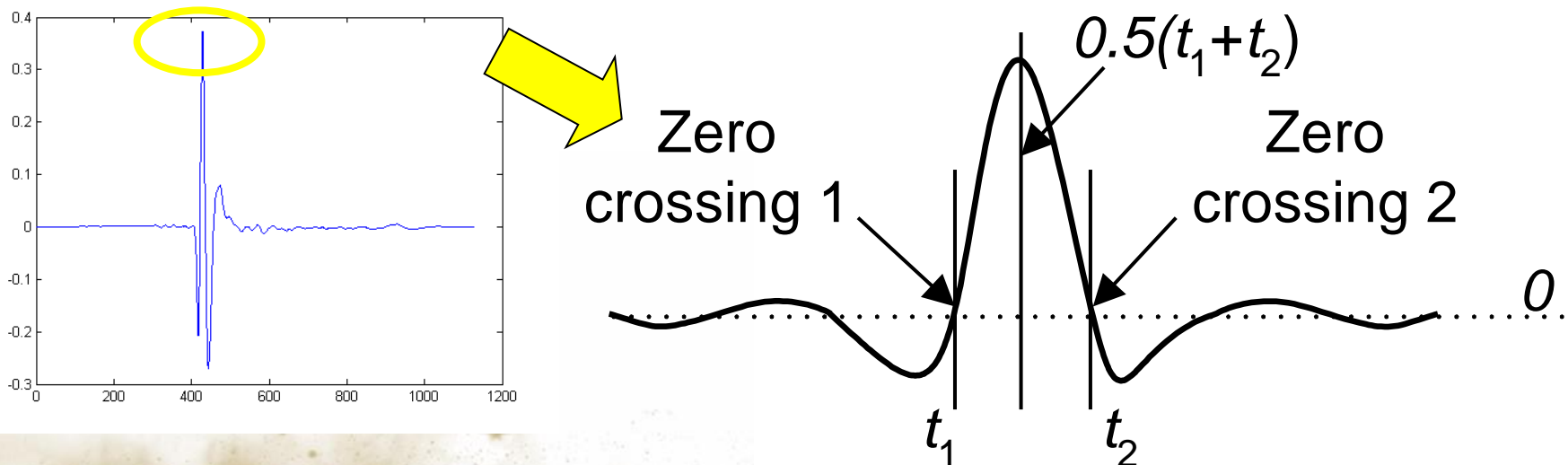
# Tof by peak location

- Find the signal peak
- Interpolate peak position using parabolic interpolation



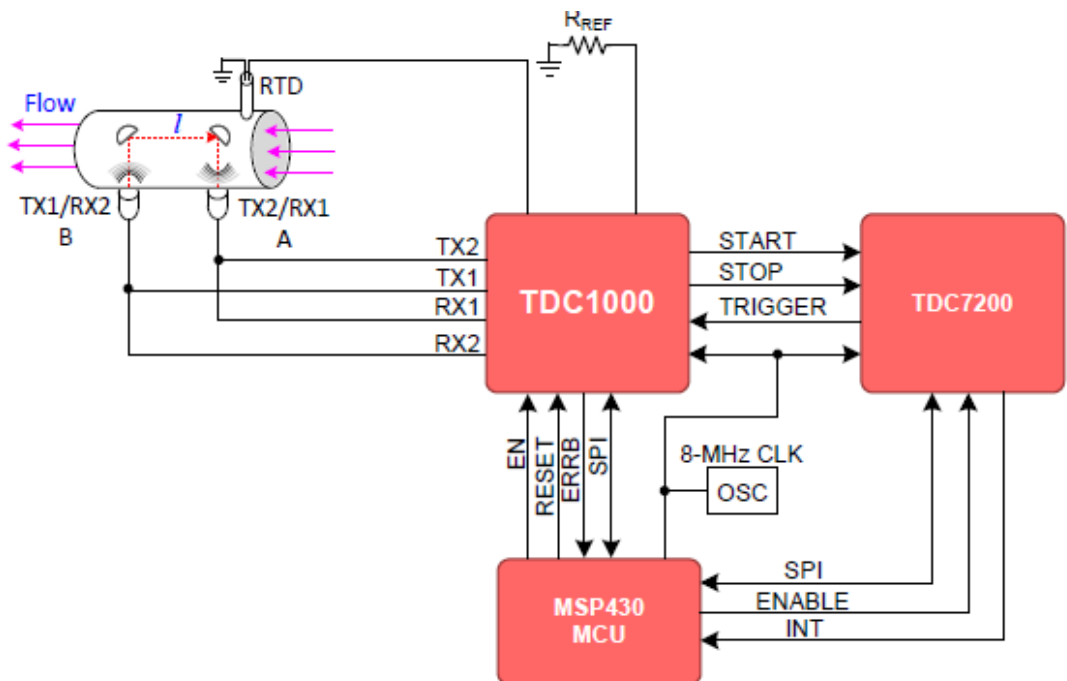
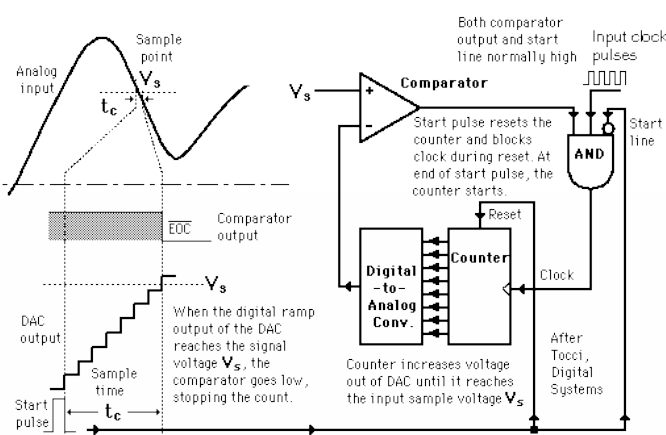
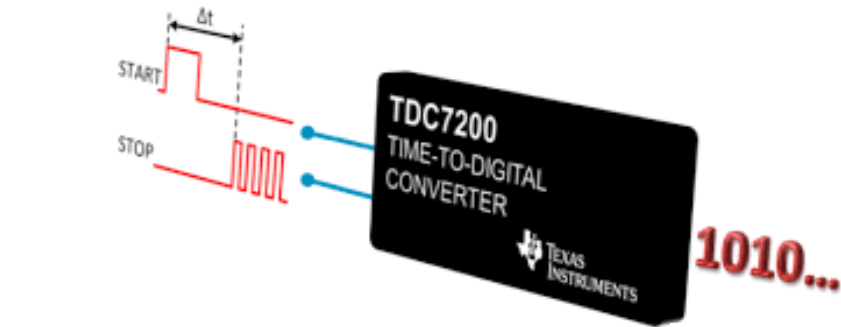
# ToF as zero crossing

- Find the signal peak/level crossing
- Descend left to the first zero crossing (Zero crossing 1)
- Find opposite side zero crossing (Zero crossing 2)
- Interpolate ZC using linear interpolation
- Take the mean:  $\text{ToF} = (\text{ZC2} + \text{ZC1})/2$

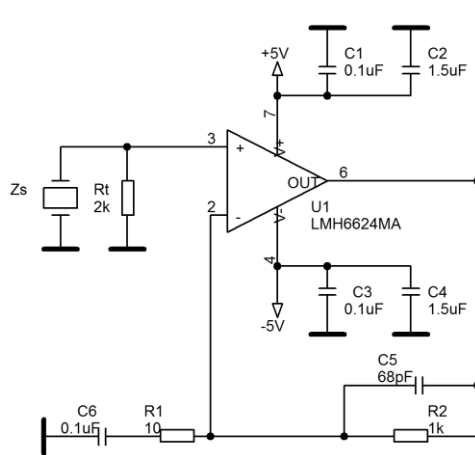


# ToF By Counting: TDC

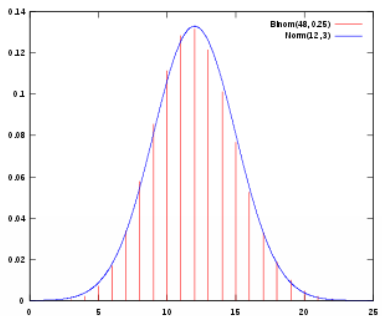
- TDC: time to digit converter



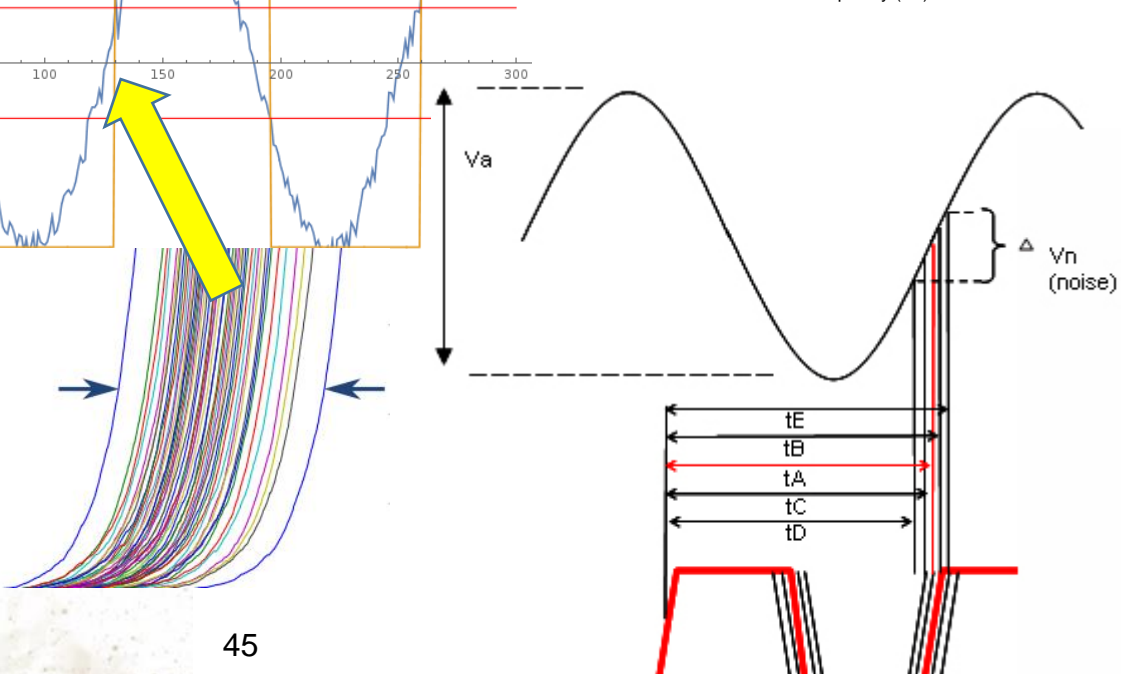
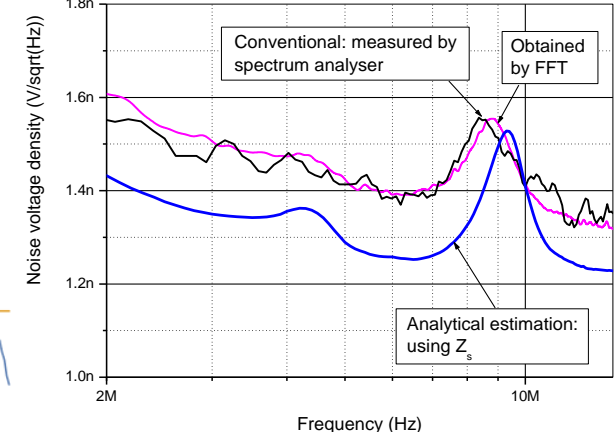
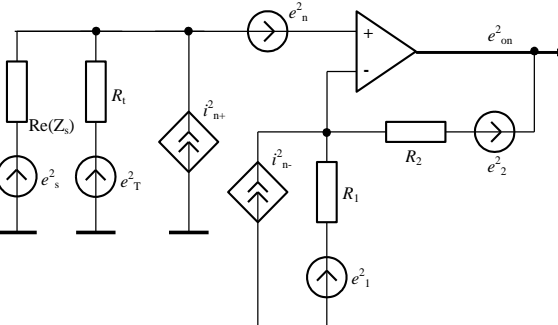
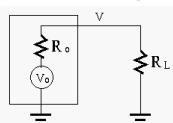
# Problem: Noise



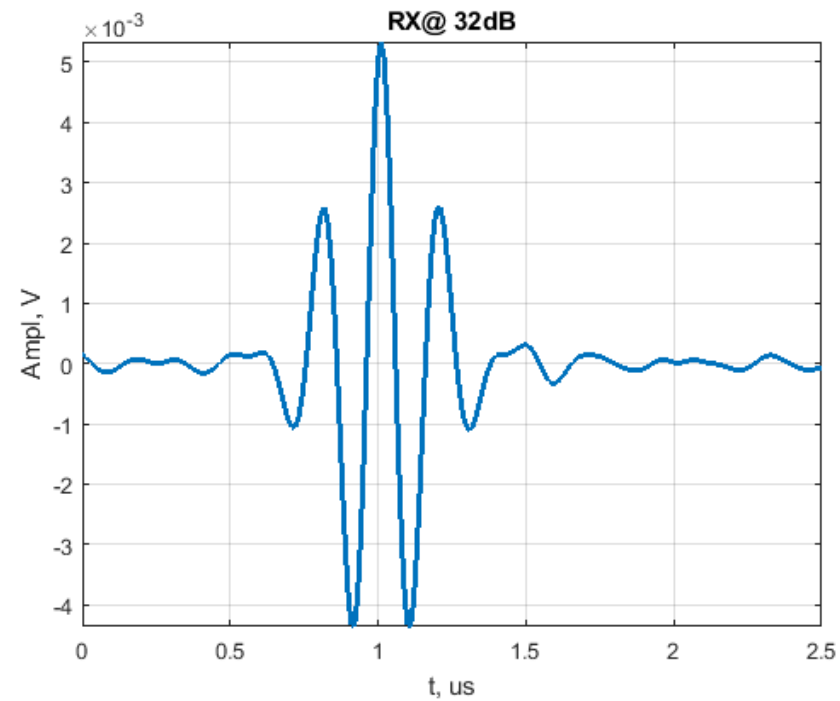
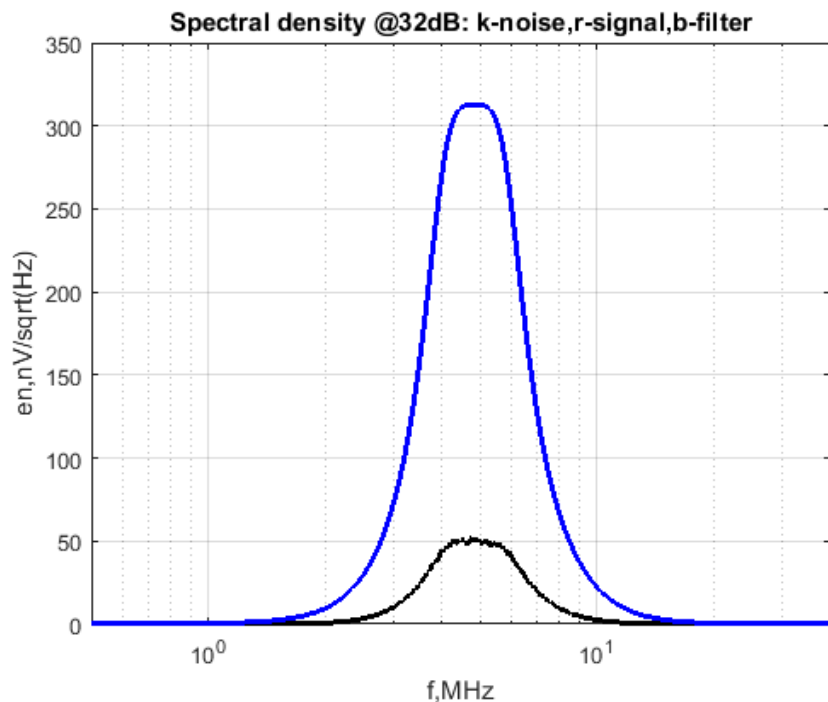
Gaussian noise



$$v_n = \sqrt{\bar{v}_n^2} \sqrt{\Delta f} = \sqrt{4k_B T R \Delta f}$$



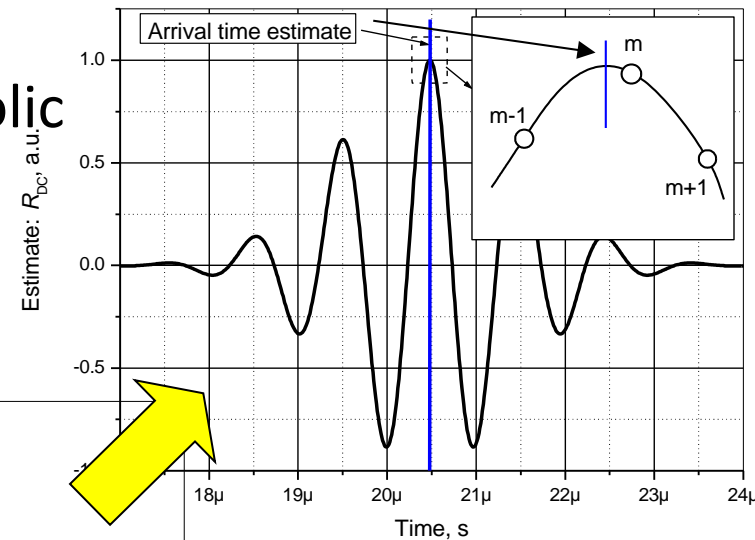
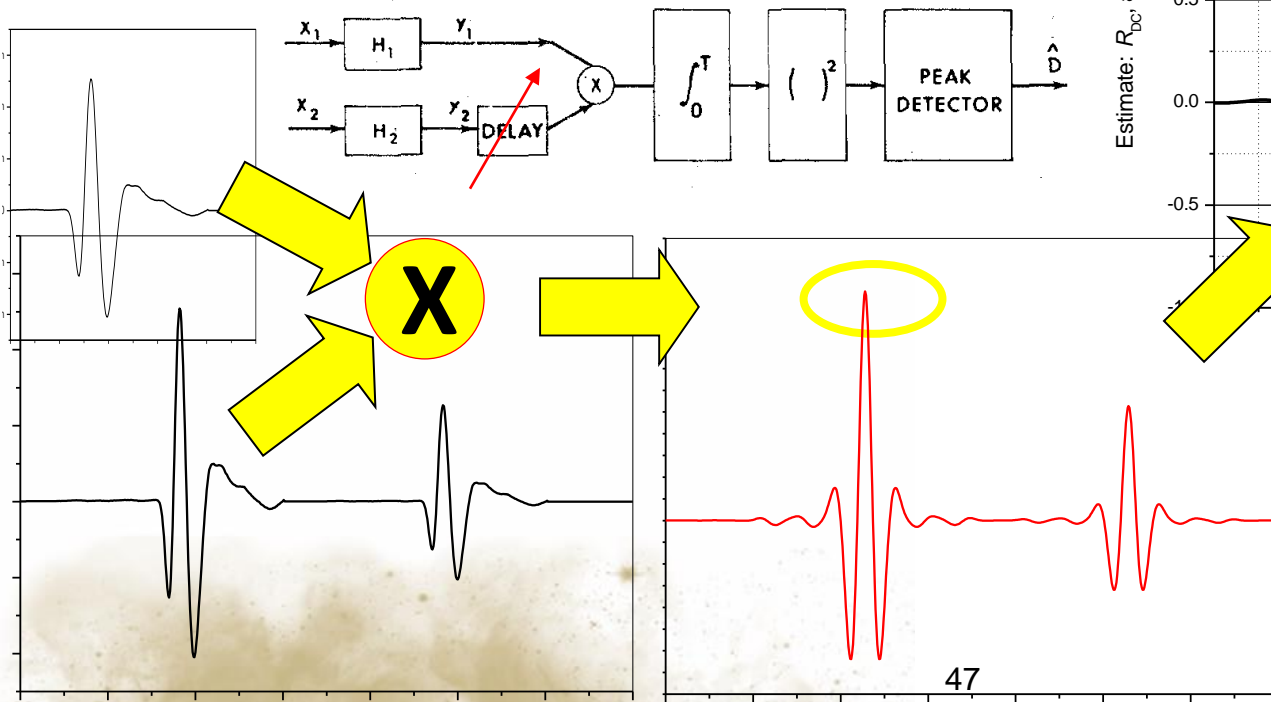
# Solution: Filtering



Optimal Filter

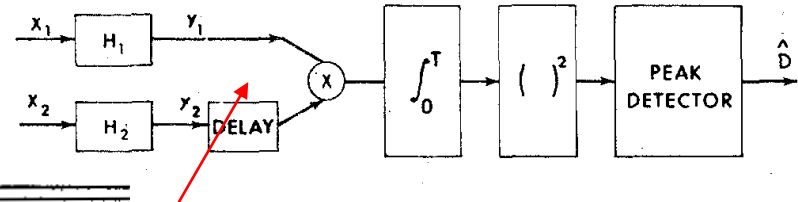
# ToF from global properties: cross-correlation peak

- Produce the reference (previously recorded, excitation signal copy, signal mathematical model)
- Calculate cross-correlation function (CCF)
- Find the CCF peak
- Interpolate using FFT, cosine or parabolic



## ToF from global properties: cross-correlation peak

- Generalized cross-correlation types




---

Processor Name	Weight $\psi(f) = H_1(f) H_2^*(f)$
----------------	---------------------------------------

---

Cross Correlation	1
-------------------	---

Roth Impulse Response	$1/G_{x_1 x_1}(f)$
-----------------------	--------------------

SCOT	$1/\sqrt{G_{x_1 x_1}(f) G_{x_2 x_2}(f)}$
------	--

PHAT	$1/ G_{x_1 x_2}(f) $
------	----------------------

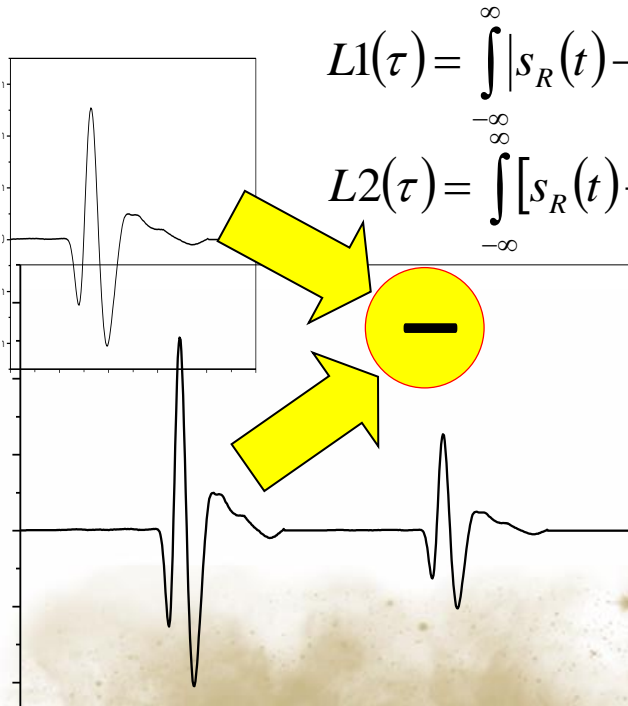
Eckart	$G_{s_1 s_1}(f)/[G_{n_1 n_1}(f) G_{n_2 n_2}(f)]$
--------	--

ML or HT	$\frac{ \gamma_{12}(f) ^2}{ G_{x_1 x_2}(f) [1 -  \gamma_{12}(f) ^2]}$
----------	---

---

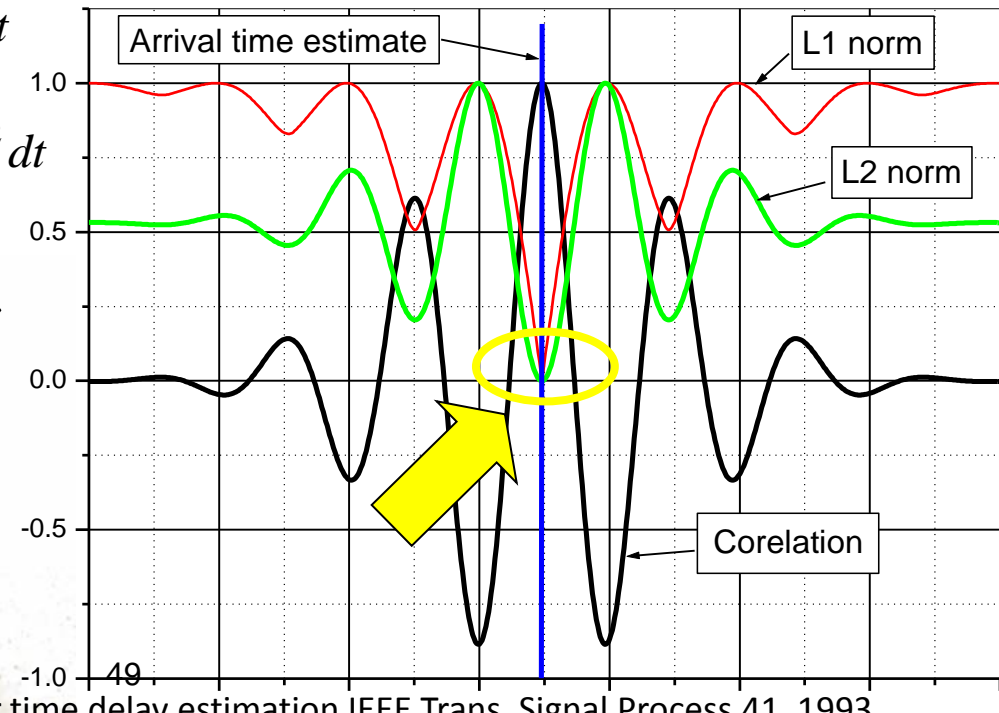
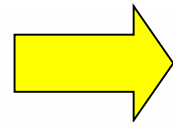
# ToF from global properties: difference minimization

- Produce the reference
- Calculate the remainder of reference subtraction for all positions
- Find the minimum of remainder L1 (magnitude, sum absolute difference SAD) or L2 norm (power, energy, sum squared difference SSD)
- Interpolate using parabolic (L2) or triangular(L1) function

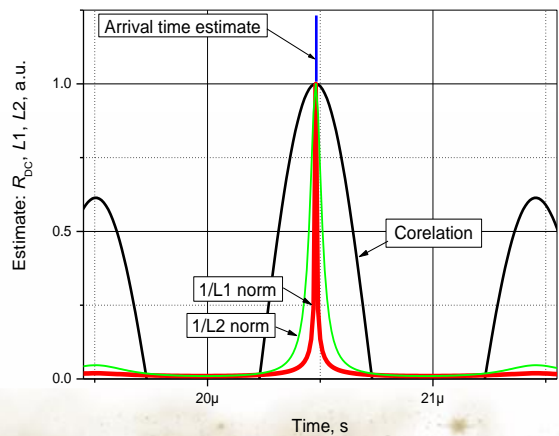
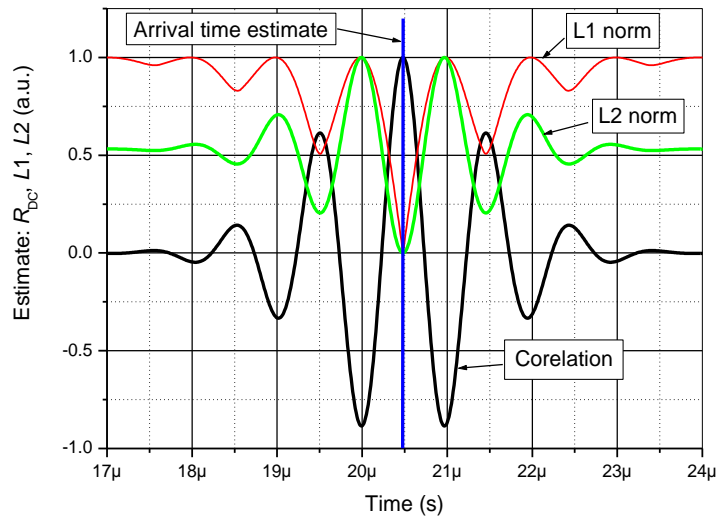


$$L1(\tau) = \int_{-\infty}^{\infty} |s_R(t) - s_T(t - \tau)| dt$$

$$L2(\tau) = \int_{-\infty}^{\infty} [s_R(t) - s_T(t - \tau)]^2 dt$$



# ToF from global properties



$$x(\tau) = \int_{-\infty}^{\infty} s(t) \cdot s_R(t - \tau) dt$$

$$ToF_{CC} = \arg[\max(x(\tau))]$$

$$L1(\tau) = \int_{-\infty}^{\infty} |s(t) - s_R(t - \tau)| dt$$

$$ToF_{L1} = \arg\{\min[L1(\tau)]\}$$

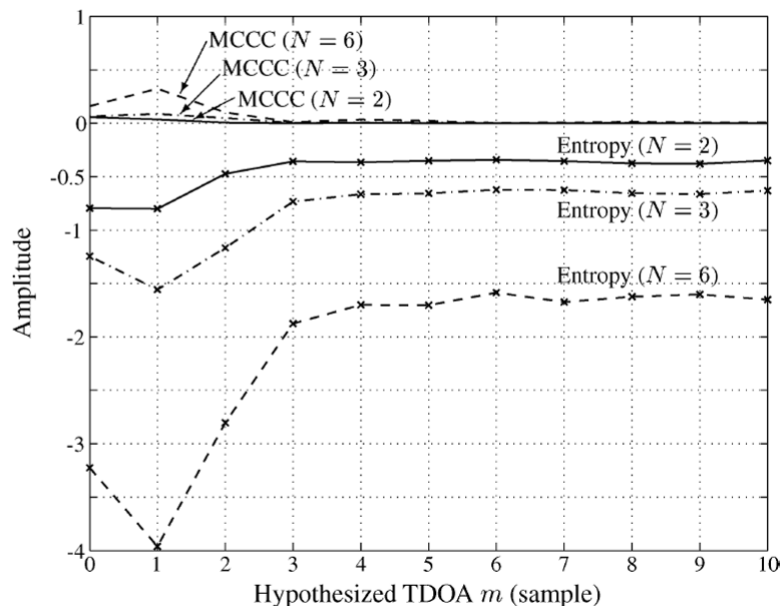
$$L2(\tau) = \int_{-\infty}^{\infty} [s(t) - s_R(t - \tau)]^2 dt$$

$$ToF_{L2} = \arg\{\min[L2(\tau)]\}$$

# ToF estimation using global properties: higher order statistics



- Establish the likelihood criteria (entropy minimum, quasi likelihood)
- Fit the criteria to received signal
- Optimal parameter is the ToF



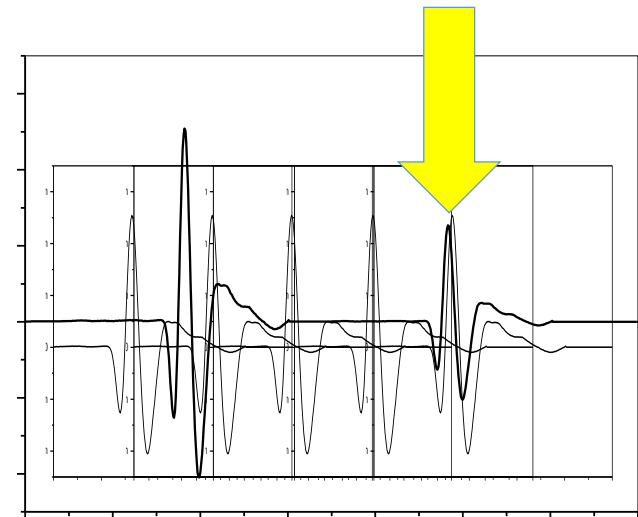
Entropy minimisation example: J Benesty, et al. 'Time Delay Estimation via Minimum Entropy', IEEE Signal Process. Lett., Vol 14, No 3, pp 157-160, 2007.

# ToF estimation for pulse (group delay)

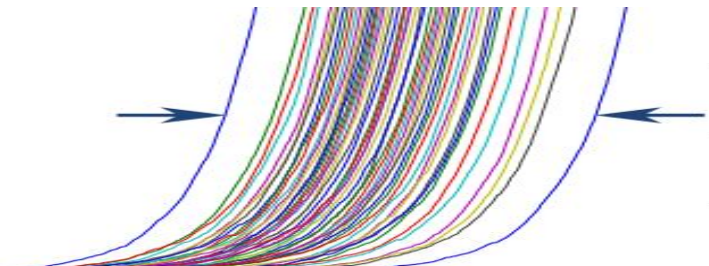
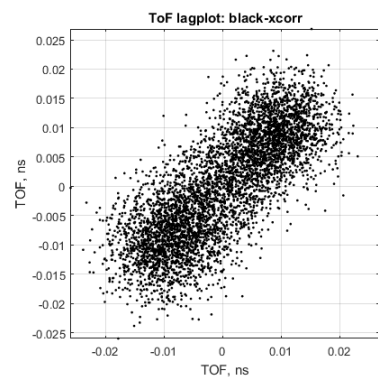
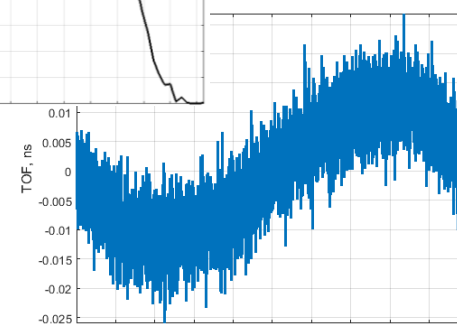
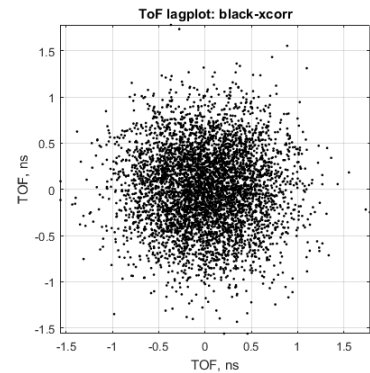
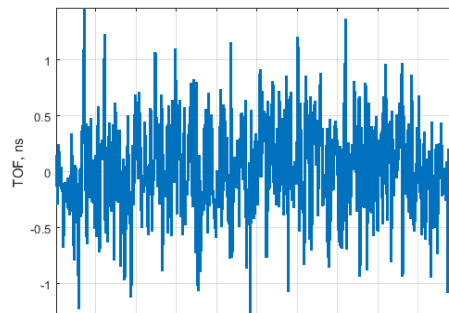
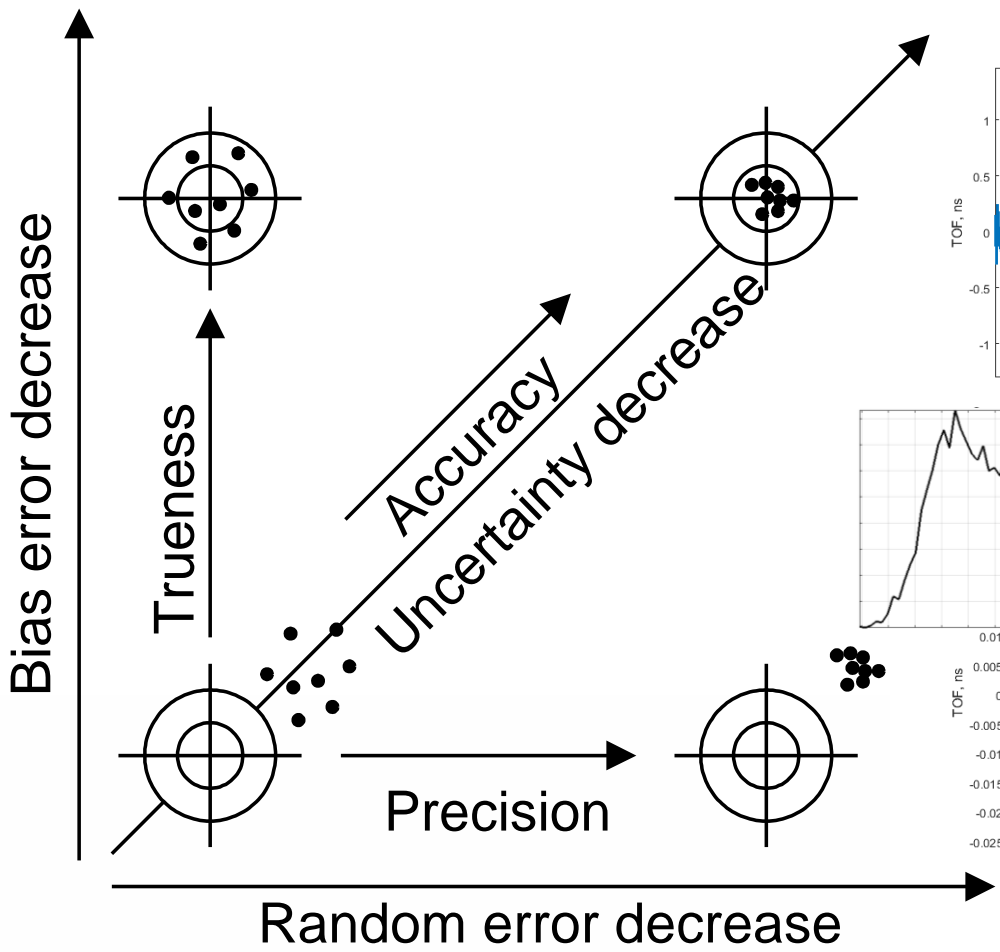
1922

## Major division

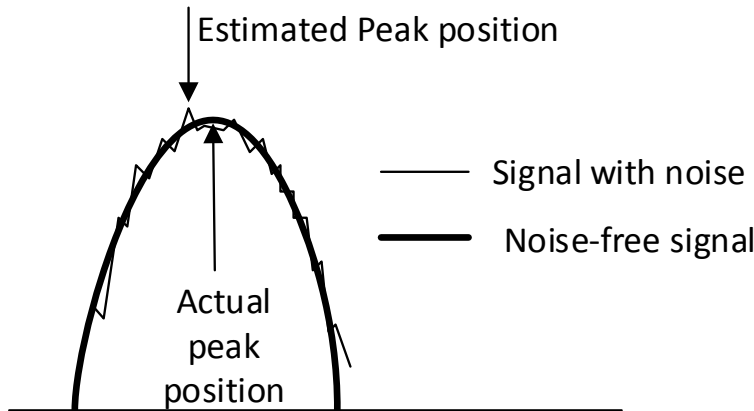
- Local properties match: no integral values (signal peak, signal derivative's zero crossing, threshold crossing, dual crossing)  
+Simple, No need for reference signal
- Global properties match: integral over time (cross correlation peak, cross correlation derivative's zero crossing, subtraction minimum, statistics)  
-Need reference signal (or model)  
+exploits full signal energy



# Measurement errors



# ToF estimation random errors



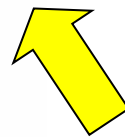
- TOF atsitiktinės paklaidos artėja prie Cramer Rao apatinės ribos (CRLB):

$$\sigma(ToF) \geq \frac{1}{F_e \sqrt{\frac{2E}{N_0}}}$$

- Efektinė juosta (Effective bandwidth, RMS bandwidth, Gabor bandwidth):

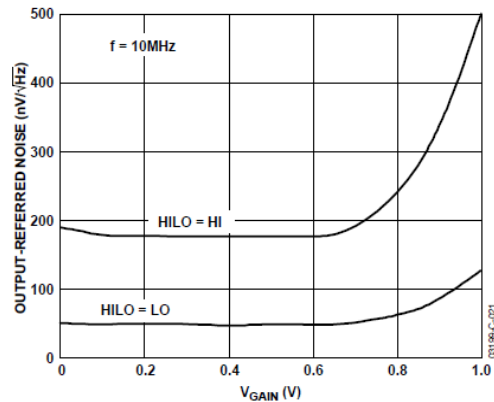
$$F_e^2 = f_0^2 + \beta^2 = \frac{\left[ \int_{-\infty}^{\infty} f |S(f)|^2 df \right]^2}{E^2} + \frac{\int_{-\infty}^{\infty} (f - f_0)^2 |S(f)|^2 df}{E}$$

Centrinis dažnis



Gaubtinės juostos plotis

# ToF estimation random errors



$$N_0 = \frac{e^2}{Z_{ADC}} n_{tot}$$

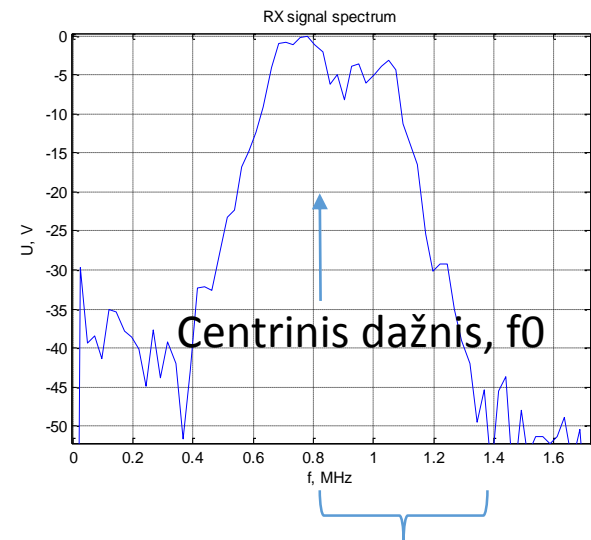
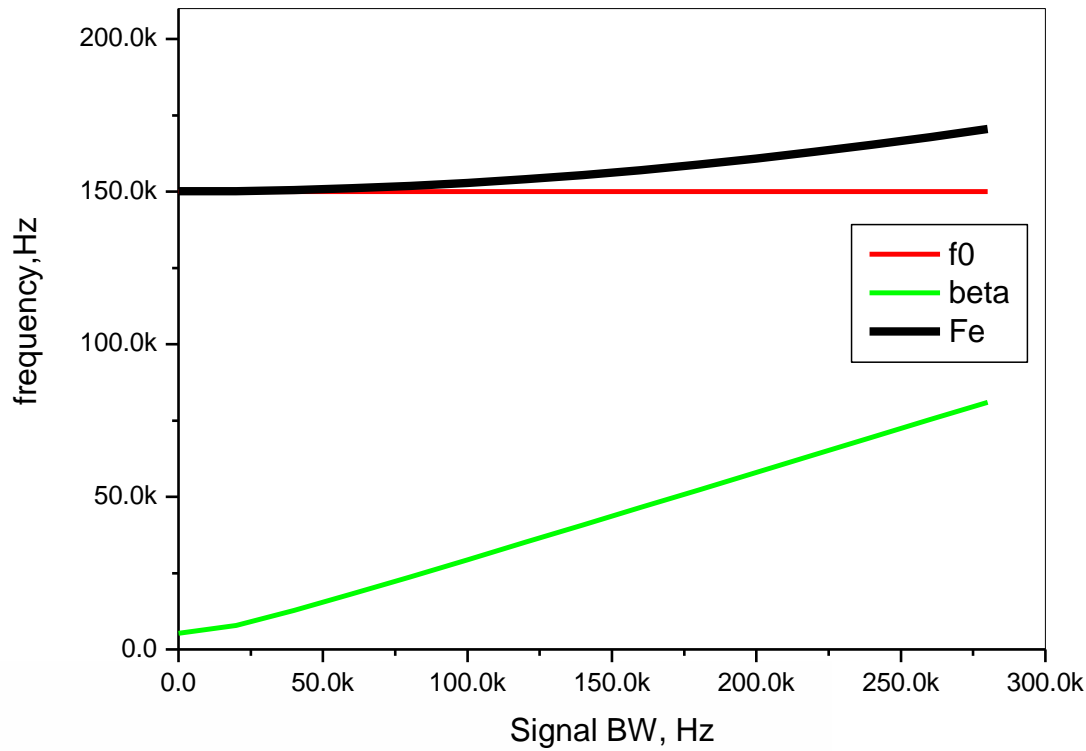
$$SNR = \frac{2E}{N_0}$$

Priimto signalo energija

Triukšmo galios spektrinė tankis

$$E = \frac{1}{Z_{ADC}} \int_{-\infty}^{\infty} |s(t)|^2 dt = \frac{2}{Z_{ADC}} \int_0^{\infty} |S(f)|^2 df$$

# fe,F0,B spectrum



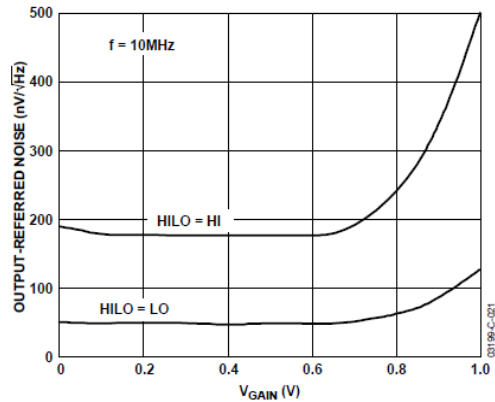
Gaubtinės juostos plotis

$$F_e^2 = f_0^2 + \beta^2 = \frac{\left[ \int_{-\infty}^{\infty} f |S(f)|^2 df \right]^2}{E^2} + \frac{\int_{-\infty}^{\infty} (f - f_0)^2 |S(f)|^2 df}{E}$$

# Noise augmentation for digital domain

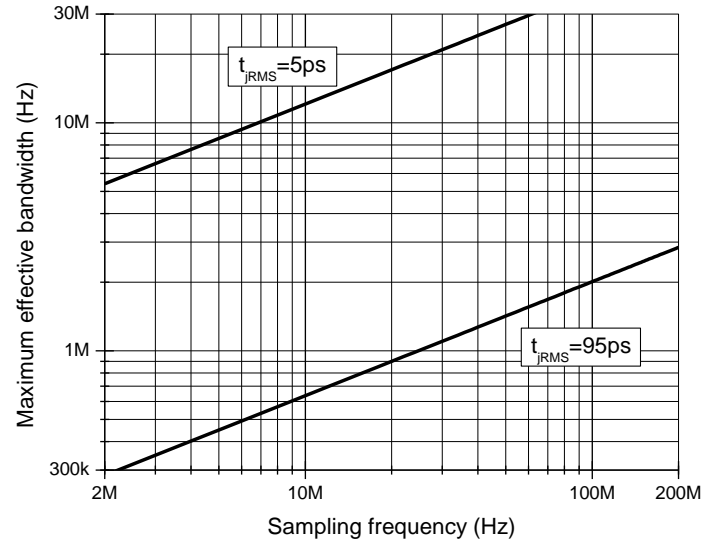
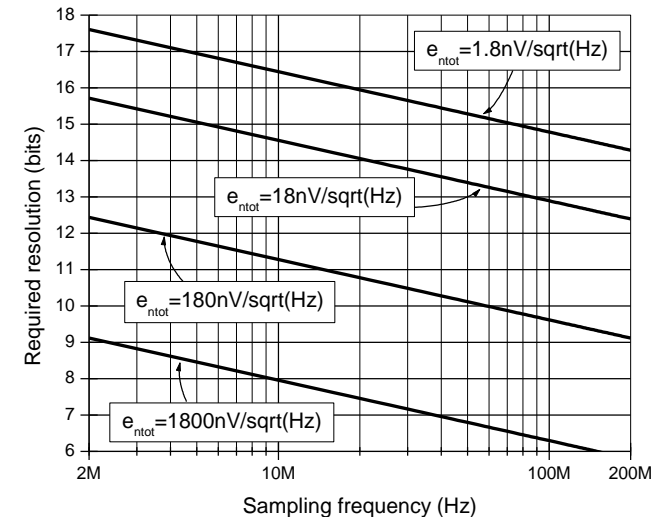


$$N_0 = N_{0A} + N_{0Q} + N_{0J}$$

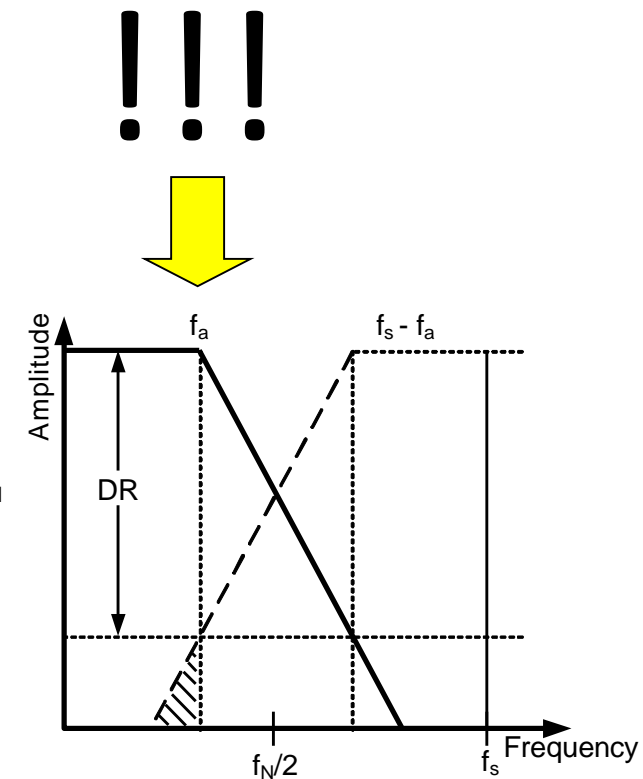
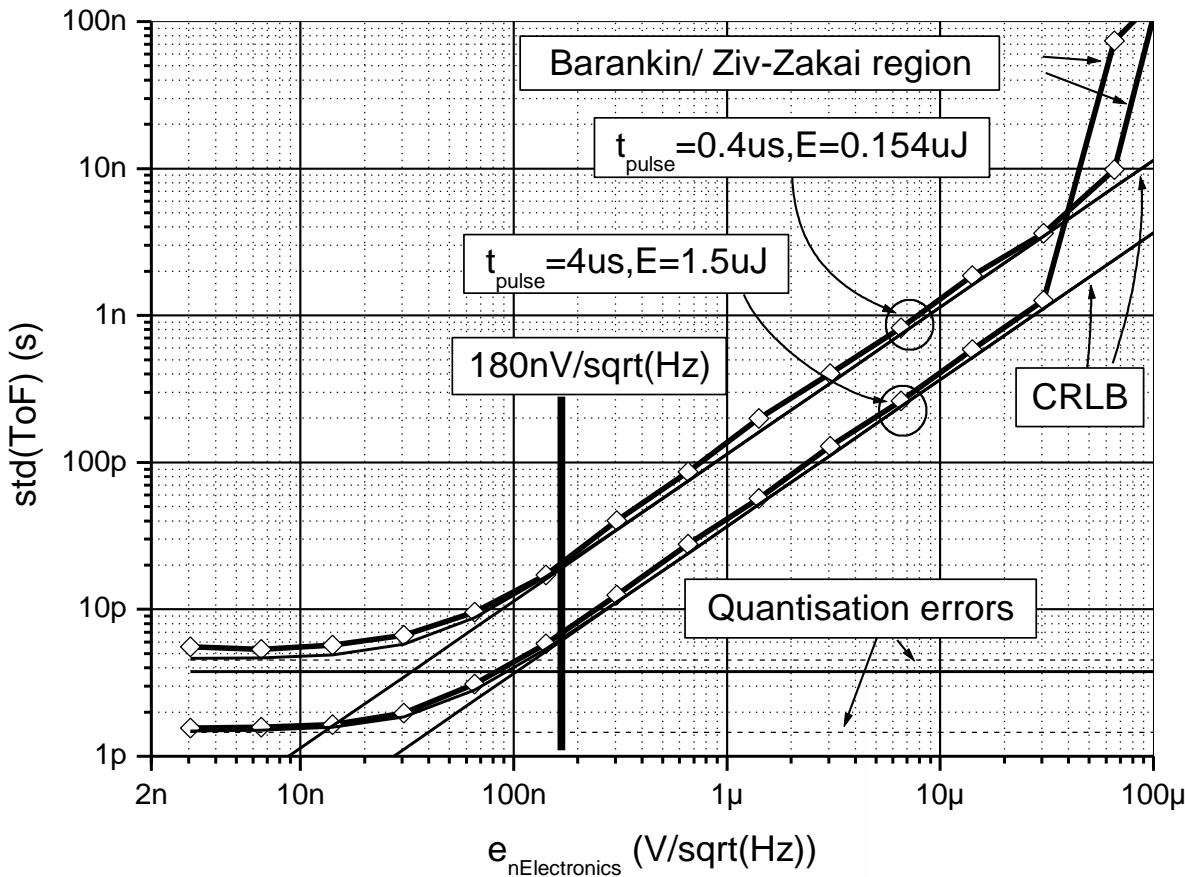


$$N_{0Q} = \frac{e_{nQ}^2}{Z_T} = \frac{V_{\text{ref}}^2}{2^{2\cdot\text{bits}} 12 \cdot Z_T}$$

$$N_{0J} = \frac{e_{nJ}^2}{Z_T} = \frac{(V_{\text{sigRMS}} \cdot 2\pi \cdot F_e \cdot t_J)^2}{0.5 f_s \cdot Z_T}$$



# Noise augmentation for digital domain

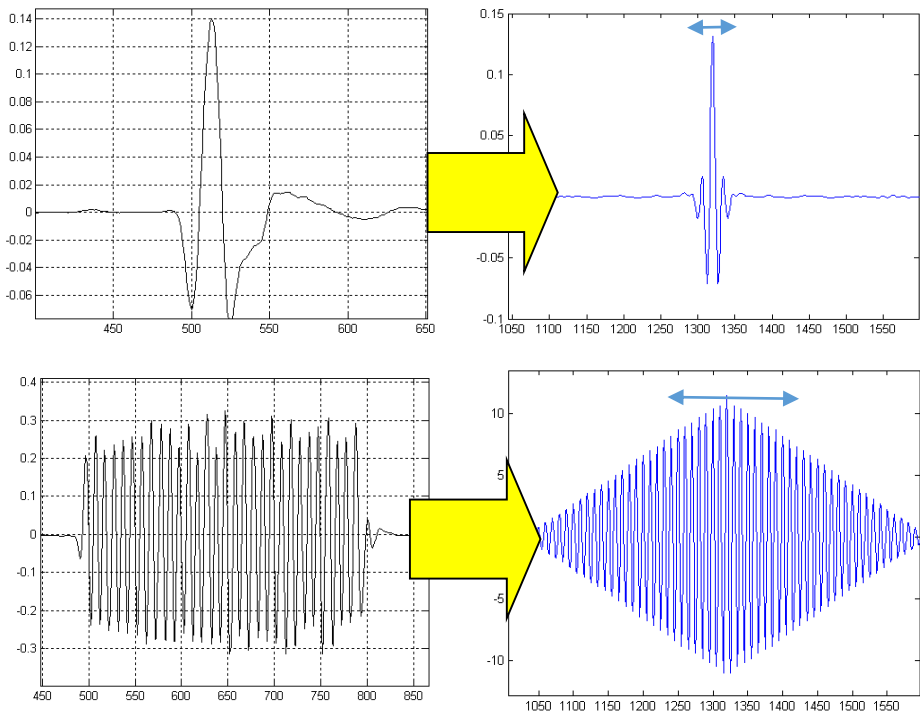
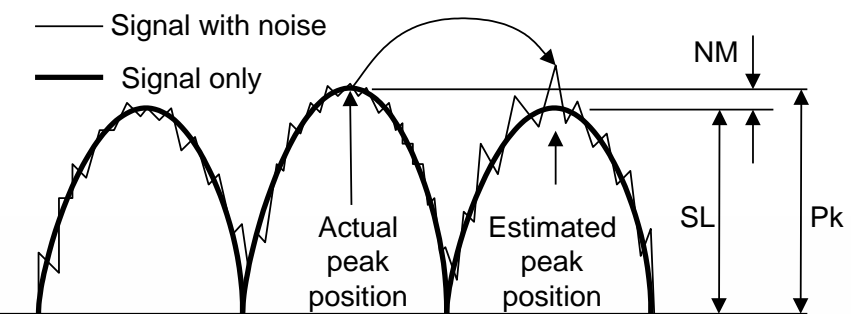


$$N_0 = N_{0A} + N_{0Q} + N_{0J}$$

# TOF random errors: full bound

- CRLB: Cramer-Rao lower bound

$$\sigma_{ToF} \geq \frac{1}{2\pi F_e \sqrt{\frac{2E}{N_0}}}$$

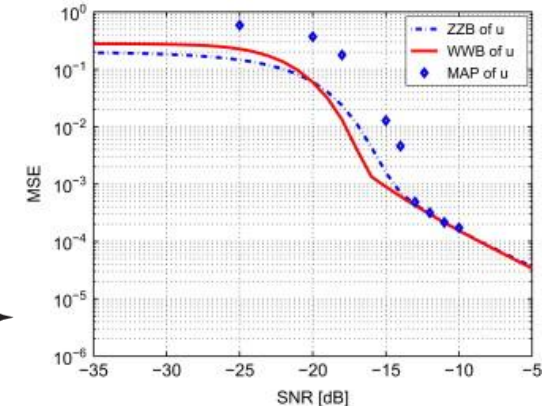
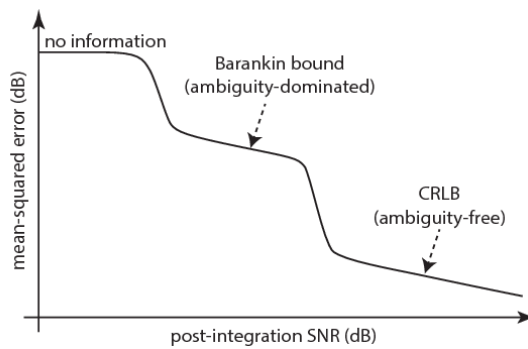
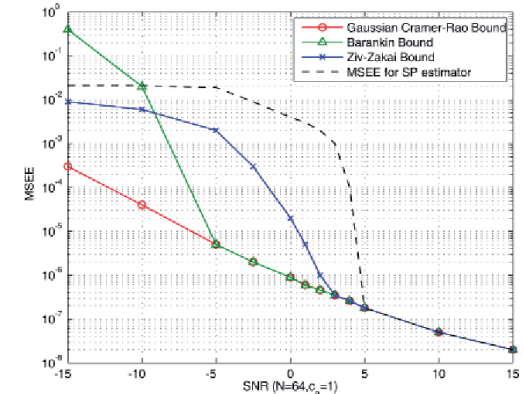
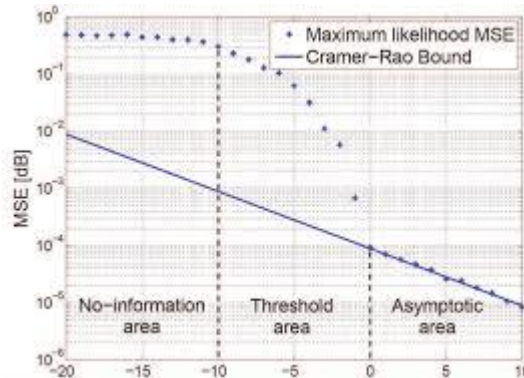
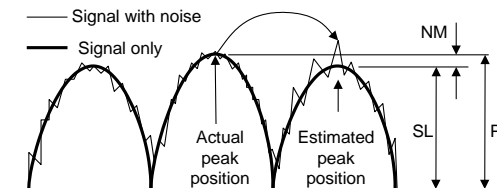


# ToF random errors: full bound

- CRLB: Cramer-Rao lower bound

$$\sigma_{ToF} \geq \frac{1}{2\pi F_e \sqrt{\frac{2E}{N_0}}}$$

- Barankin (1949) bound
- Ziv-Zakai (1969) bound
- Weiss-Weinstein (1982) bound



E. W. Barankin, "Locally best unbiased estimates," Ann. Math. Statist., pp. 477-501, 1949

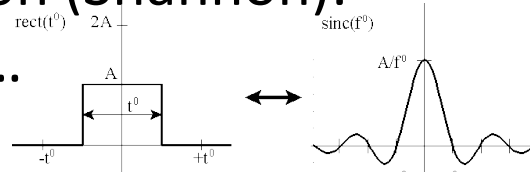
J. Ziv and M. Zakai, "Some lower bounds on signal parameter estimation," IEEE Trans. Inform. Theory, vol. IT-15, pp. 386-391, 1969.

A. J. Weiss and E. Weinstein, "Composite bound on the attainable mean square error in passive time-delay estimation from ambiguity prone signal," IEEE Trans. Inform. Theory, vol. IT-28, pp. 977-979, Nov. 1982.

# Subsample ToF: interpolation

ToF errors can be less than  $T_{\text{sampl}}$

Ideal reconstruction (Shannon):  
*sinc* function, but...



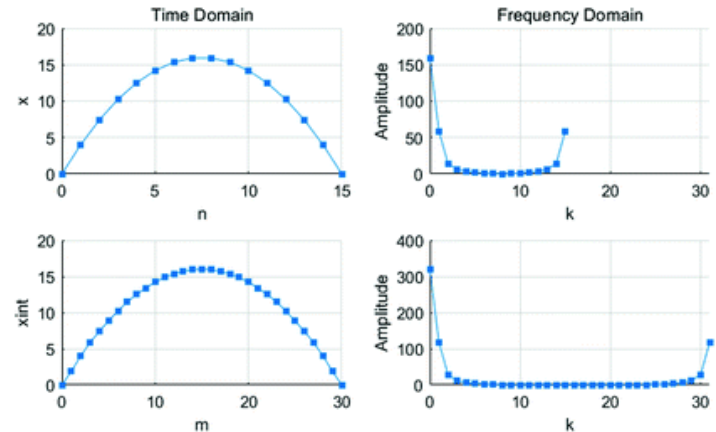
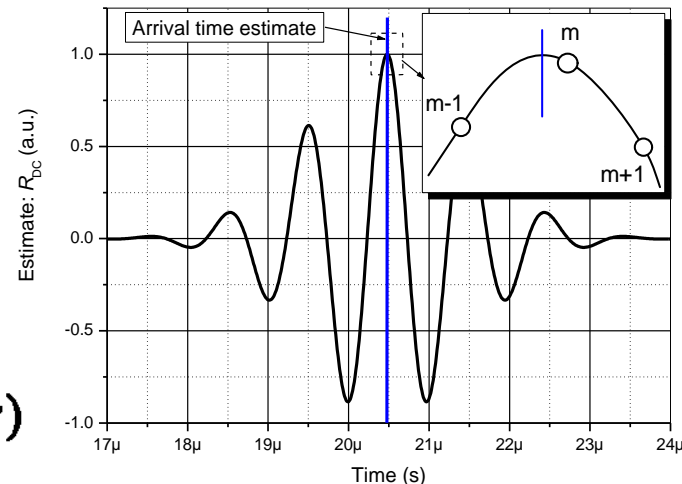
## 1. Truncated *sinc* (Cespedes)

$$x(t) = \sum_{n=-N_s/2}^{N_s} x(n) \operatorname{sinc} \left[ \pi(t - nT_s) / T_s \right] w_h((t - nT_s) / T_s)$$

## 2. Zero-padding

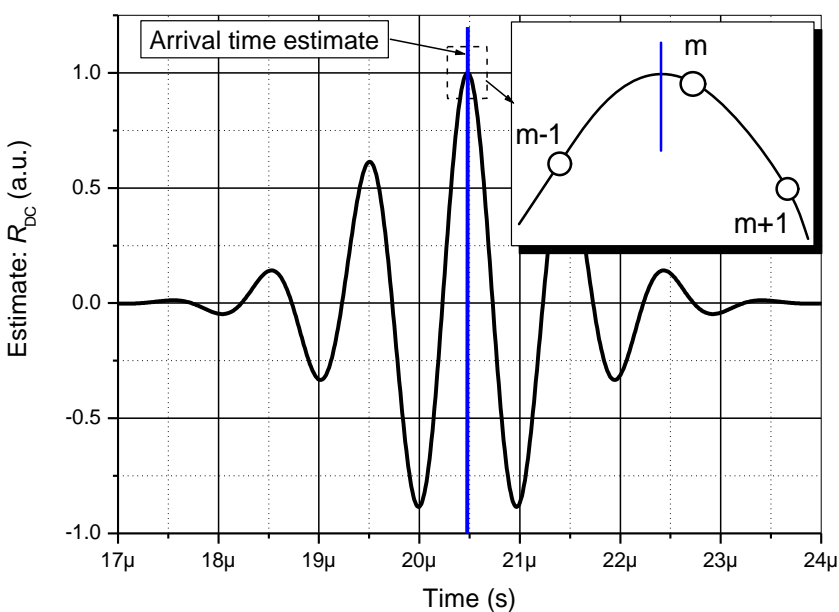
$$\hat{R}_{xy}(\tau) = IFT \{ X(\omega_k) \times Y^*(\omega_k) \},$$

## 3. Iterative subsample shift



- I. Cespedes, et al. 'Methods for estimation of subsample time delays of digitized echo signals', Ultrason. Imag., 1995.
- C.A. Teixeira et al. 'A method for sub-sample computation of time displacements between discrete signals based only on discrete correlation sequences' Biomedical Signal Processing and Control, 2017

# Subsample ToF: interpolation



$$\Delta ToF_p = -\frac{b}{2af_s} = \frac{x_{m-1} - x_{m+1}}{2f_s(x_{m-1} - 2x_m + x_{m+1})}$$

$$\Delta ToF_G = -\frac{c}{f_s} = \frac{\ln(x_{m+1}) - \ln(x_{m-1})}{f_s(4\ln(x_m) - 2\ln(x_{m-1}) - 2\ln(x_{m+1}))}$$

$$\Delta ToF_{FFT\phi}^w = \frac{\sum_{m=1}^M \varphi(X^0_m) \cdot |X^0_m|^2}{M \sum_1^M |X^0_m|^2}$$

Matlab depository: [GetTOFcos](#), [GetTOFfftPhase](#)

<https://www.mathworks.com/matlabcentral/fileexchange/65229-gettofcos-mysignal-refsignal>

$$\Delta ToF_{\cos} = -\frac{\theta}{f_s \omega_0}, \omega_0 = \arccos\left(\frac{x_{m-1} + x_{m+1}}{2x_m}\right), \theta = \arctan\left(\frac{x_{m-1} - x_{m+1}}{2x_m \sin \omega_0}\right)$$

R.E.Boucher, J.C.Hassab, 'Analysis of discrete implementation of generalized cross correlator', IEEE TASSP, 1981

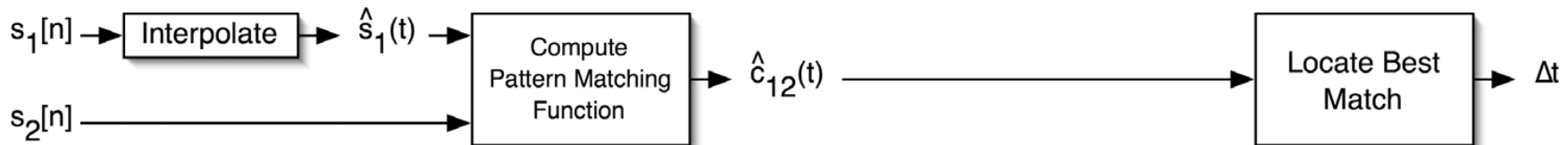
L.Zhang, 'On the application of cross correlation function to subsample discrete time delay estimation', DSP, 2006

Z. Zhao, Z. Q. Hou, 'The generalized phase spectrum method for time delay estimation' Acta Acustica, 1985

PGM de Jong, et al., 'Determination of tissue motion velocity by correlation interpolation of pulsed ultrasonic echo signals' Ultrason. Imag., 1990.

I. Cespedes, et al. 'Methods for estimation of subsample time delays of digitized echo signals', Ultrason. Imag., 1995

# Interpolation: spline

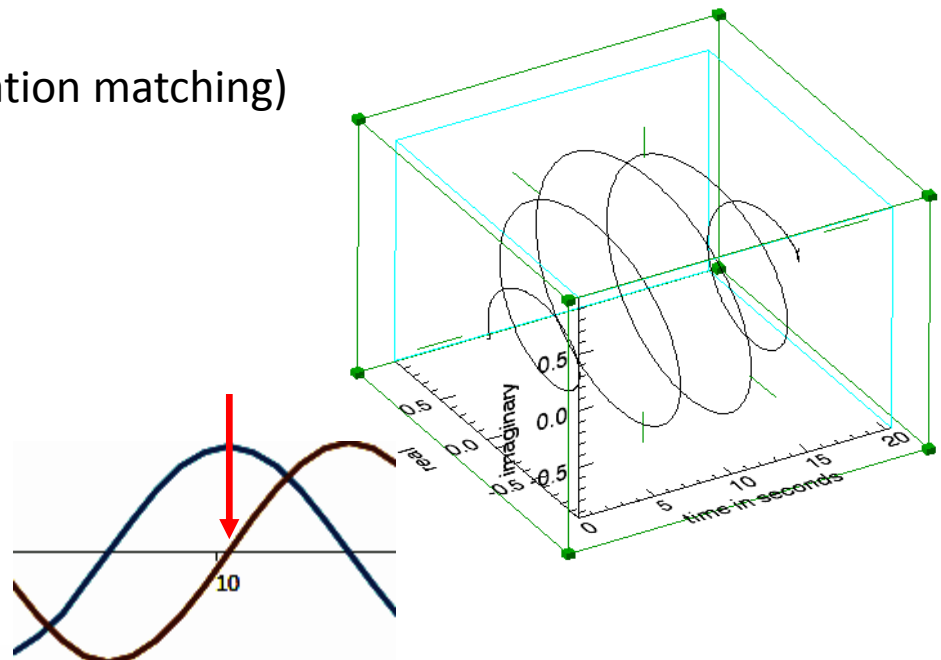
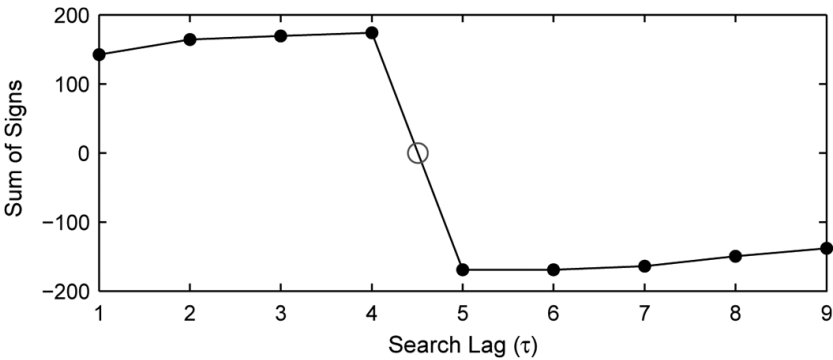


Use splines to produce a continuous time representation of the reference signal.  
Then input to xcorr with the discrete measured signal.  
Yields an analytical function => continuous time-delay estimate.

$$\sigma(\Delta t - \hat{\Delta}t) \geq \sqrt{\frac{3}{2f_o^3 \pi^2 T (B^3 + 12B)} \left( \frac{1}{\rho^2} \left( 1 + \frac{1}{SNR^2} \right)^2 - 1 \right)}$$

# Other interpolation techniques

- Linear approximation at zero crossing of binary correlation [Shaswary ]
- Imaginary part of correlation function obtained by Hilbert transform [Grennberg]
- All-pass filter
- MSX and MXS (auto- and cross-correlation matching)



$$s_R(t) = s_T(t - \Delta t) = IDFT(DFT(s_T) \cdot e^{\omega_m \Delta t})$$

E. Shaswary et al, 'A New Algorithm for Time-Delay Estimation in Ultrasonic Echo Signals' IEEE TUFFC, 2015

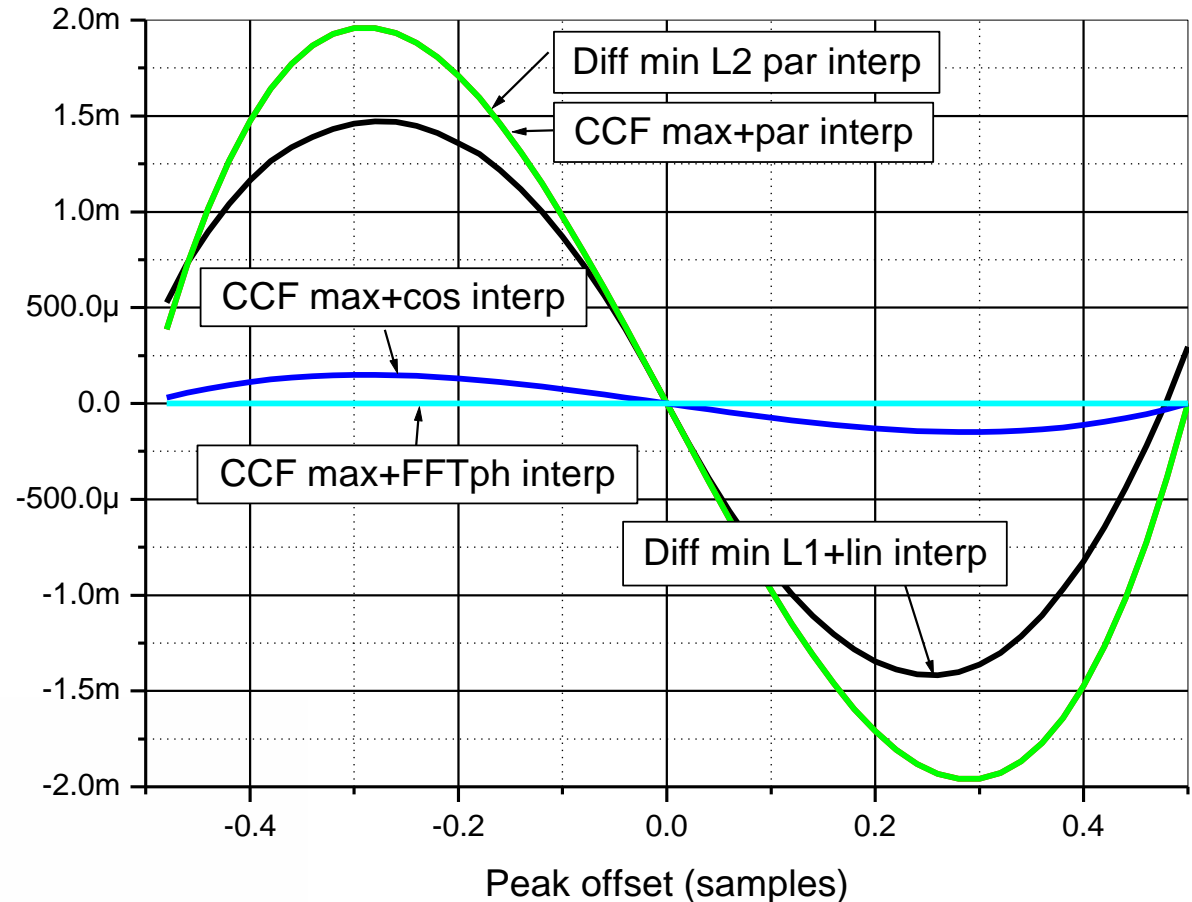
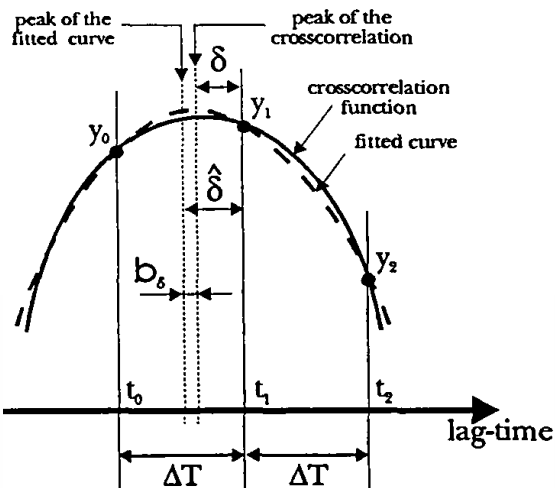
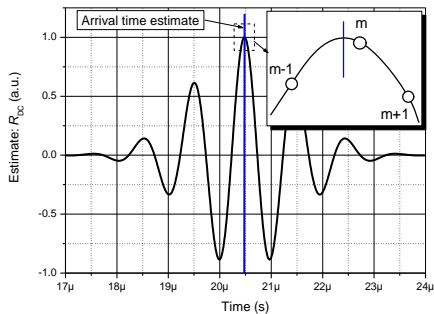
A. Grennberg, M. Sandell, 'Estimation of subsample time delay differences in narrow-band ultrasonic echoes using the Hilbert transform correlation' IEEE TUFFC, 1994

S.Hirata, et al. 'Cross-correlation by single-bit signal processing for ultrasonic distance measurement' IEICE TFECCS, 2008

S.Tanaka, 'A Model-Based Adaptive Algorithm for Determination of Time-of-Flight in Ultrasonic Measurement' SICE 1997

A.K. Nandi, 'On the Subsample Time Delay Estimation of Narrowband Ultrasonic Echoes', TUFFC 1995

# Bias error: interpolation

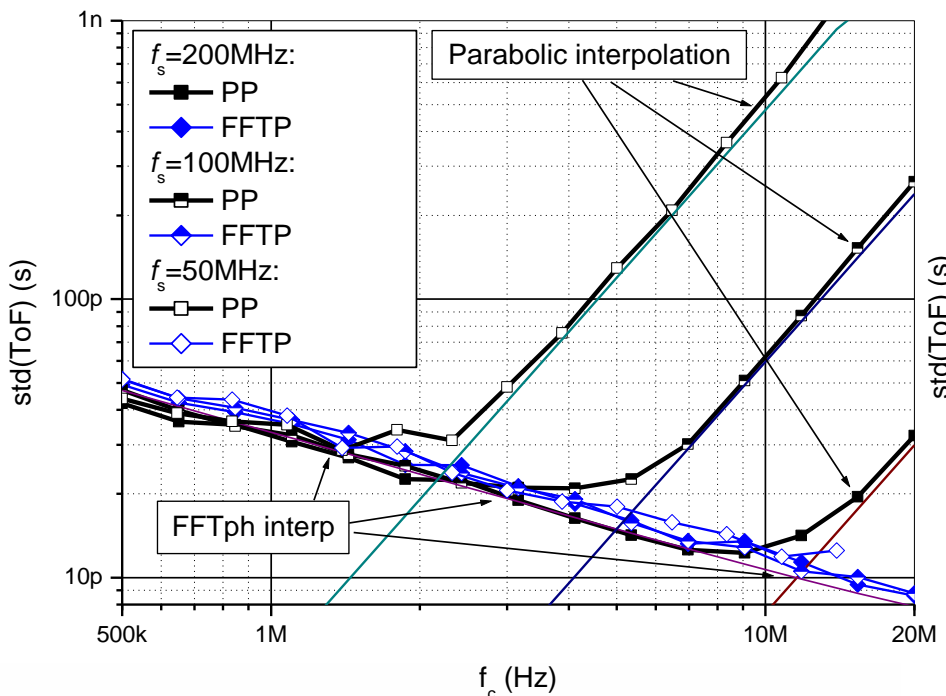


L.Svilainis, et al. 'Subsample interpolation bias error in time of flight estimation by direct correlation in digital domain'. Measurement, 2013

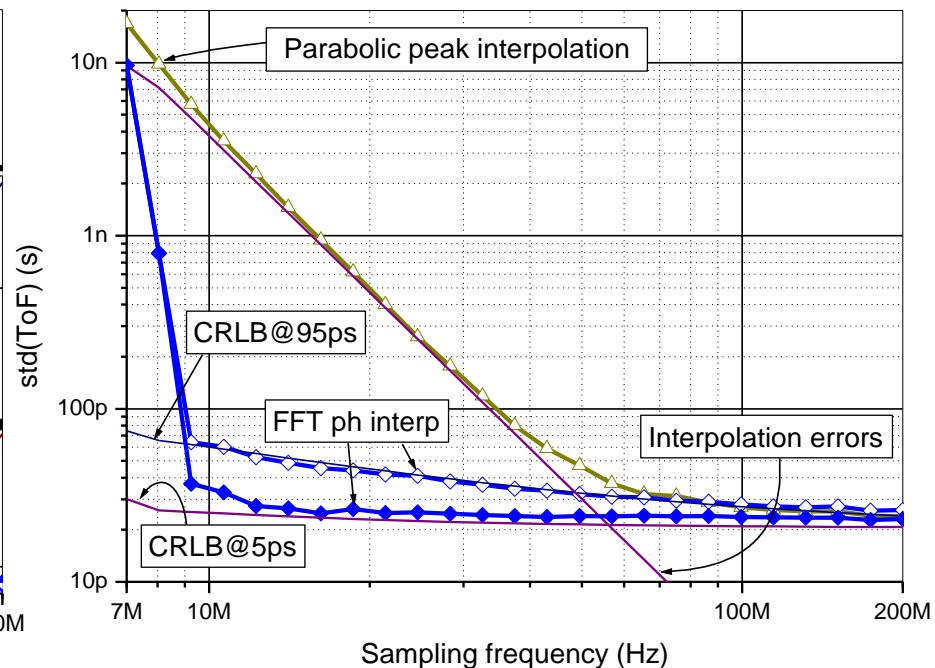
J.F.S. Costa-Júnior, 'Measuring uncertainty of ultrasonic longitudinal phase velocity estimation using different time-delay estimation methods based on cross-correlation: Computational simulation and experiments', Measurement 2018

S. R. Dooley, A. K. Nandi, 'Comparison of discrete subsample time delay estimation methods applied to narrowband signals' MST, 1998

# Bias errors: interpolation



Center frequency influence



Sampling frequency influence

# Bias errors: interpolation

Maximum error amplitude can be predicted

$$\max[\varepsilon(ToF_c)] = \sqrt{\pi} \frac{\beta^2}{f_s^3}$$

$$\max[\varepsilon(ToF_p)] = \sqrt{\pi} \frac{\beta^2}{f_s^3} + \frac{f_0^2}{\sqrt{2} f_s^3} = \max[\varepsilon(ToF_c)] + \frac{f_0^2}{\sqrt{2} f_s^3}$$

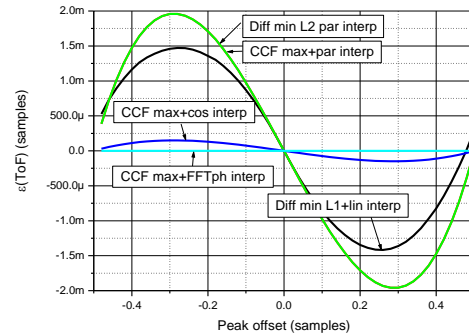
- no centre frequency influence on bias errors of cosine interpolation;
- bias error for cosine interpolation is defined by envelope bandwidth and sampling freq.;
- for parabolic interp., bias error is defined mostly by centre frequency and sampling freq.;
- sampling frequency has essential influence on interpolation bias error ( $1/f_s^3$ ).

Minimum necessary sampling frequency can be derived

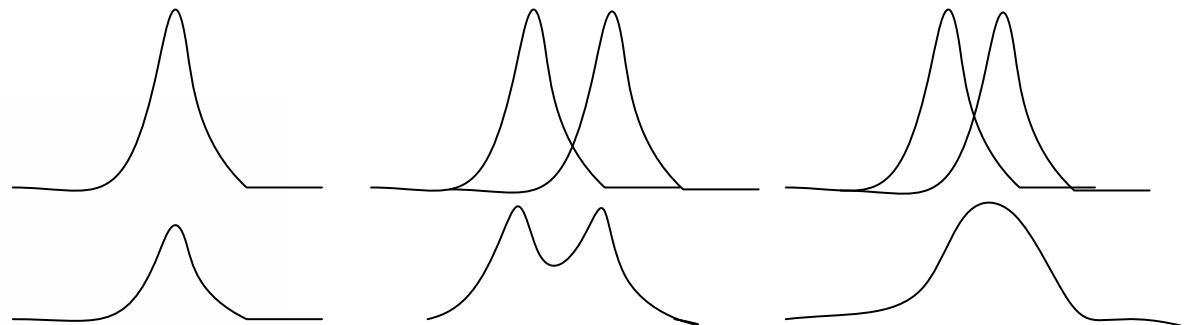
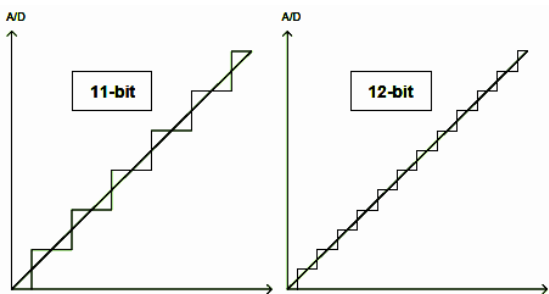
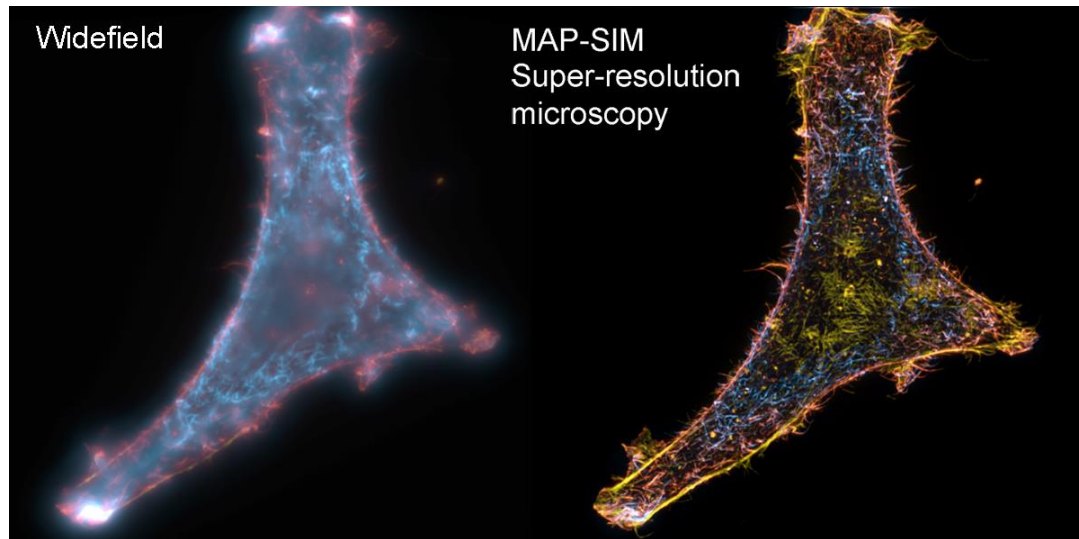
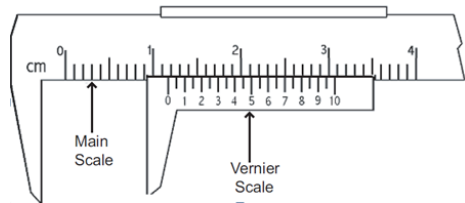
$$f_{s\_min\_cos} \geq \sqrt[3]{\sqrt{18\pi^3} \cdot \beta^2 F_e \sqrt{SNR}}$$

$$f_{s\_min\_par} \geq \sqrt[3]{3\pi \cdot (f_0^2 + \sqrt{2\pi}\beta^2) F_e \sqrt{SNR}}$$

L.Svilainis, et al. 'Subsample interpolation bias error in time of flight estimation by direct correlation in digital domain'. Measurement, 2013

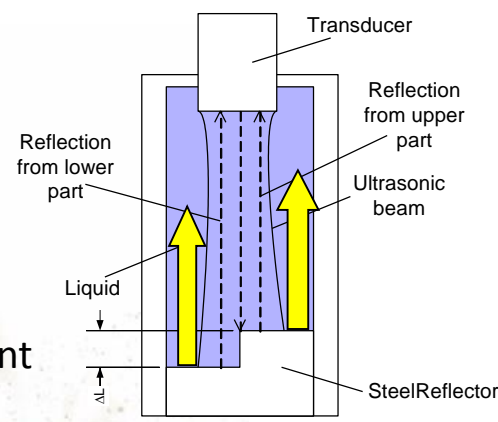
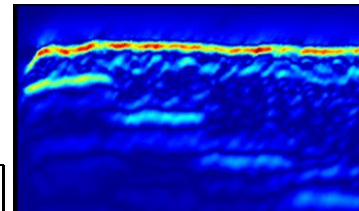
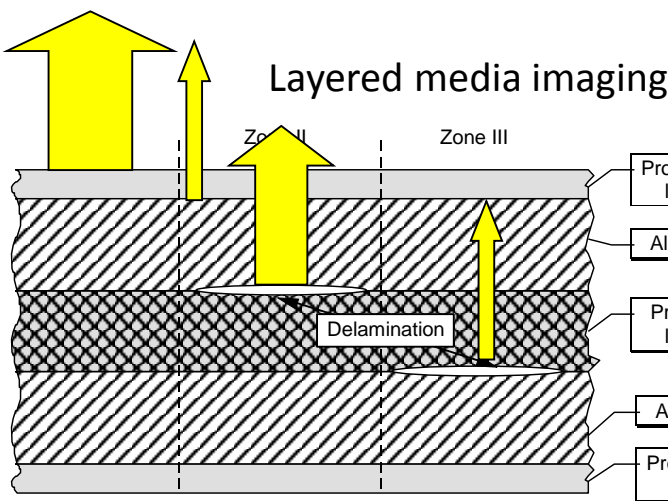


# Resolution

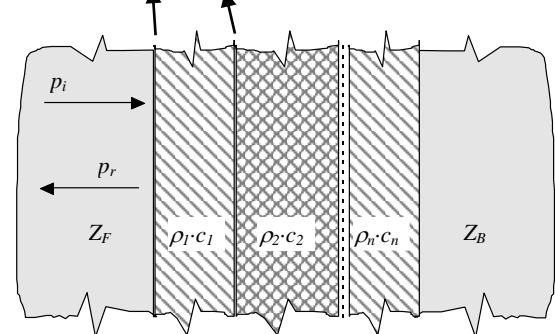
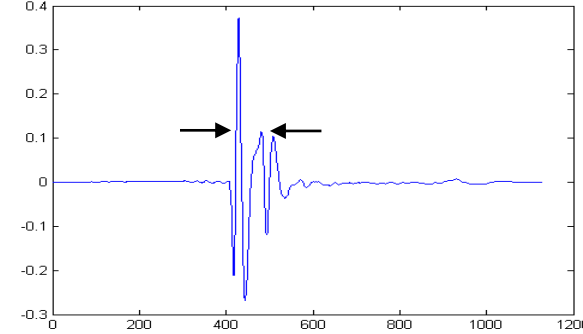
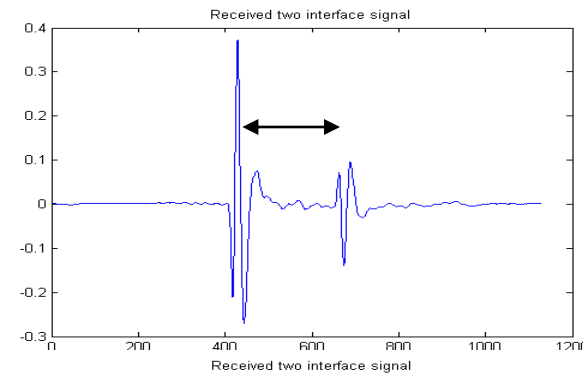


# Multiple reflections: resolution

- Multiple reflections overlap.

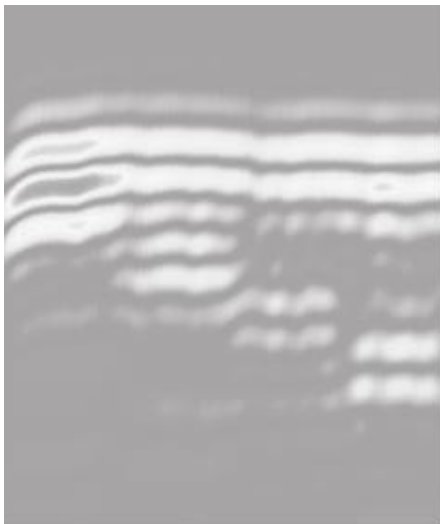


- Ultrasound Velocity measurement using dual reflection

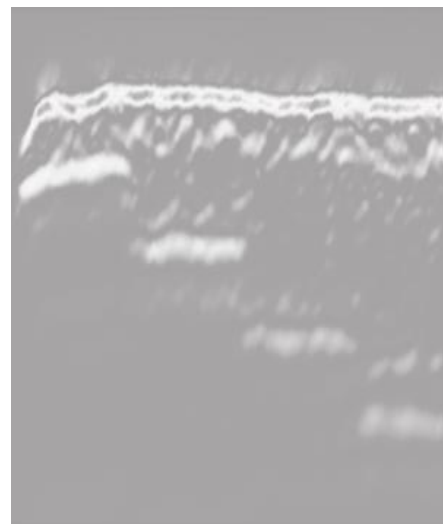


# Resolution: signal bandwidth limitation

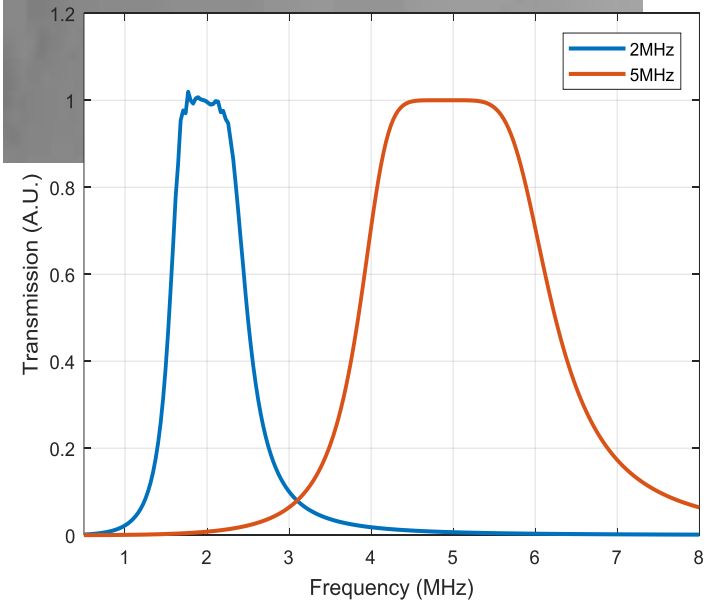
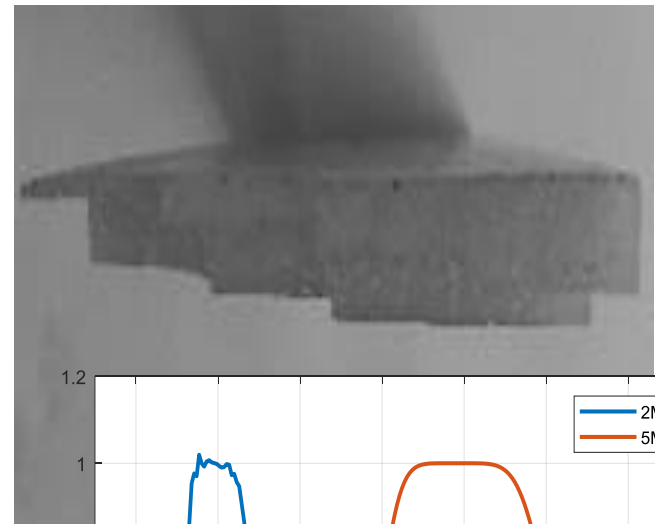
- Wider bandwidth=better resolution,
- Higher frequency~better resolution.



$F_c=2\text{MHz}$

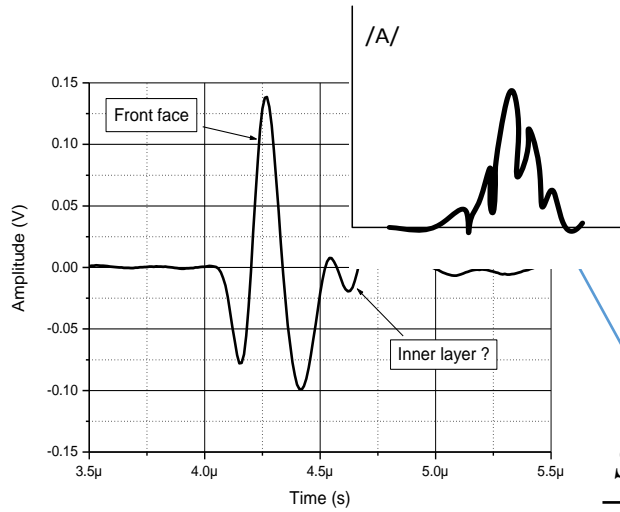


vs.  $5\text{MHz}$

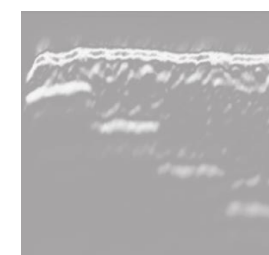
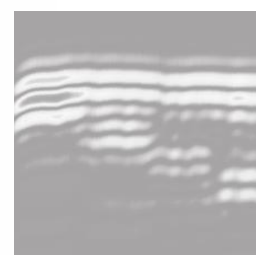
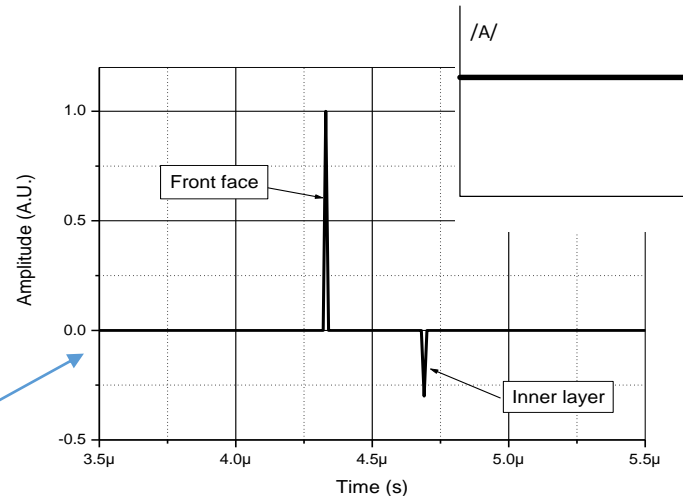
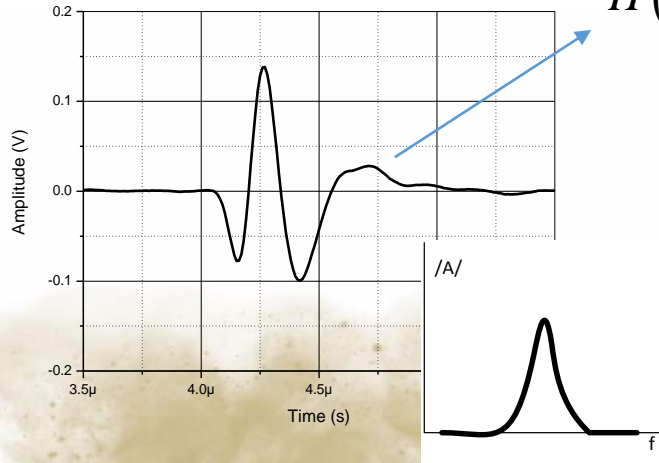


# Solution: loss compensation=deconvolution

- Losses=limited bandwidth,
- Loss compensation= wider bandwidth=better resolution.

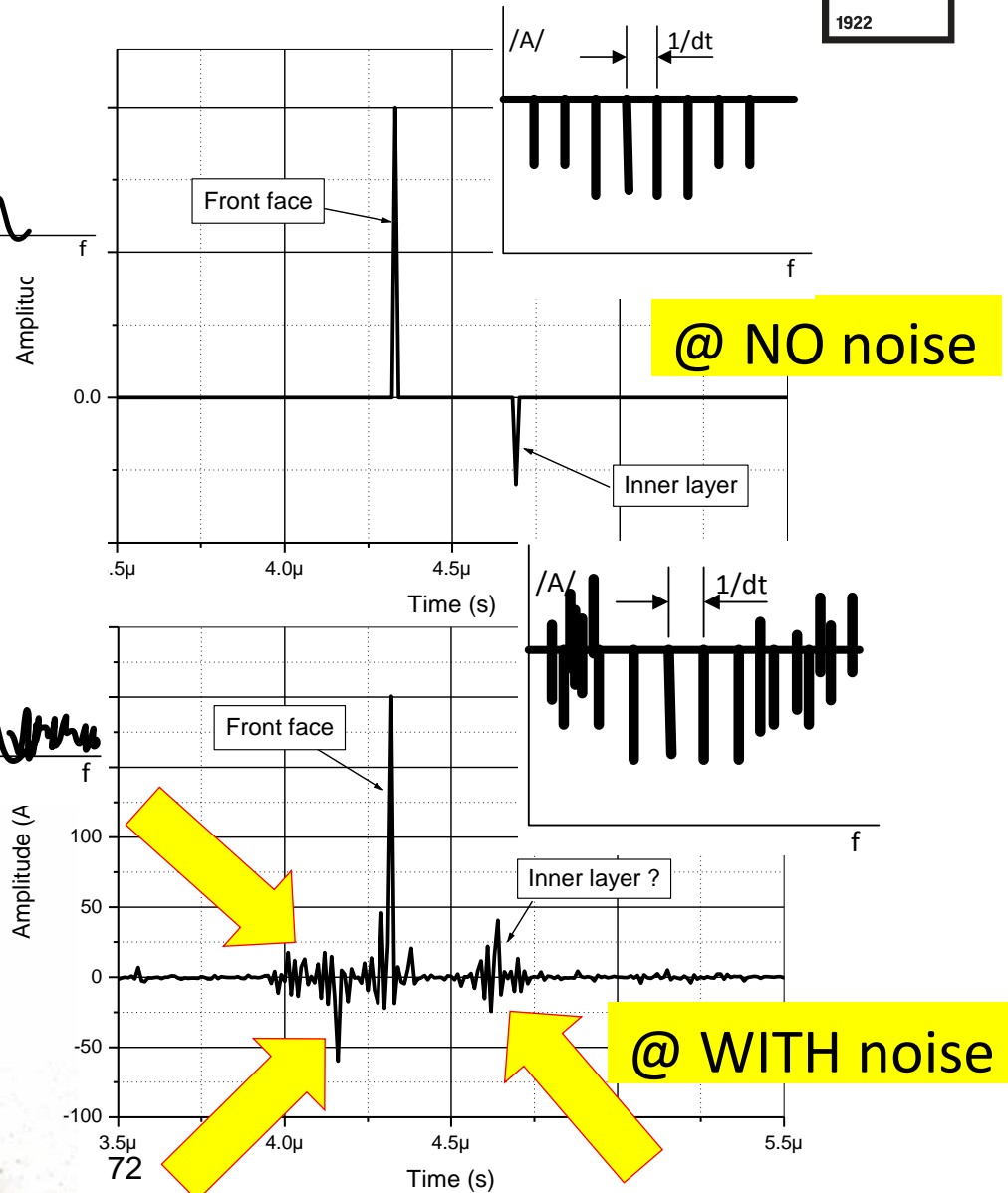
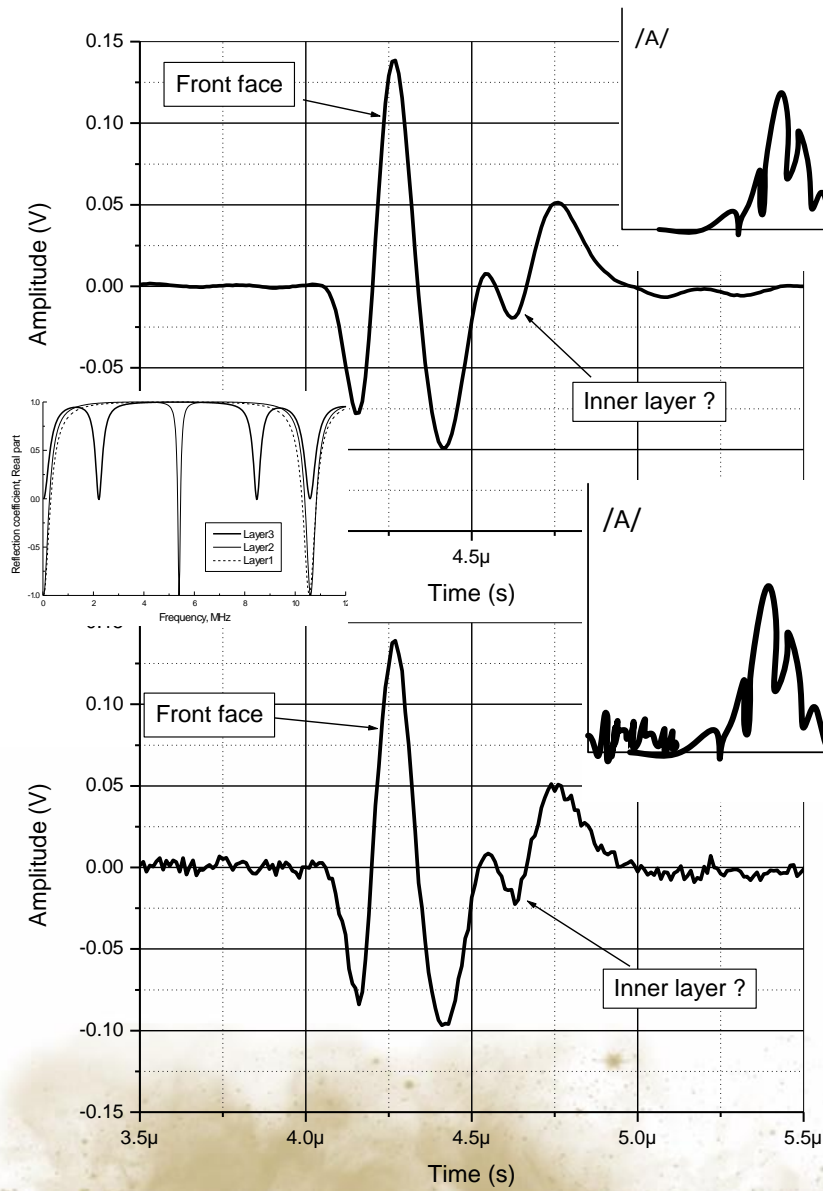


$$\frac{S(f)}{H(f)} = S_{cmp}(f)$$



$F_c=2\text{MHz}$  to  $5\text{MHz}$  or even more

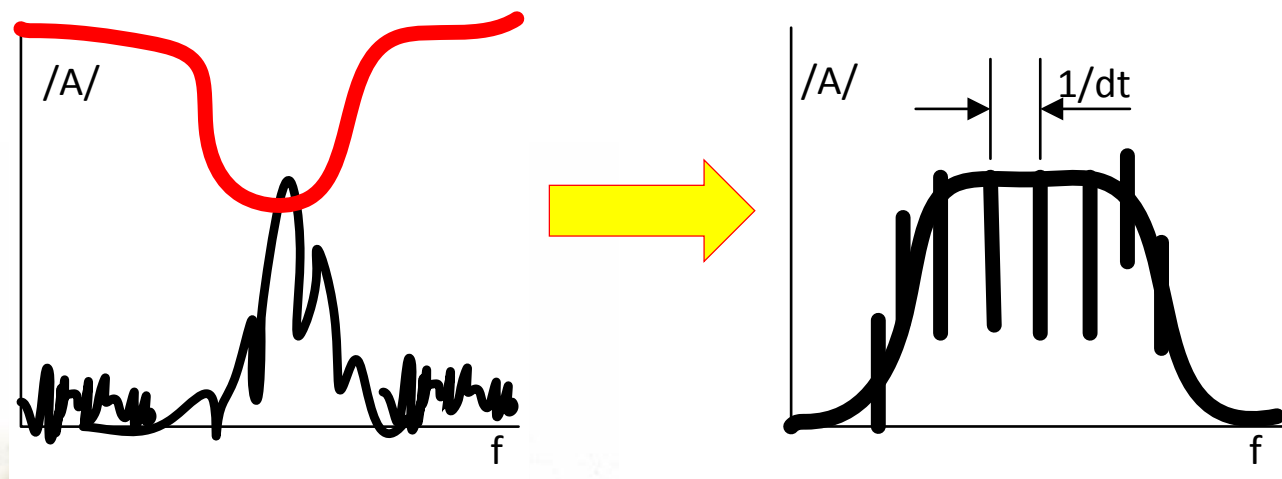
# Loss compensation: deconvolution @ noise



# Loss compensation @ noise: wiener filter

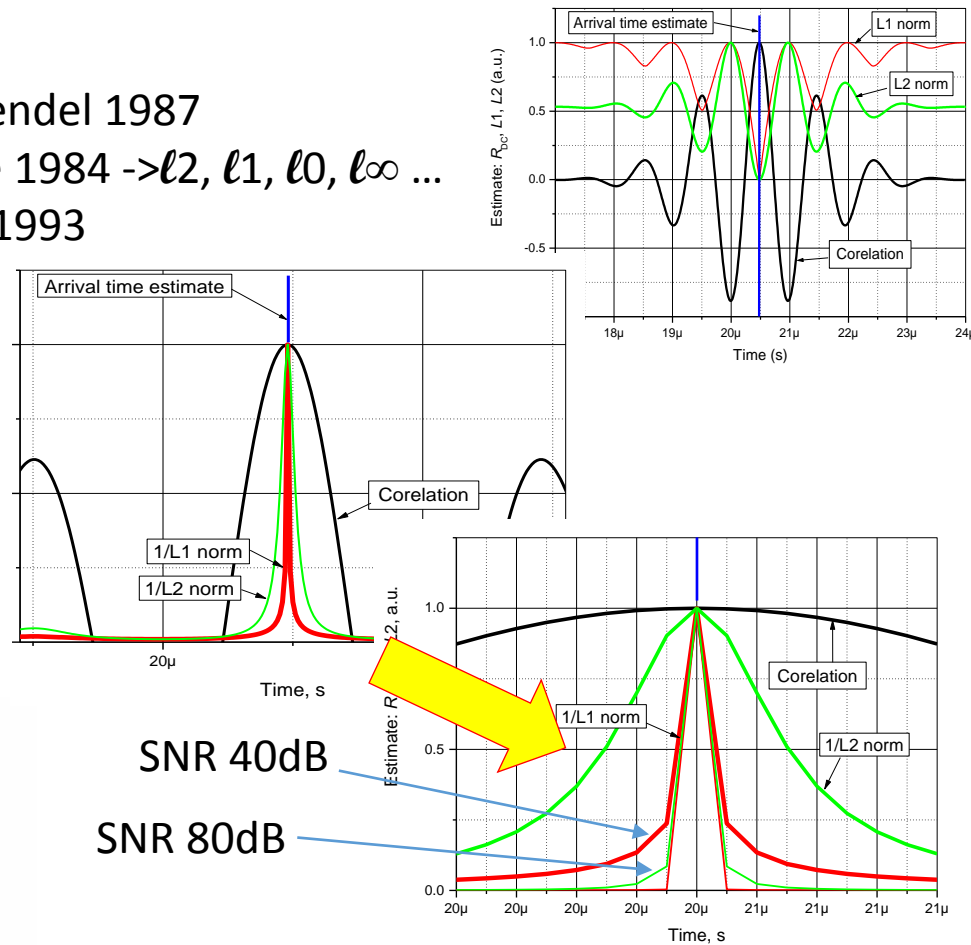
$$\frac{S(f)}{H(f)} = S_{cmp}(f)$$

$$\frac{H^*(f)S(f)}{|H(f)|^2 S(f) + N(f)} = \frac{1}{H(f)} \left[ \frac{|H(f)|^2}{|H(f)|^2 + \frac{N(f)}{S(f)}} \right] = \frac{1}{H(f)} \left[ \frac{|H(f)|^2}{|H(f)|^2 + \frac{1}{SNR(f)}} \right]$$



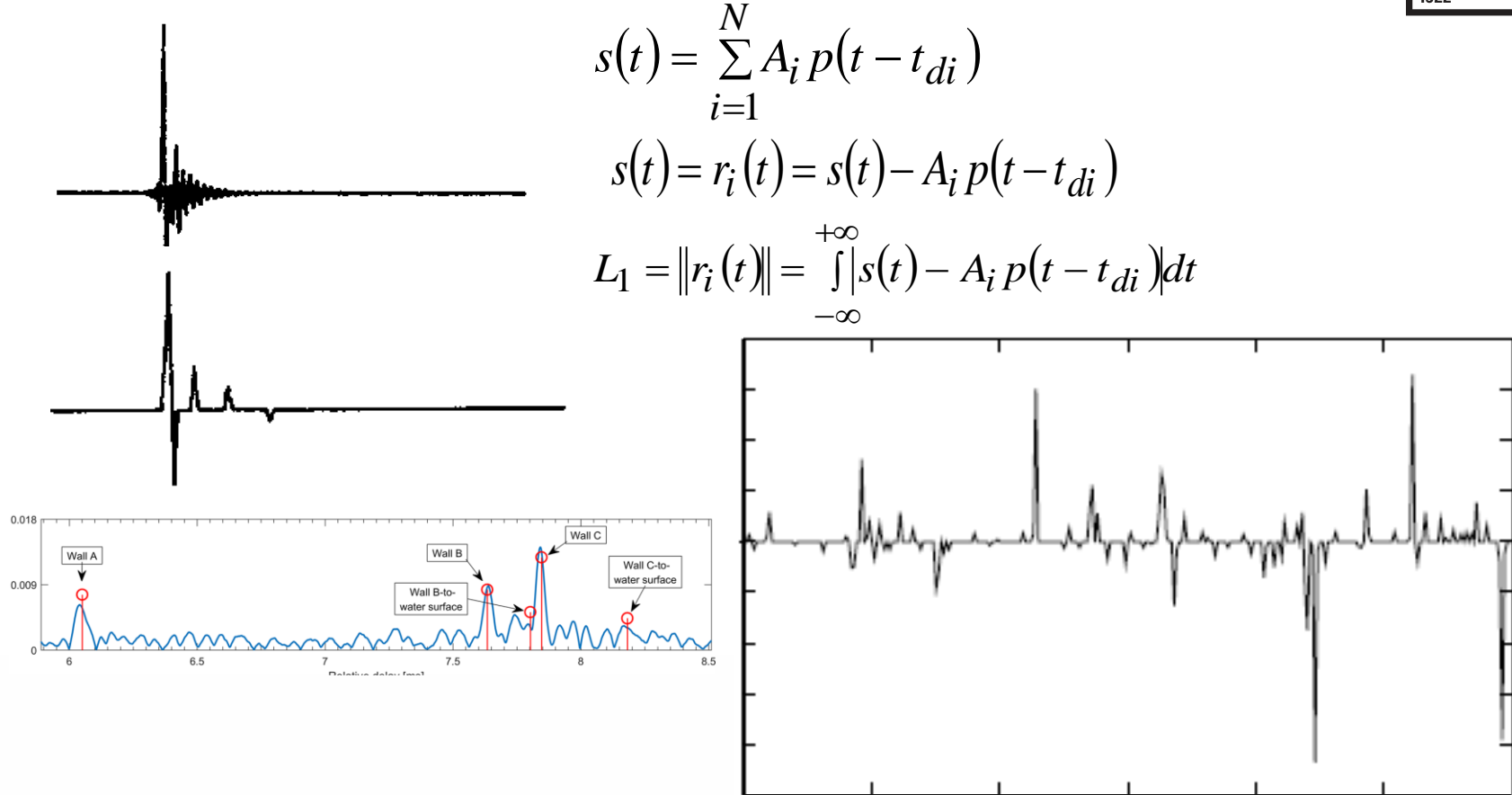
# Better solution: iterative deconvolution

- Wiener 1960
- Spectral extrapolation Burg alg. 1980
- Minimum variance deconvolution, Mendel 1987
- Iterative deconvolution, Zala Barodale 1984 -> $\ell_2, \ell_1, \ell_0, \ell_\infty \dots$
- Matching pursuit (MP), Mallat Zhang 1993
- Orthogonal MP, Patte Razzaifar 1993
- Basis Pursuit, Chen Donoho 1994
- Method of frames, Wang 1997  $\min \ell_2$
- Best ortho basis, Donoho 1997
- Support MP, E.Mor, Azoulay 2010
- Gradient pursuit
- Greedy Basis pursuit, LASSO
- Sparse deconvolution
- Iterated window maximization
- Genetic optimization
- Adaptive deconvolution



Wiener N. The interpolation, extrapolation and smoothing of stationary time series. Report of the Services 19, MIT, 1942.  
 Chen S.S.B., Donoho D.L., Saunders M.A. Atomic decomposition by basis pursuit. SIAM Review, 2001.  
 Guo J., Xin Y., Reconstructing outside pass-band data to improve time resolution in ultrasonic detection. NDT&EInt, 2012.

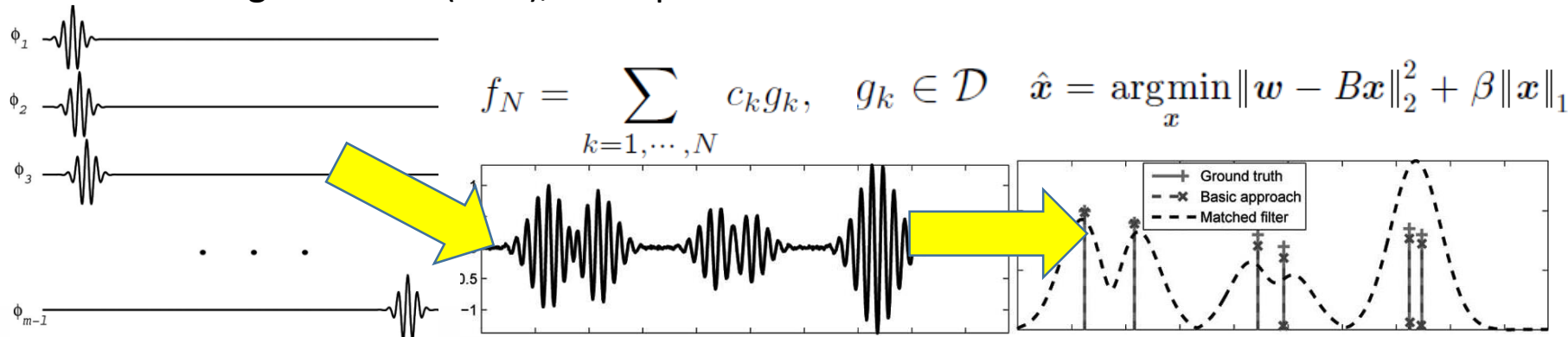
# Iterative deconvolution



Barrodale I., Zala C.A., et al. Comparison of the L1 and L2 norms applied to one-at-a-time spike extraction from seismic traces. GF, 1984.  
 Sam-Kit Sin, 'A Comparison of Deconvolution Techniques for the Ultrasonic Nondestructive Evaluation of Materials', IEEE TIP 1992  
 Yongsung Park, 'Compressive time delay estimation off the grid', JASA 2017  
 Mu Z., Plemmons R.J., Santiago P. Iterative ultrasonic signal and image deconvolution for estimation of the complex medium response. International Journal of Imaging Systems and Technology, Vol. 15, Issue 6, 2005, p. 266–277.

# Iterative deconvolution = matching pursuit

- Method of frames (MOF)
- MP (matching pursuit): greedily add non-zero coefficients to  $x$  one at a time, based on which basis vector is most correlated with the current residual.
- If D-orthogonal – OMP (Orthogonal matching pursuit)+update of all  $x$  in each iteration
- Best orthogonal basis (BOB), Basis pursuit=LASSO



G.Shi, 'Narrowband Ultrasonic Detection With High Range Resolution: Separating Echoes via Compr. Sensing and SVD' IEEE TUFFC 2012  
 Zhang G.M., Zhang C.Z., Harvey D.M. Sparse signal representation and its applications in ultrasonic NDE. Ultrasonics, 2012.

Mallat S.G., Zhang Z., Matching pursuits with time-frequency dictionaries. IEEE Transactions on Signal Processing, 1993.

Mu Z., et al. 'Iterative ultrasonic signal and image deconvolution for estimation of the complex medium response' IJIST, 2005.

E.Mor et al. 'A matching pursuit method for approximating overlapping ultrasonic echoes' IEEE TUFFC, 2010

High-resolution pursuit for detecting flaw echoes close to the material surface in ultrasonic NDT. IEEE Proc 2006

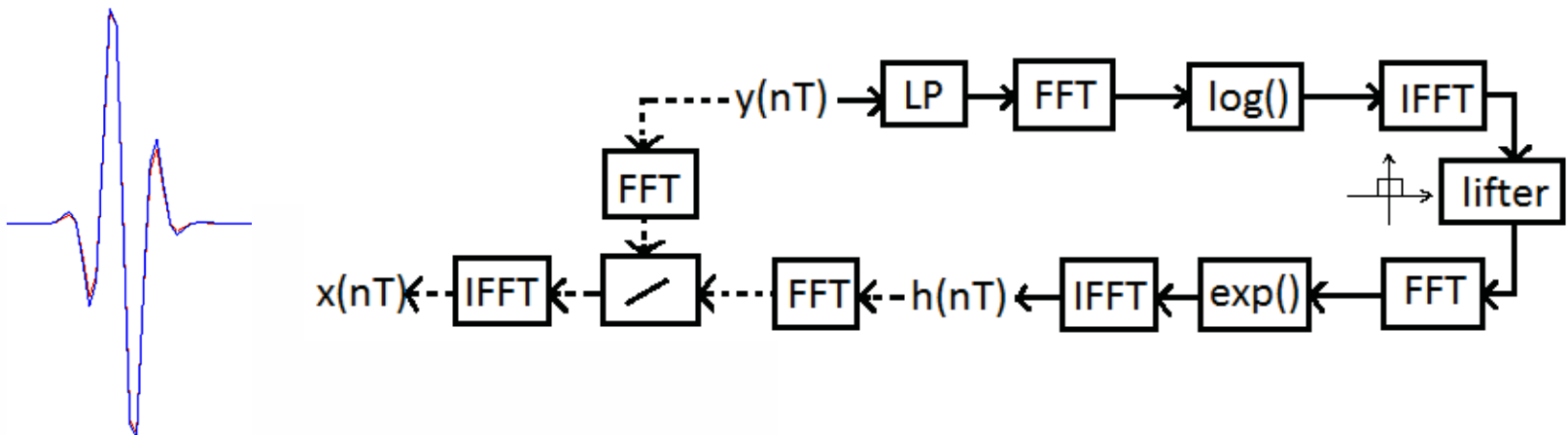
Recovery of sparse translation invariant signals with continuous basis pursuit, IEEE Trans. Signal Process. 2011,

Ruiz-Reyes, et al. High-resolution pursuit for detecting flaw echoes close to the material surface in ultrasonic NDT. 2006.

Atomic Decomposition by Basis Pursuit 2001,

# Better solution: approximate prony method (APM)

- MP is restricted to a grid for the time-shifts
- MP is greedy: it will find the most significant amplitudes just by comparison of correlations of the shifted dictionary to measured
- MP can fail in further iterations once wrong shift is assumed
- APM can detect arbitrarily distributed time-shifts
- Problem – signal model is needed, better Gabor...
- Other solution: cepstrum + adaptive reference signal (dictionary)
- Extract the reference from the measured taking first term in cepstrum.



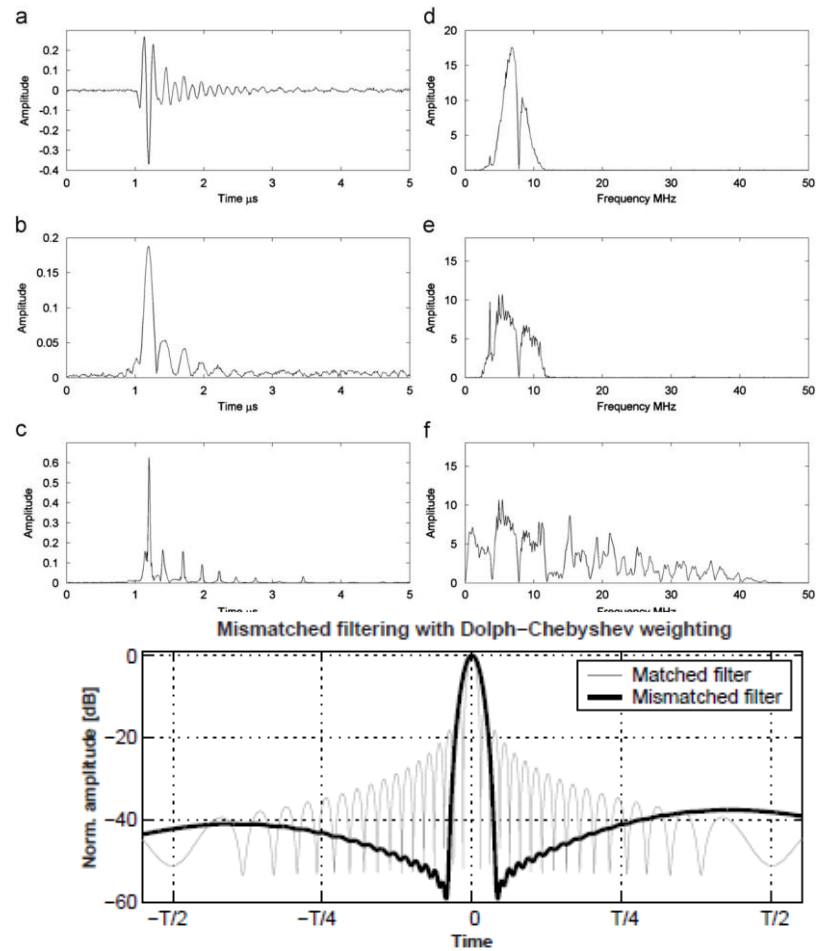
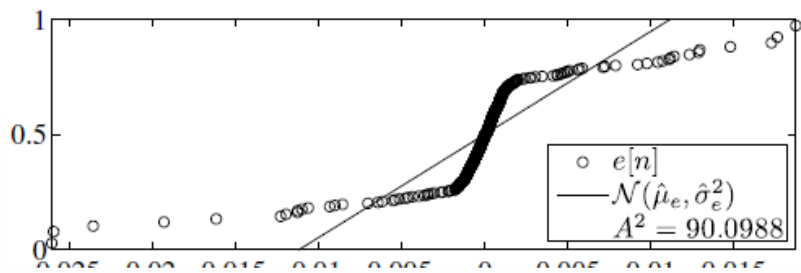
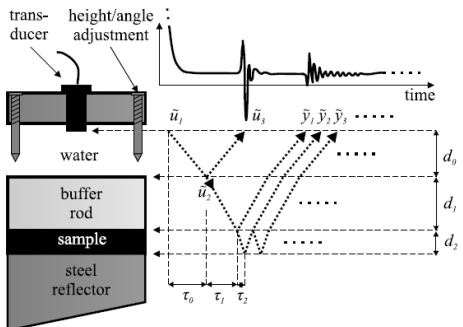
F.Boßmann, Plonka G, et al. 'Sparse deconvolution methods for ultrasonic NDT' J. Nondestruct. Eval., 2012

K.F.Kaarensen, E.Bolviken Blind Deconvolution of Ultrasonic Traces Accounting for Pulse Variance. IEEE TUFFC, 1999.

G.Cardoso, J. Saniie Ultrasonic Data Compression via Parameter Estimation. IEEE TUFFC, 2005

# Direct approach: spectra

- Autoregressive Spectral Extrapolation
- Hard+Soft modelling.
- “Decorrelation” - Mismatched filtering



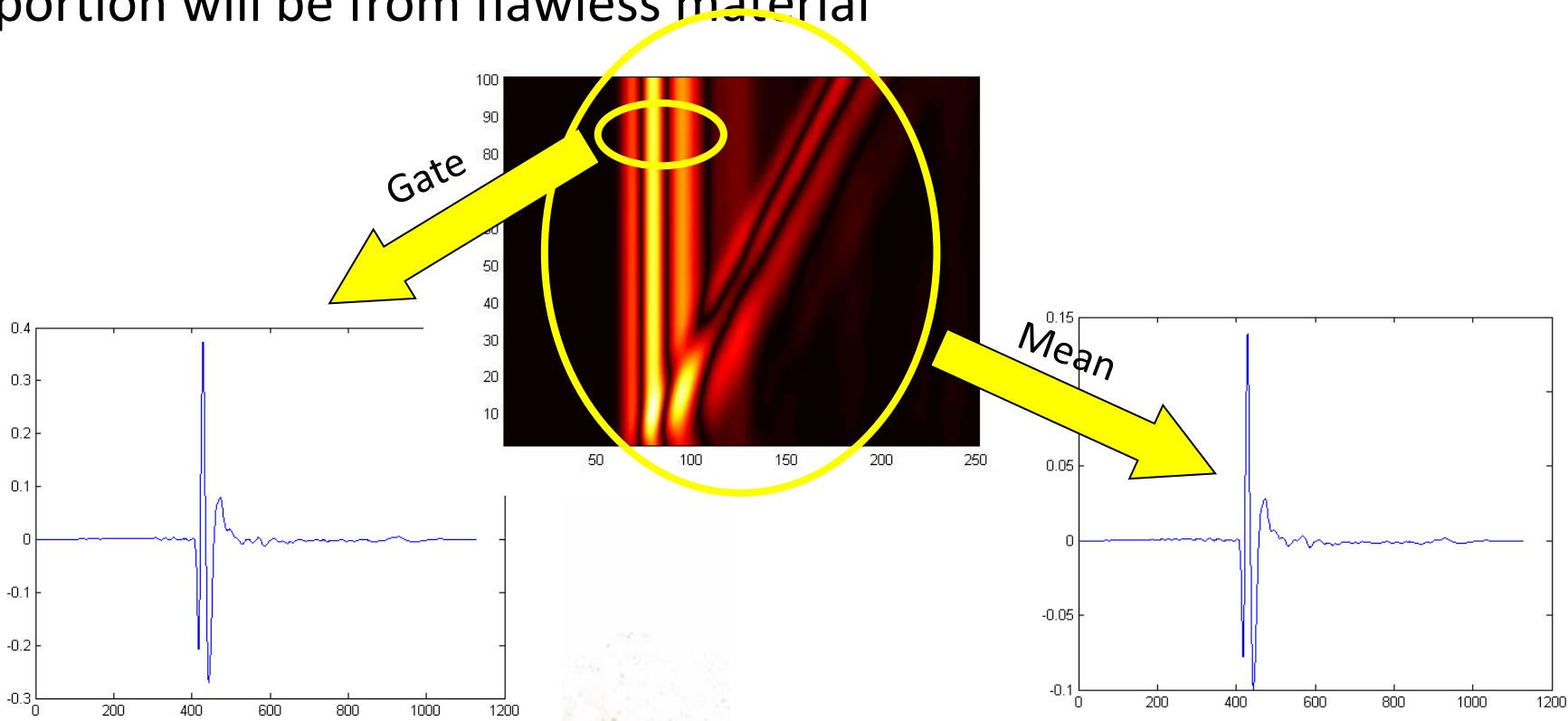
A.N. Sinclair et al. ‘Enhancement of ultrasonic images for sizing of defects by time-of-flight diffraction’, NDTE 2010

J. Martinsson et al., ‘Complete post-separation of overlapping ultrasonic signals by combining hard and soft modeling’, Ultrasonics, 2008

T.Misaridis, ‘Ultrasound Imaging Using Coded Signals’, PhD thesis, Technical University of Denmark, August 2001

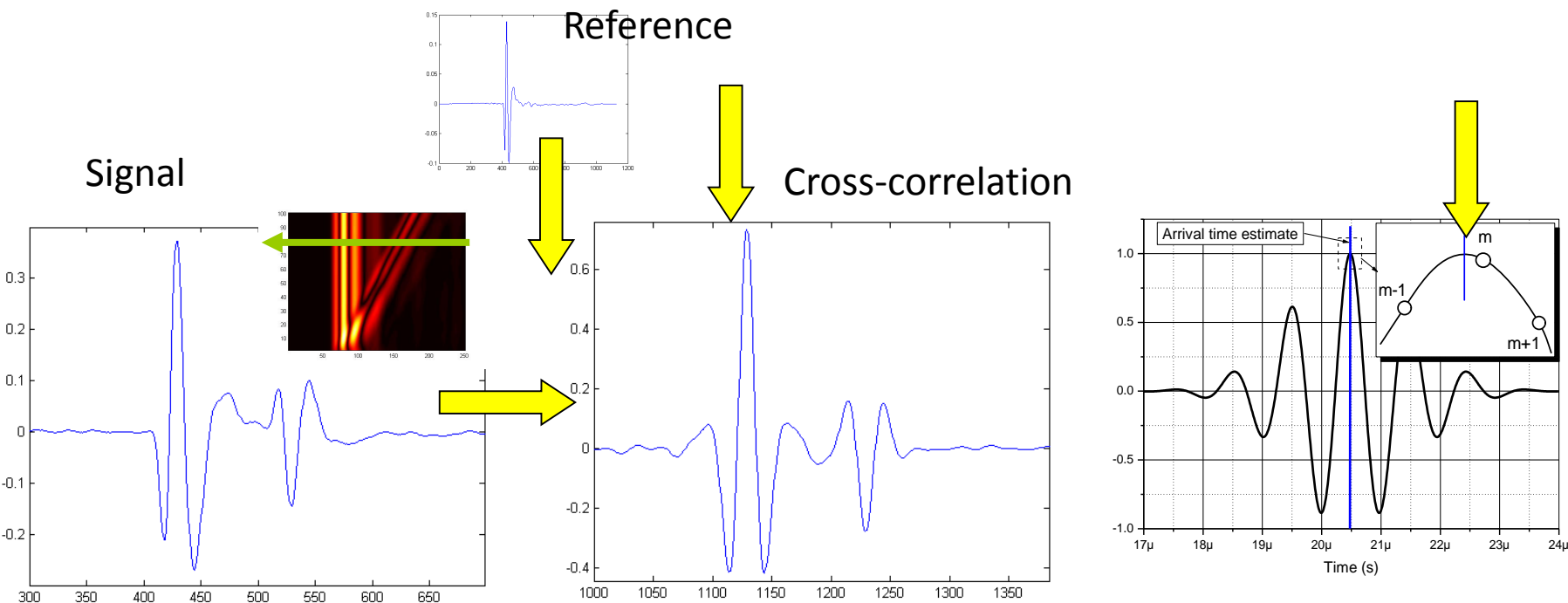
# Iterative deconvolution example: stripping 1

- Produce the reference:
- 1: area where ONLY front face reflection is present
- 2: average signal from whole specimen, assuming that major portion will be from flawless material



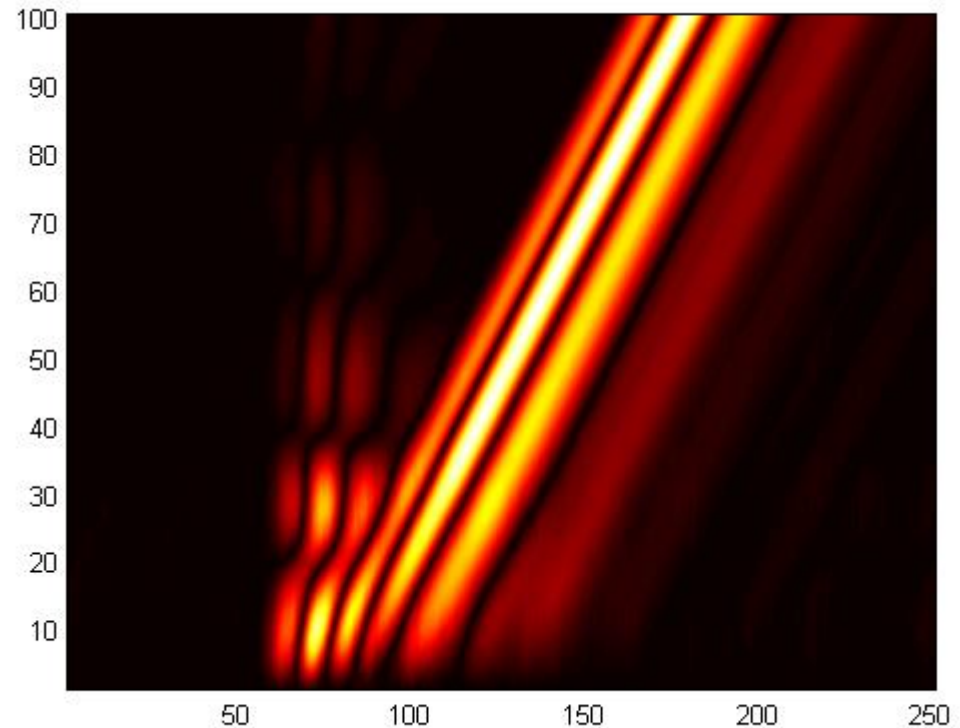
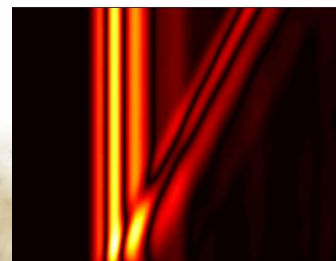
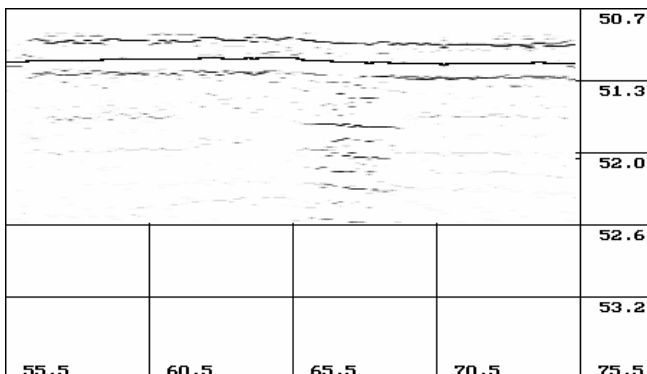
# Iterative deconvolution example: stripping 2

- Find the strongest reflector correlating with reference:
- i) cross-correlate
- ii) find correlation peak position
- iii) peak position SUBSAMPLE interpolation = TOF

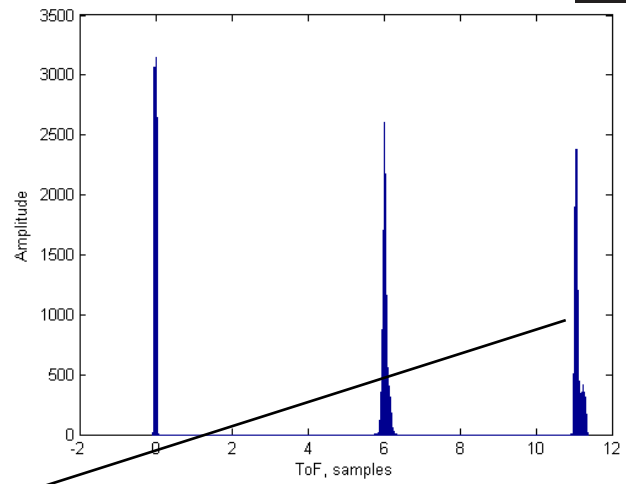
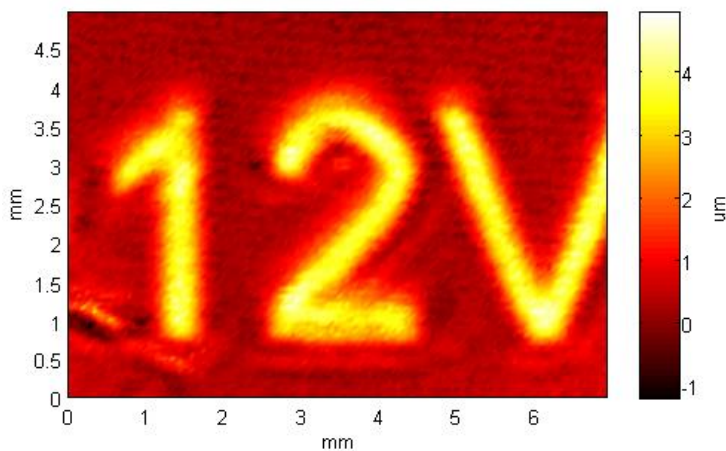


# Iterative deconvolution example: stripping 3

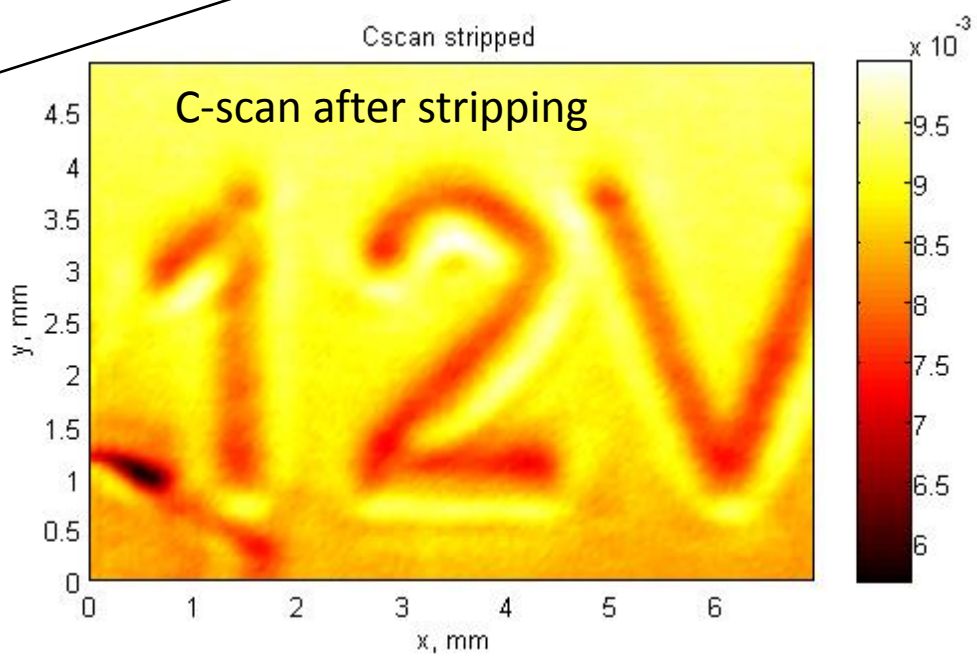
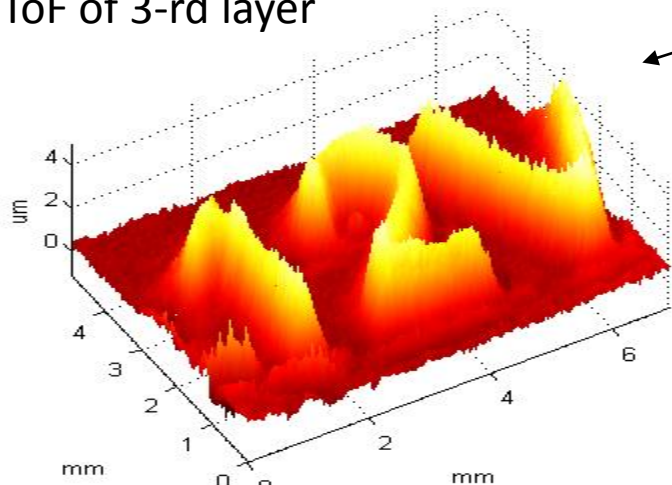
- Subtract the reference at TOF position, amp=cross-correlation
- Use remainder or iterate



# Iterative deconvolution example: layers

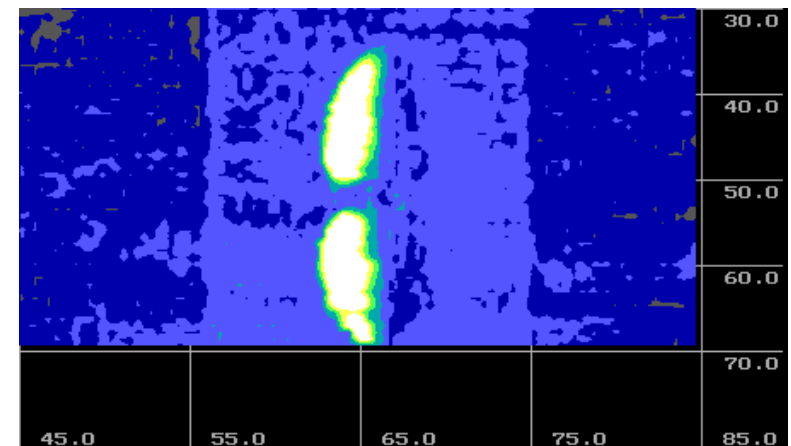
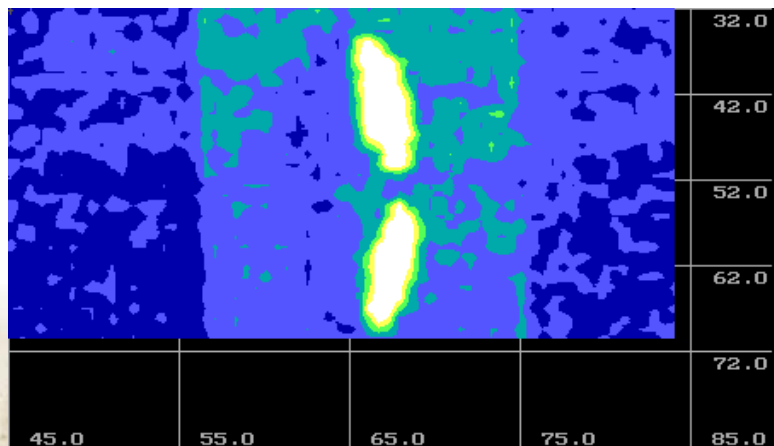
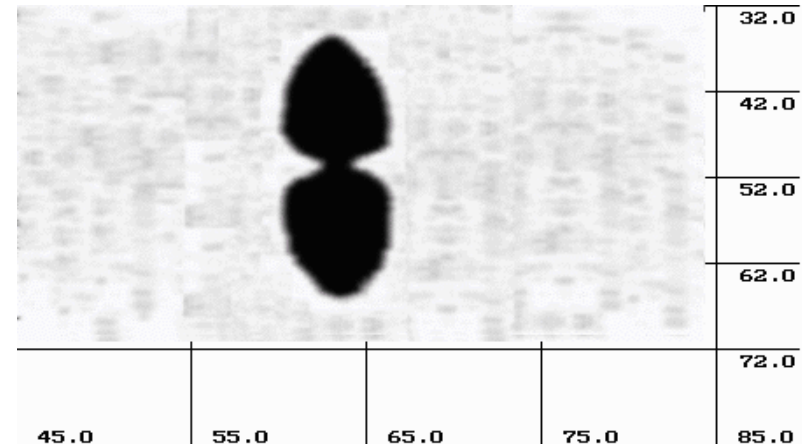
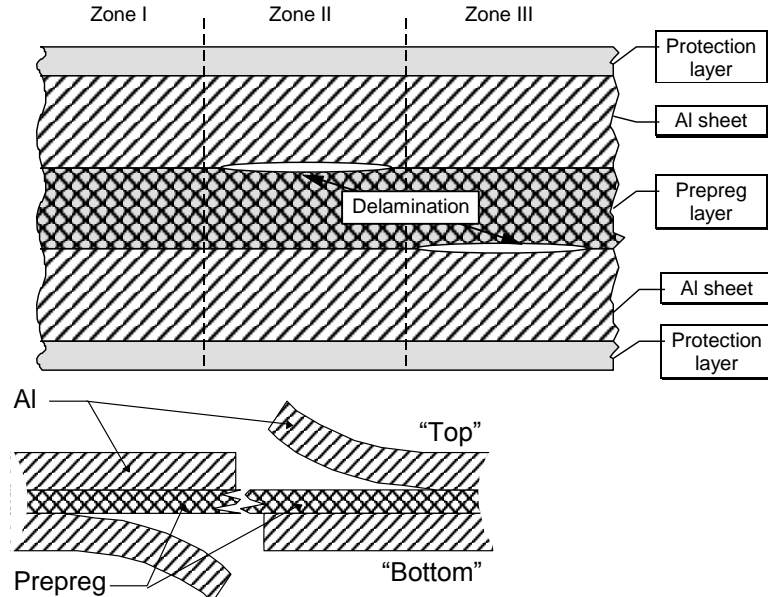


ToF of 3-rd layer

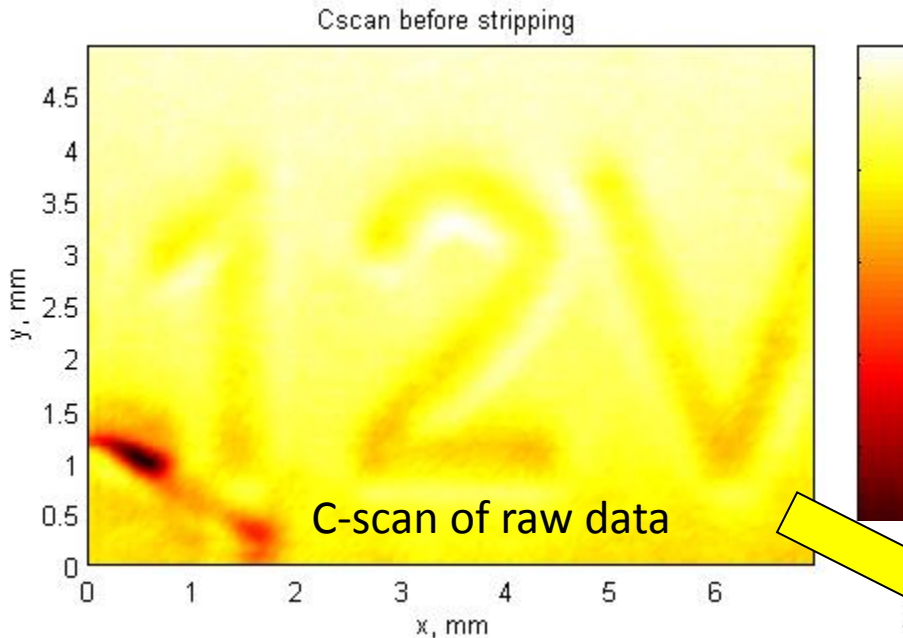


# Iterative deconvolution example: layers

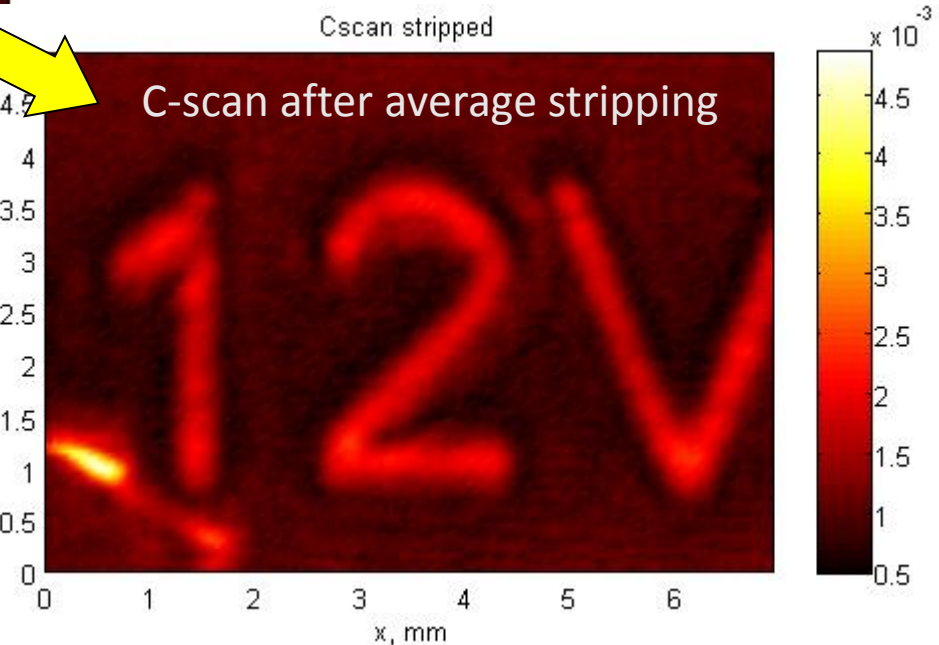
- GLARE, ARAL delamination



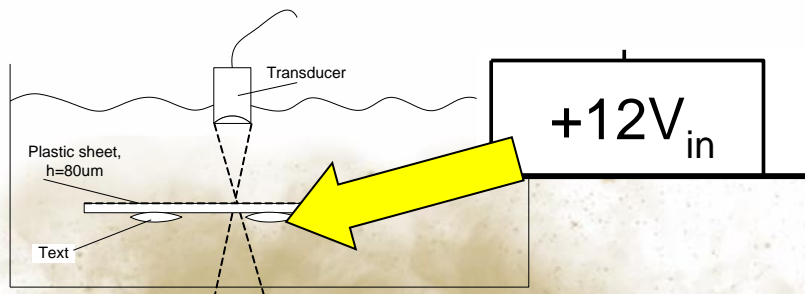
# Iterative deconvolution example: remainder



- Focused transducer IRY220 from NDT Transducers LLC
- 20 MHz 81% BW
- D=0.35mm focal spot



- Plastic 80  $\mu\text{m}$  thick
- Text on opposite side: 5  $\mu\text{m}$
- 2.5 mm letter height



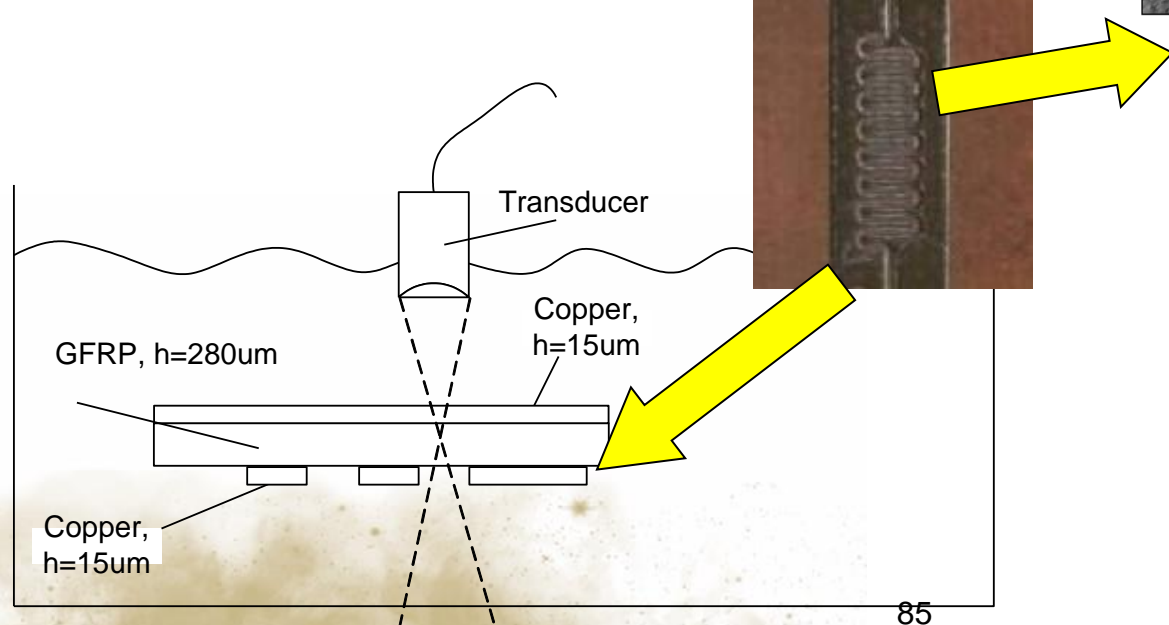
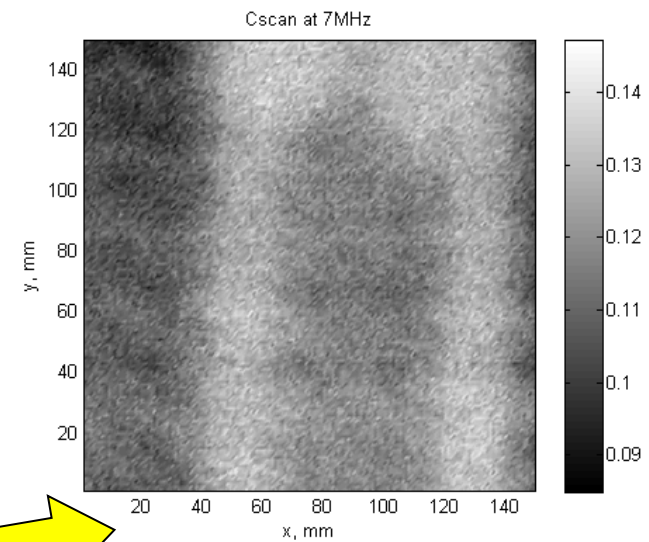
# Spectroscopy alone on PCB

PCB,  $h=280\text{ }\mu\text{m}$ .

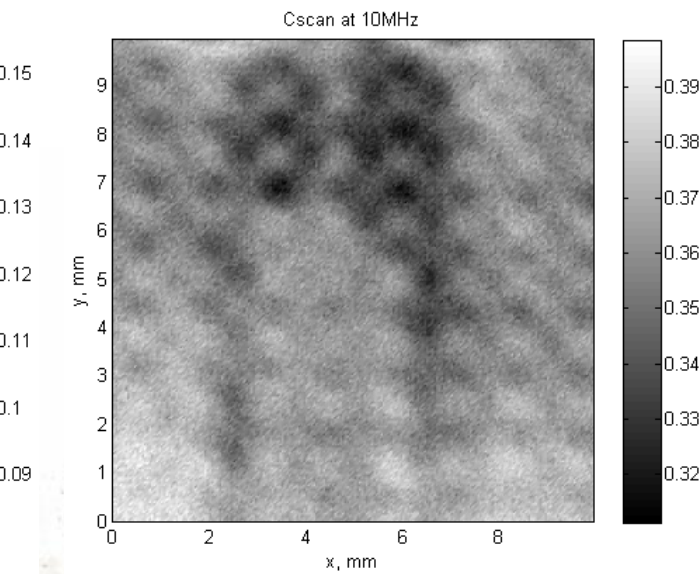
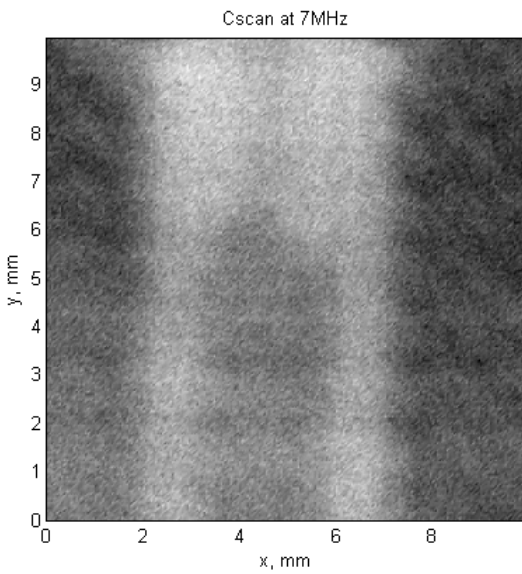
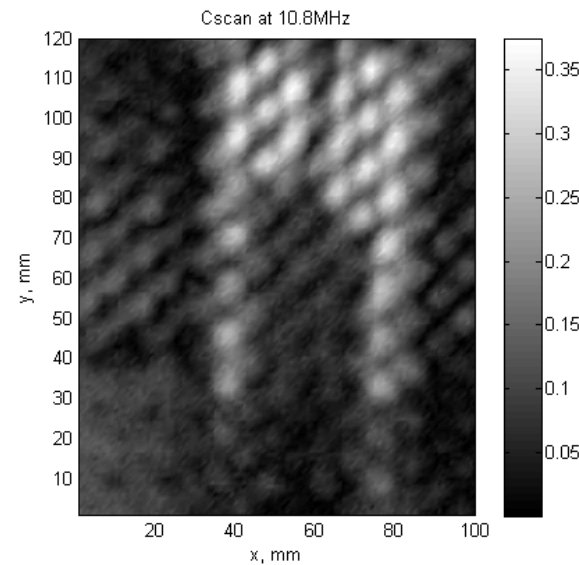
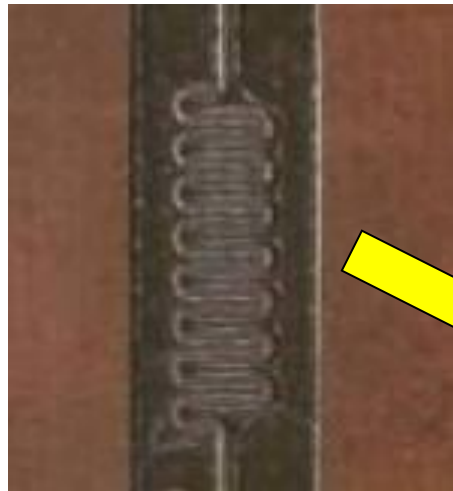
Top: 15 $\mu\text{m}$  copper,

Bottom: delay line ( $w=200\text{ }\mu\text{m}$ ).

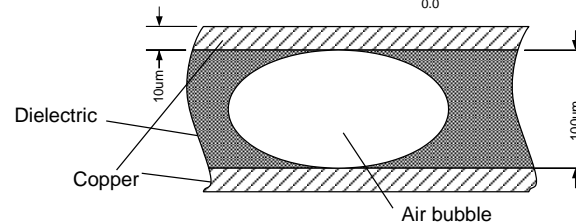
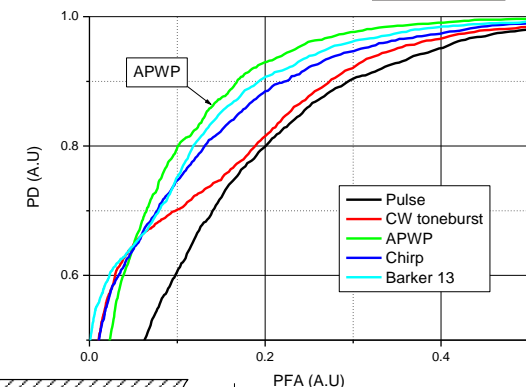
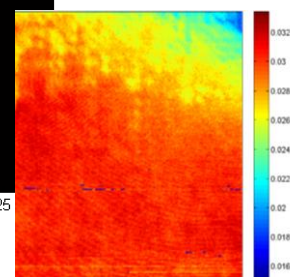
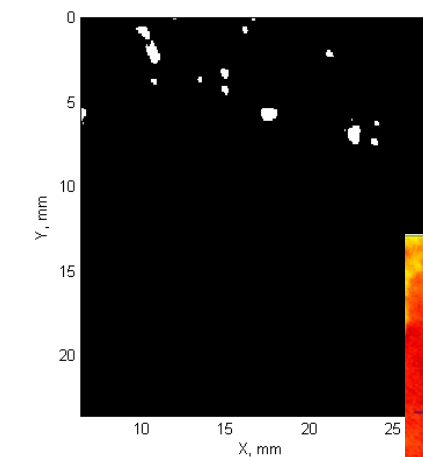
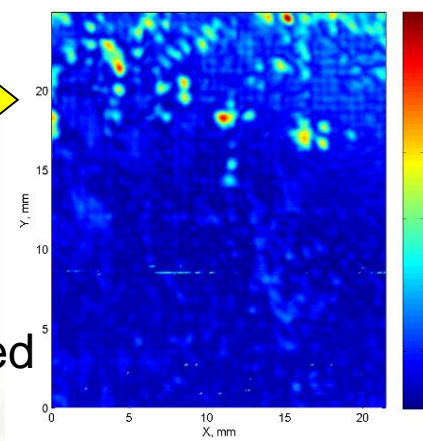
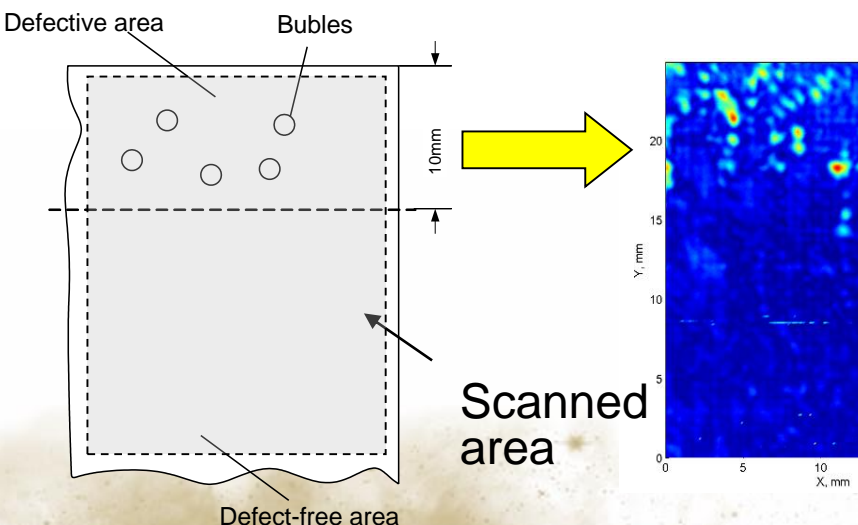
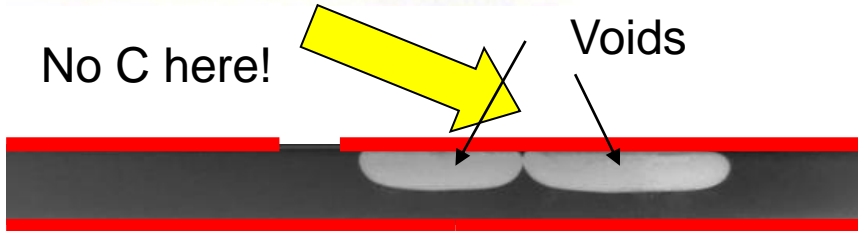
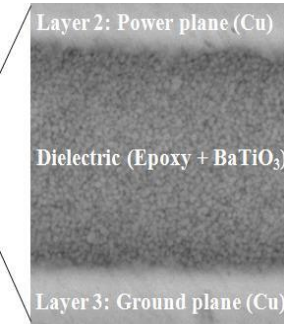
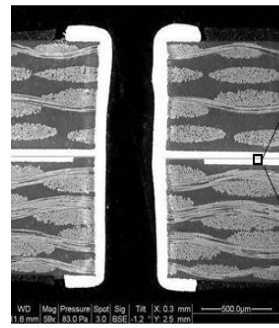
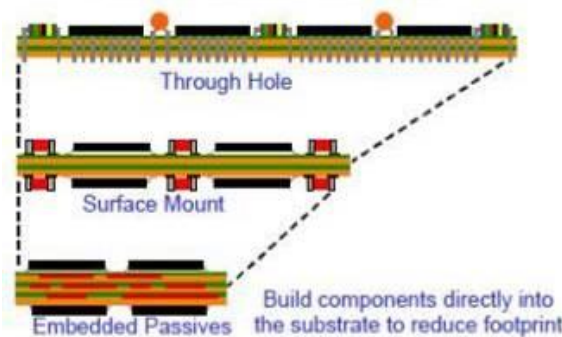
Same 20 MHz WB focused transducer



# Spectroscopy on PCB after stripping



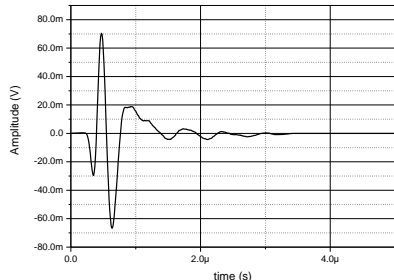
# Iterative deconvolution example: remainder



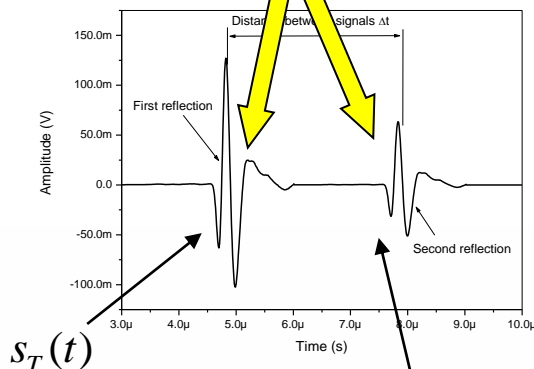
Receiver  
operating  
curve  
(ROC)

# Neighbor reflection induces bias on ToF

Real signal from delay line:



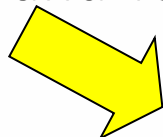
Artificial multilayer:



$$s_R(t) = A(t) \cdot s_T(t - \Delta t)$$

$\Delta t$  – artificial delay,  
distance between signal

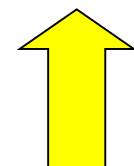
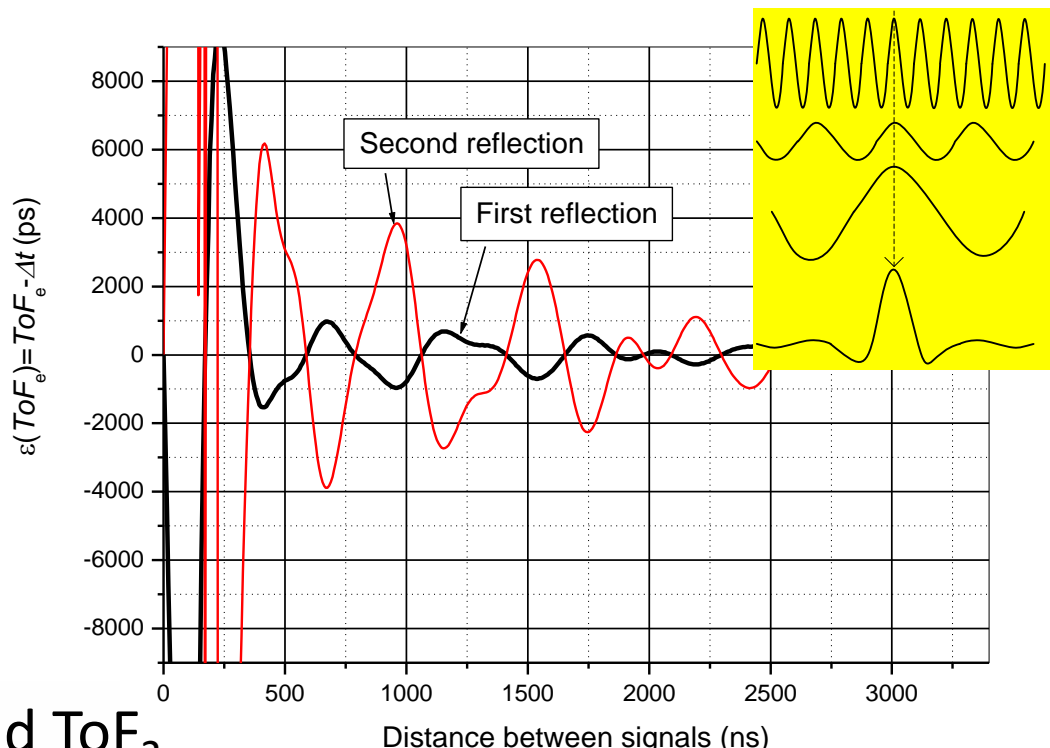
ToF<sub>1</sub> and ToF<sub>2</sub>



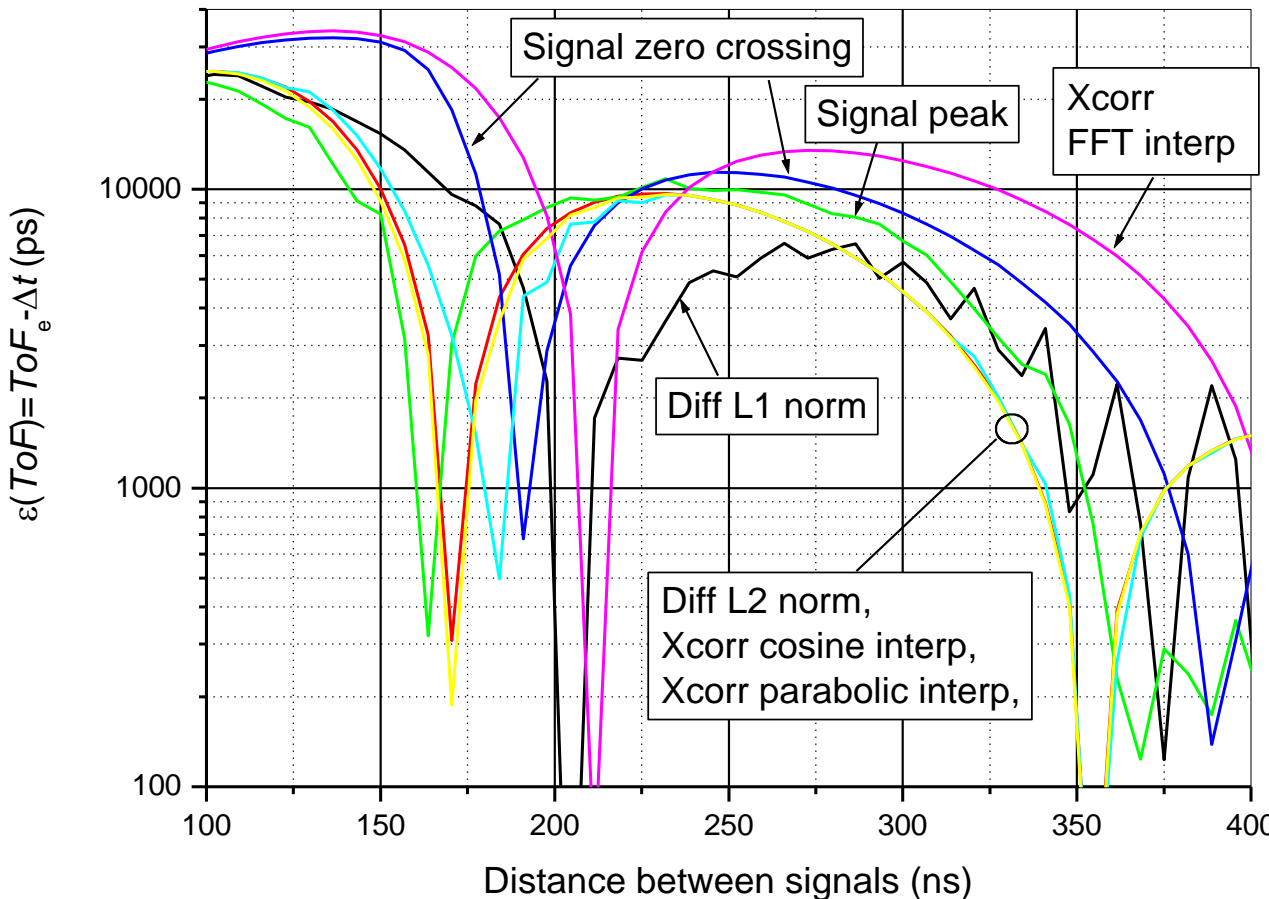
$\varepsilon$  – bias error

$$\varepsilon(\Delta \text{ToF}_1) = \text{ToF}_{e1} - 0$$

$$\varepsilon(\Delta \text{ToF}_2) = \text{ToF}_{e2} - \Delta t$$



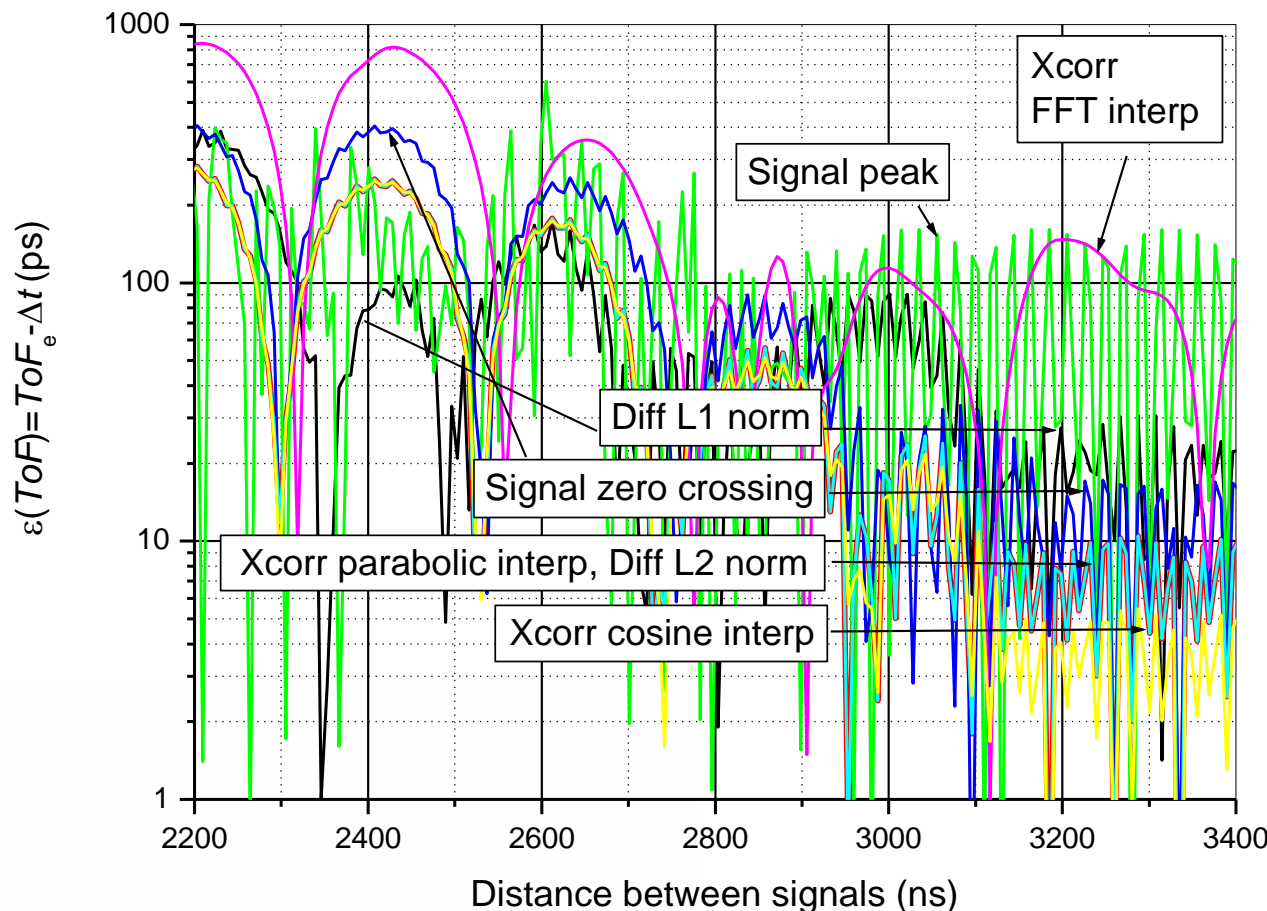
## Bias error due to close reflection: close proximity



Best performers: CCF peak interpolation using cosine or parabola and diff L2 norm  
 Techniques using local properties (signal peak and zero crossing) do not perform better

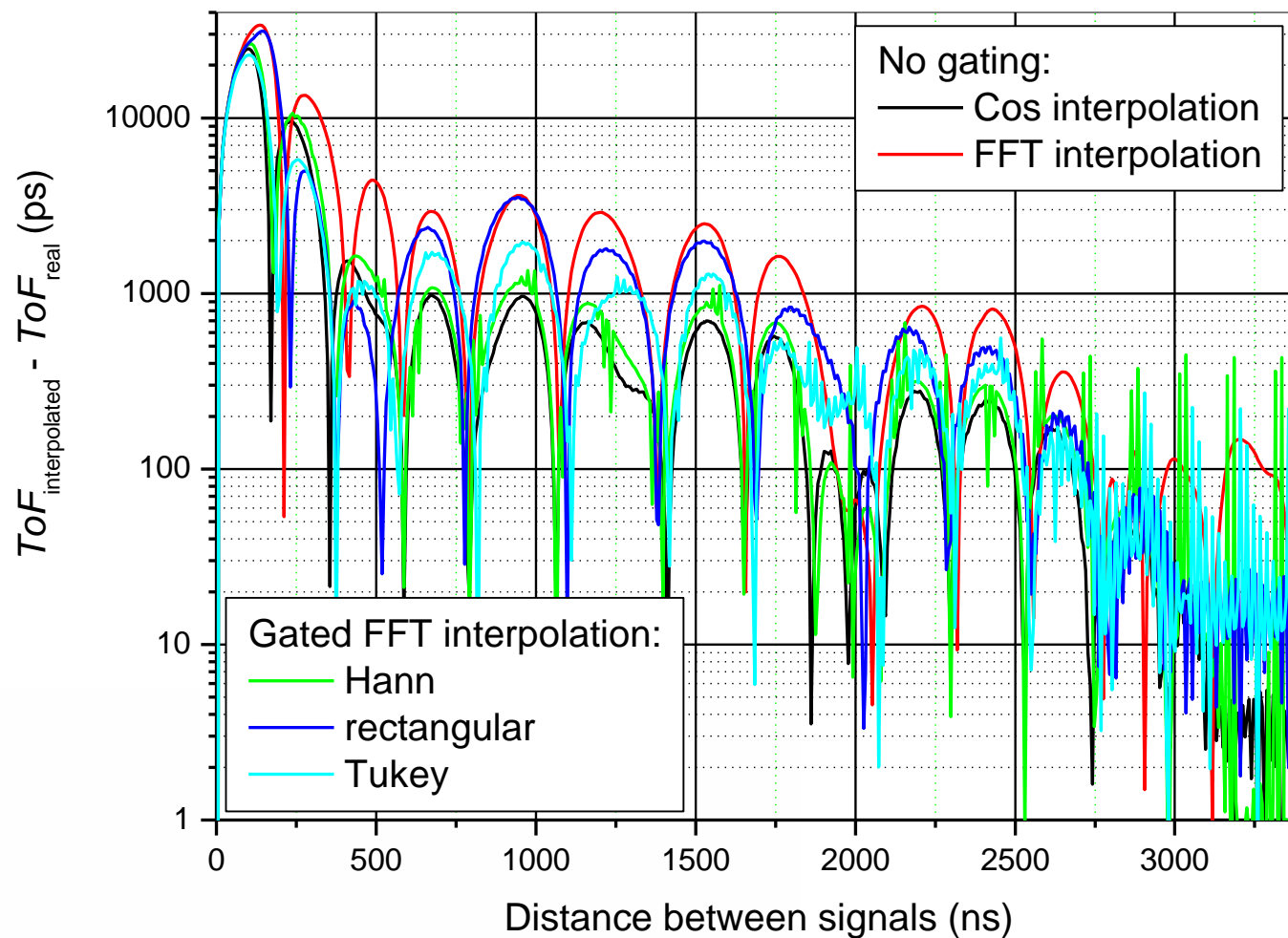
# Bias error due to close reflection: large spacing

Pulse



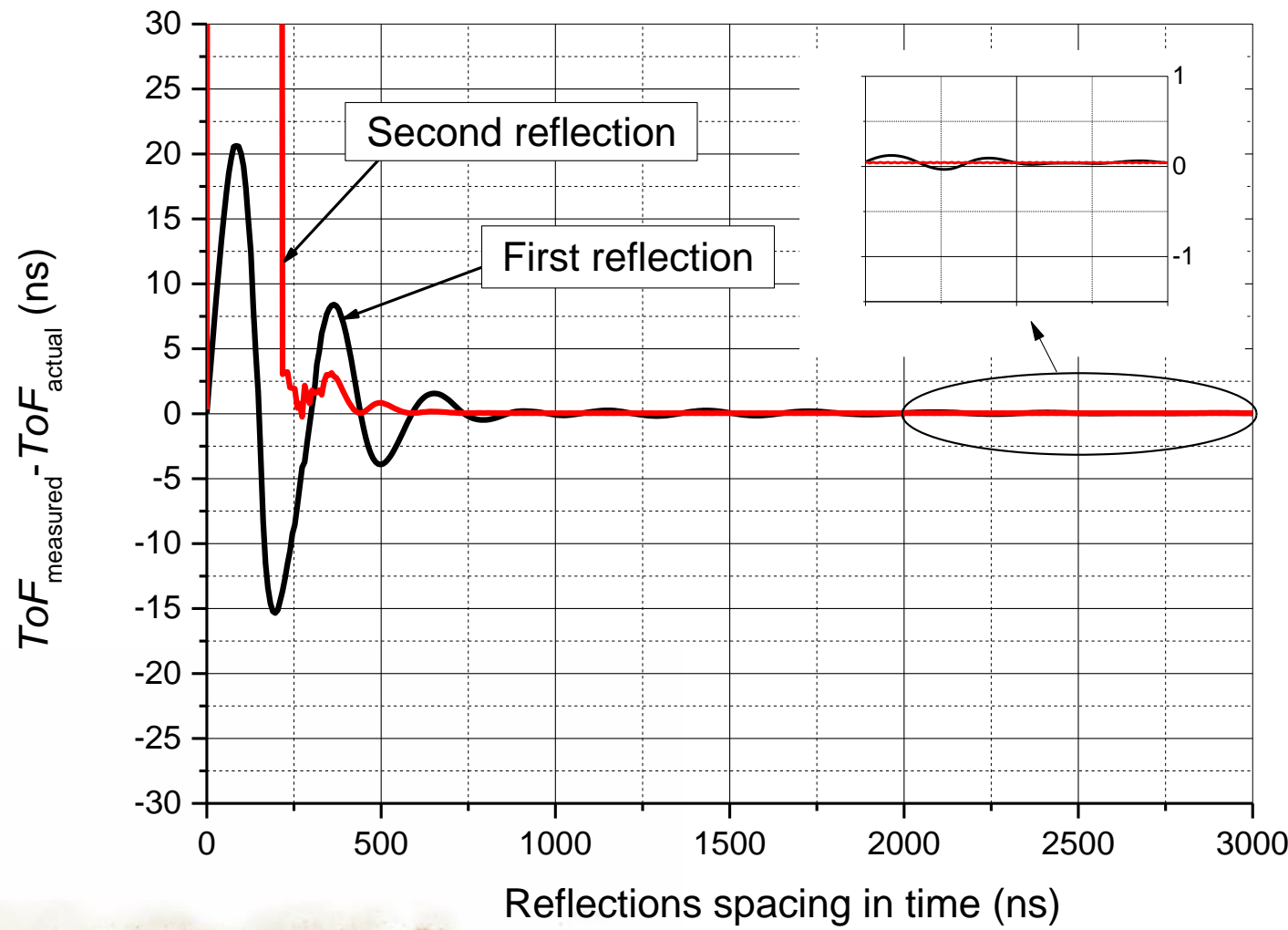
Best performers: CCF peak interpolation using cosine or parabola and diff L2 norm  
 Techniques using local properties (signal peak and zero crossing) do not perform better

## Bias error due to close reflection: gating

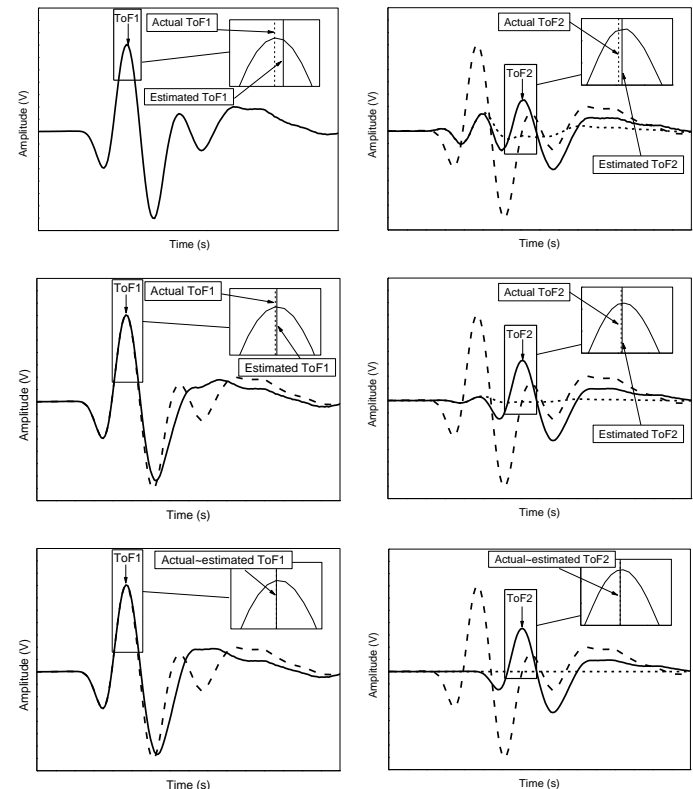
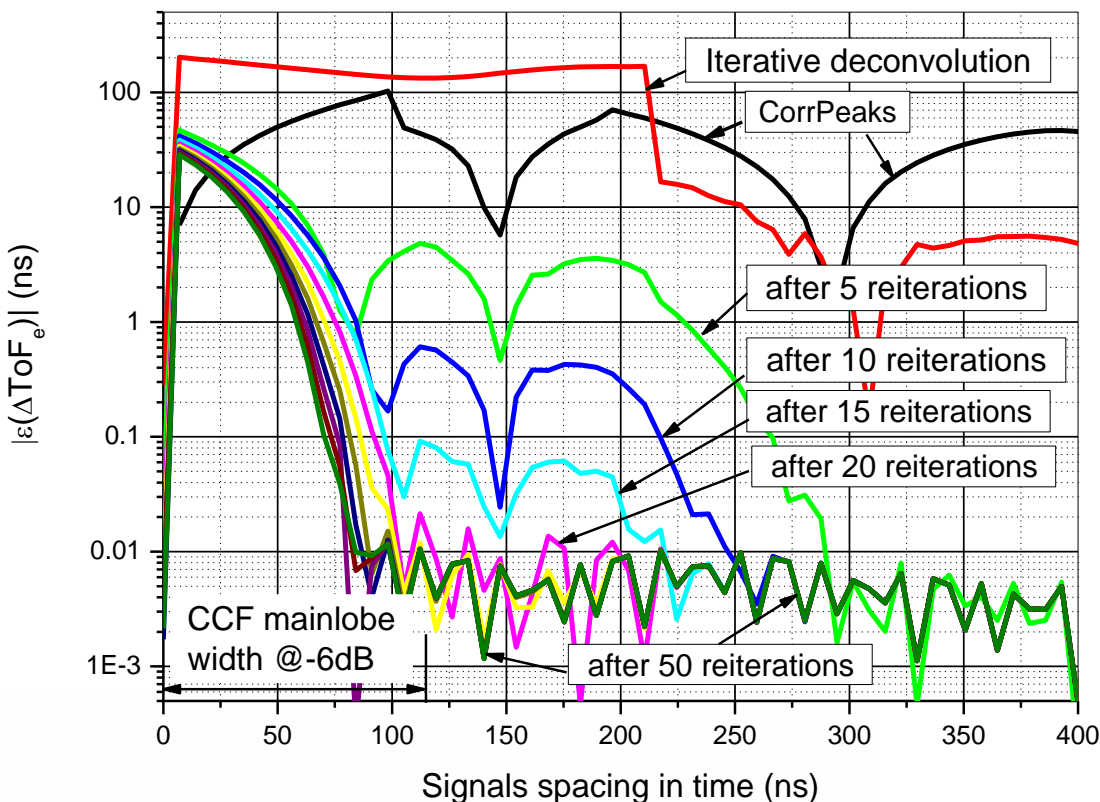


Gating does not reduce bias error induced by neighboring reflections

## Bias error due to close reflection: iterative deconvolution

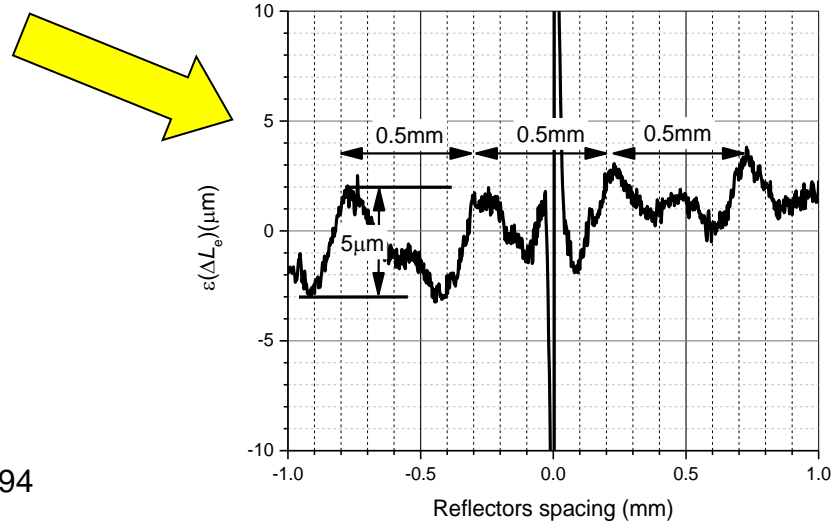
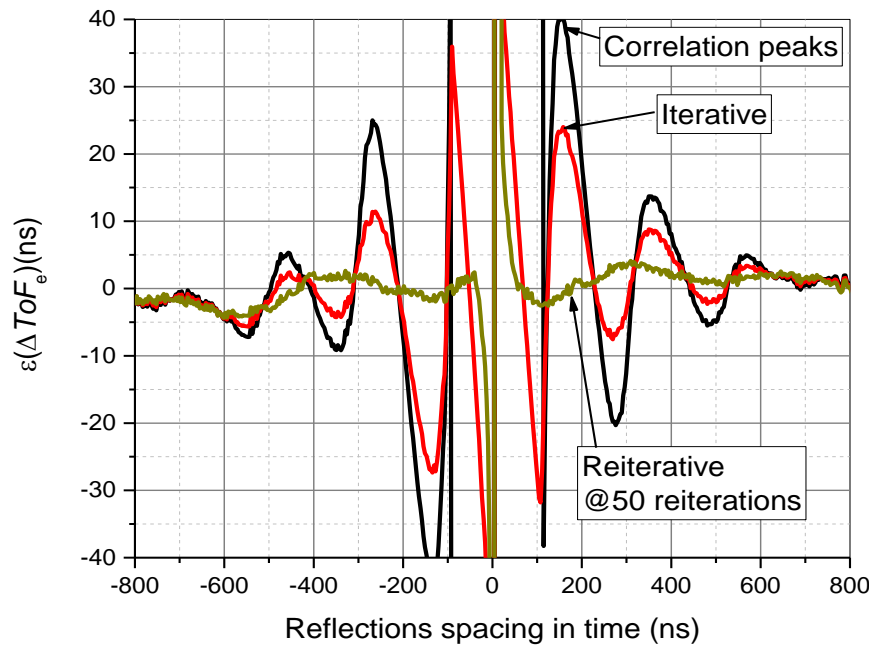
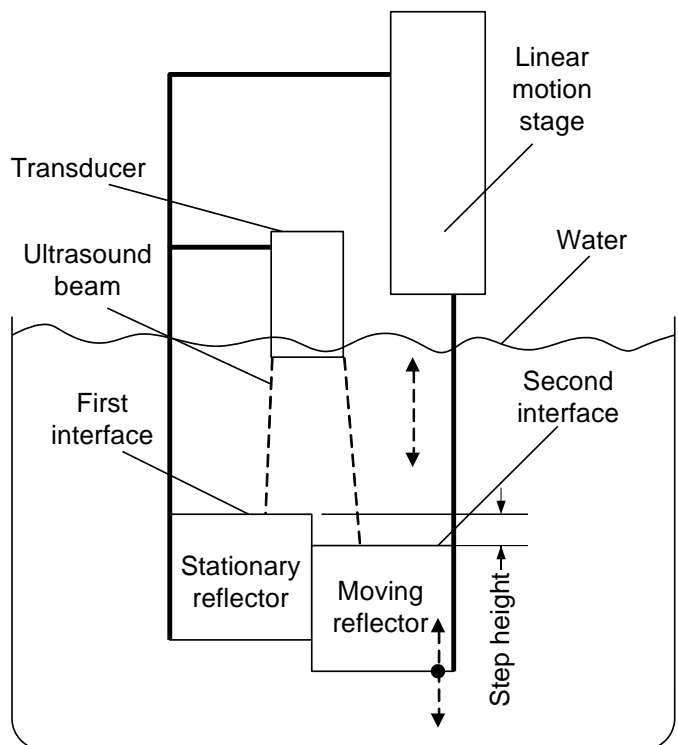


# Bias error due to close reflection: re-iterative deconvolution



L.Svilainis, K.Lukoseviciute, D.Liaukonis, Reiterative deconvolution: New technique for time of flight estimation errors reduction in case of close proximity of two reflections, Ultrasonics, 76, pp 154-165, 2017

# Reiterative deconvolution – down to leadscrew errors



# Reference signal production

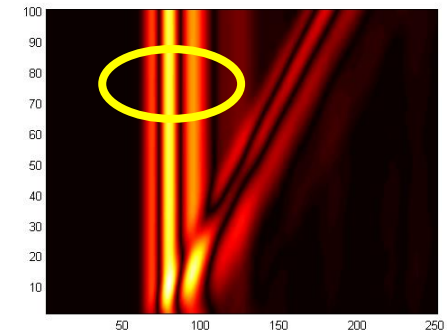
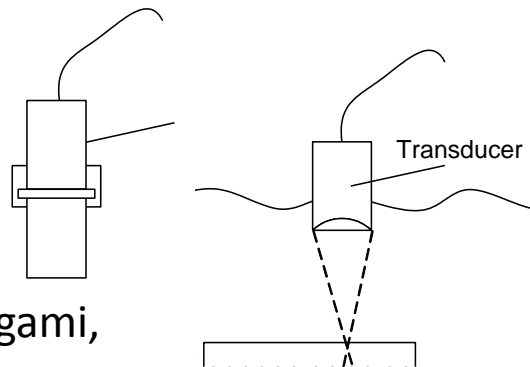
Reference signal:  
Water-air interface

Steel slab

Average

Model-based: Gabor, chirplet, Nakagami,  
time-warped Causal, Morlet

Adaptive



R.Demirli, J Saniie, 'Model-Based Estimation of Ultrasonic Echoes Part I: Nondestructive Evaluation Applications', IEEE TUFFC, Vol 48, No 3, pp 787-802, 2001.

Y.Lu, E. Oruklu and J. Saniie 'Chirplet signal and empirical mode decompositions of ultrasonic signals for echo detection and estimation' J. Signal and Inform. Process., 41,49–57, 2013

High-resolution pursuit for detecting flaw echoes close to the material surface in ultrasonic NDT. IEEE Proc 2006

Asymmetric Gaussian Chirplet model for ultrasonic echo analysis. IEEE Proc (2010)

Ultrasonic guided-waves characterization with warped frequency transforms, IEEE TUFFC. 56 (2009)

Efficient algorithm for discrimination of overlapping ultrasonic echoes", Ultrasonics 73 (2017)

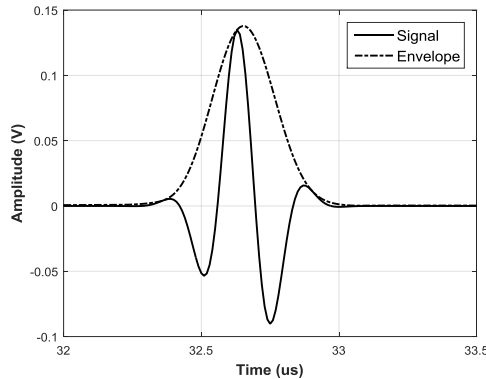
Zhou J., Zhang X., Zhang G., Chen D. Optimization and Parameters Estimation in Ultrasonic Echo Problems Using Modified Artificial Bee Colony Algorithm. Journal of Bionic Engineering, Vol. 12, 2015, p. 160-169.

Lu Y., Demirli R., Cardoso G., Saniie J. A Successive Parameter Estimation Algorithm for Chirplet Signal Decomposition. IEEE TUFFC, Vol. 53, Issue 11, 2006, p. 2121 2131.

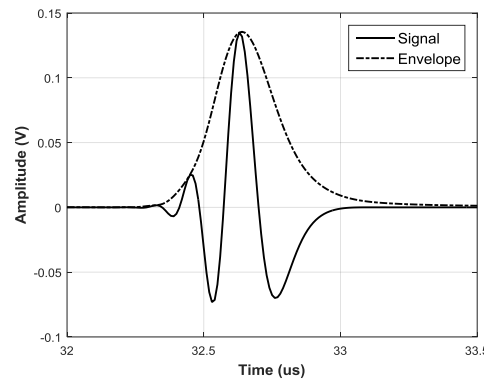
M. Alessandrini, L. De Marchi, 'Recursive Least Squares adaptive filters for ultrasonic signal deconvolution', 2008

# Reference signal production: model

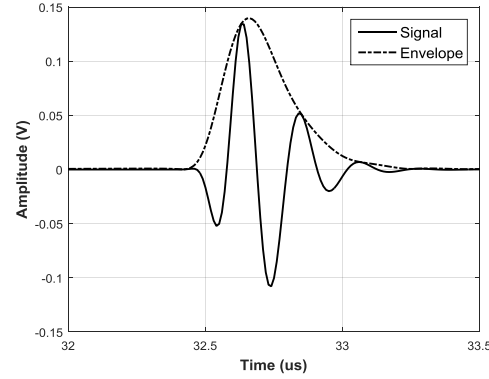
1922



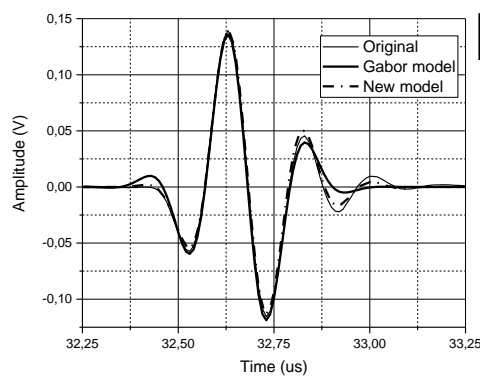
Gabor



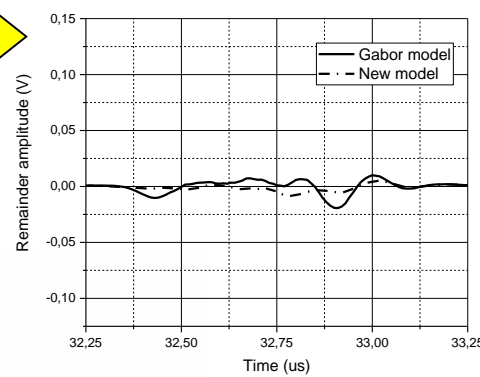
Gaussian Chirplet



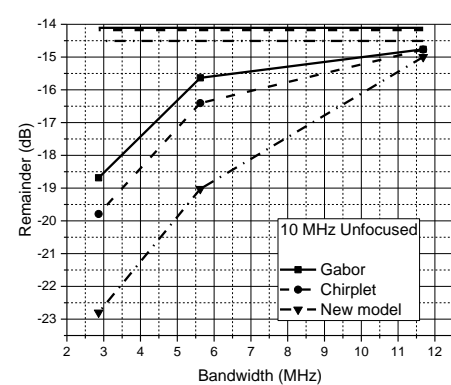
time-warped Causal



Original vs model

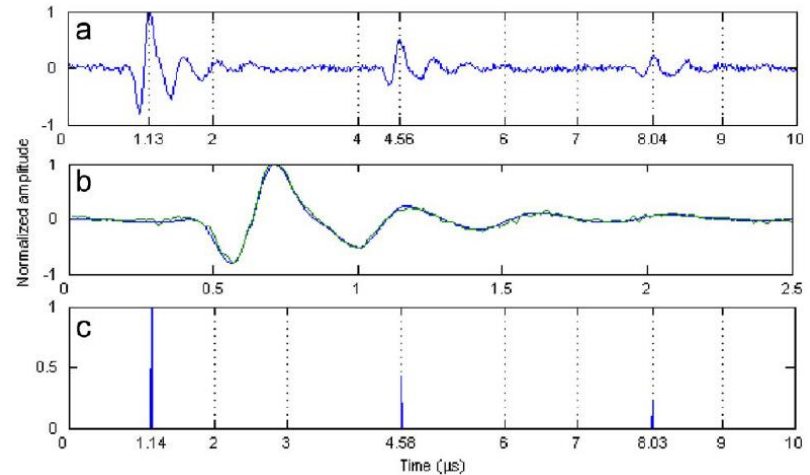
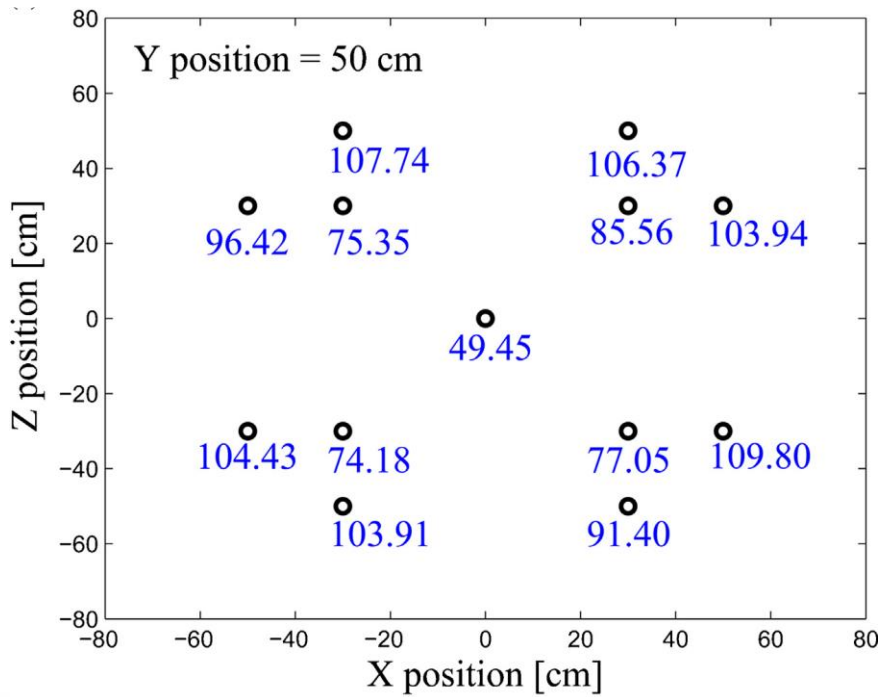


Remainder



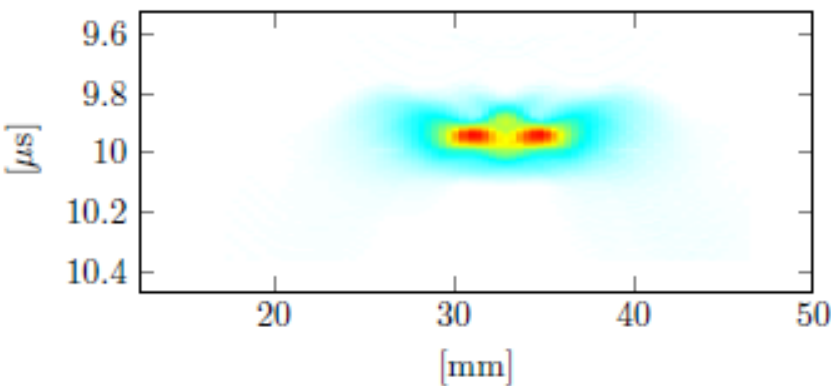
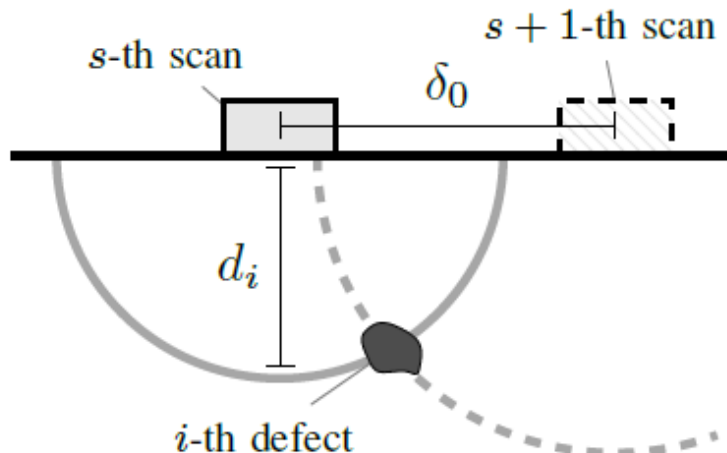
Remainder energy /  
original energy

# Model-based deconvolution: compressive sensing

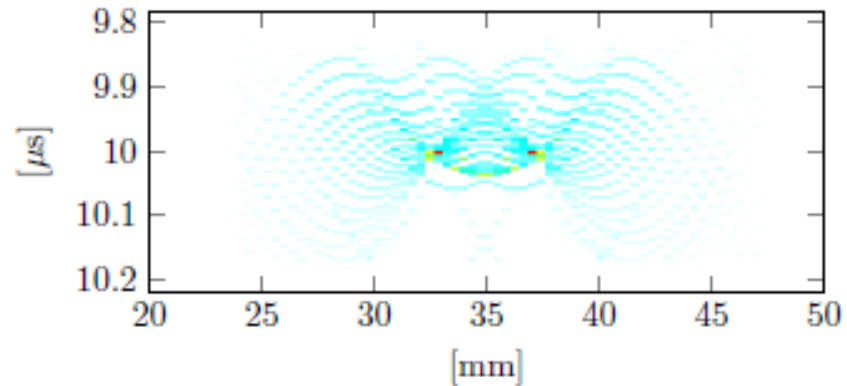
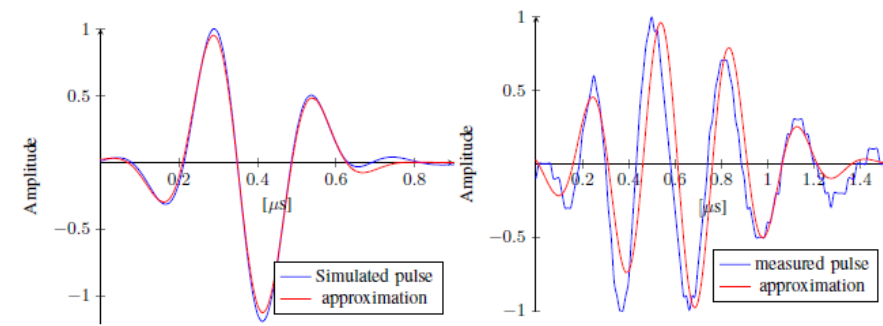


- R. Demirli, J. Saniie 'Model-based estimation pursuit for sparse decomposition of ultrasonic echoes' 2012  
M. F. Schiffner, et al, 'Compressed sensing for fast image acquisition in pulse-echo ultrasound' BT, 2012.  
Liang Wei et al. Sparse deconvolution method for improving the time-resolution of ultrasonic NDE signals' NDTE 2009  
N.Thong-un, S. Hirata, et al. 'A linearization-based method of simultaneous position and velocity measurement using ultrasonic waves' SENSORS AND ACTUATORS A-PHYSICAL 2015

# Deconvolution: 2D/3D model



**BP+SAFT (2.8 s + 0.188 s)**



**OMP+SAFT (0.26 s + 0.006 s)**

J.Kirchhof 'Speeding up 3D SAFT for ultrasonic NDT by Sparse Deconvolution' IEEE IUS 2016

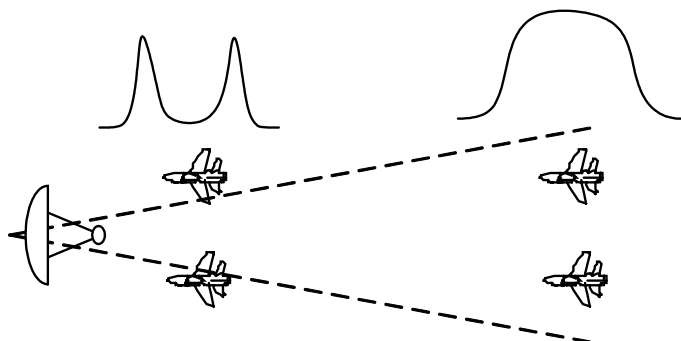
M. Wuest et al. 'A matched model-based synthetic aperture focusing technique for acoustic microscopy' NDTE 2019

M.F. Schiffner and Georg Schmitz 'Pulse-Echo Ultrasound Imaging Combining Compressed Sensing and the Fast Multipole Method' IEEE IUS 2014

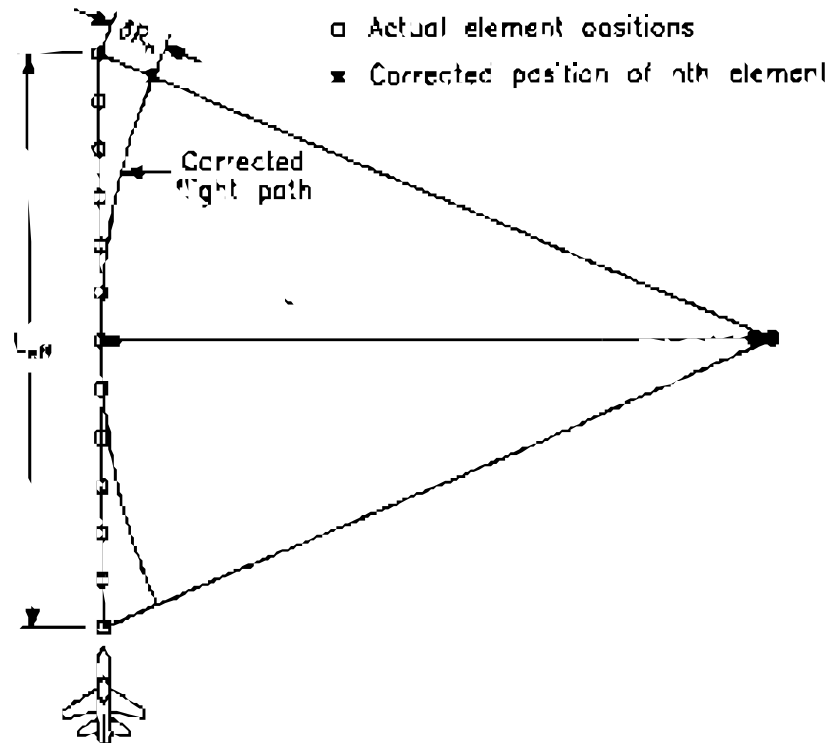
# SAR/SAFT

SAR: Synthetic aperture radar

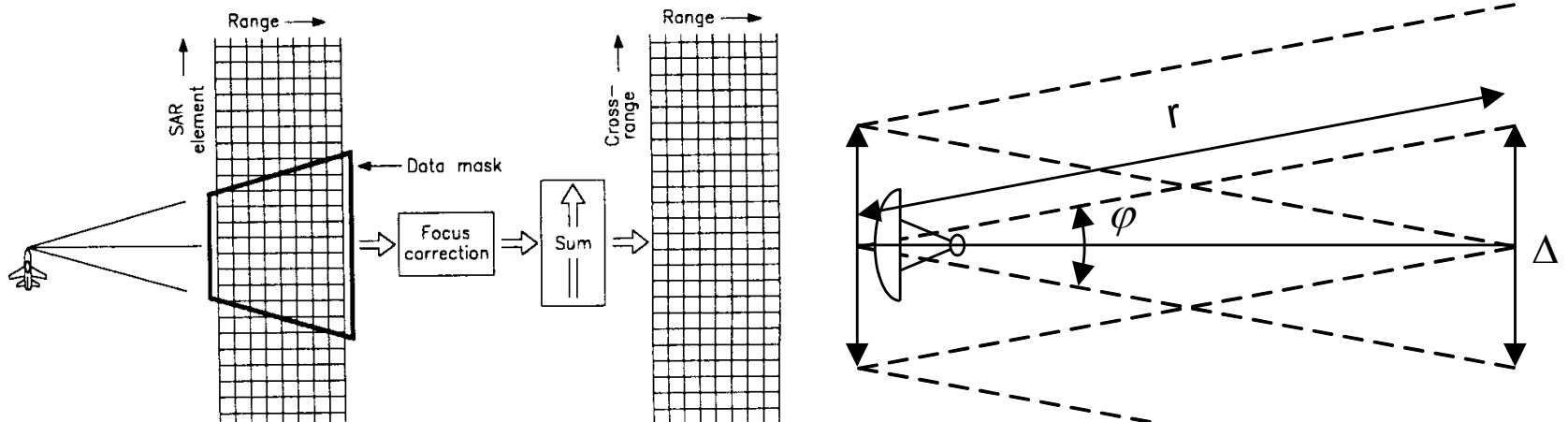
SAFT: Synthetic aperture focusing technique



$$\varphi_{0.5} = \frac{\lambda}{D_{ef}}$$



# SAR/SAFT



SAR resolution is defined by the size of primary antenna

$$\varphi_{0.5} = \frac{\lambda}{L_A} \rightarrow \Delta = 2r \sin\left(\frac{\varphi_{0.5}}{2}\right) \approx r\varphi_{0.5} \approx r \frac{\lambda}{L_A} \rightarrow L_{SAR} = \Delta$$

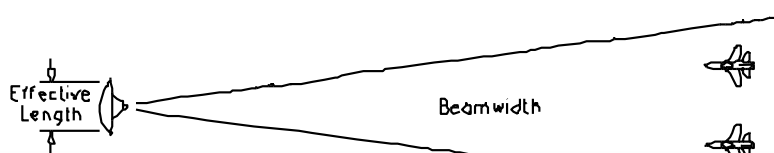
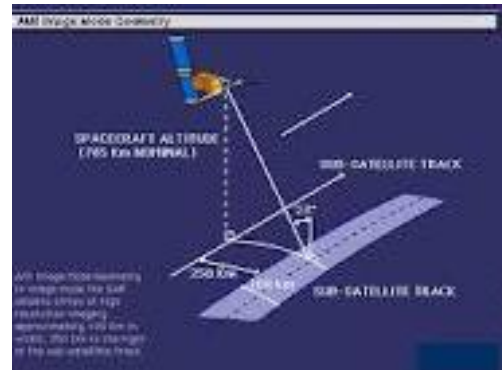
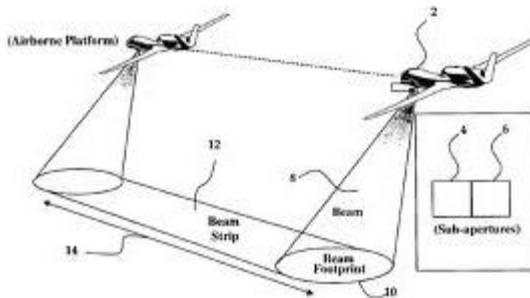
$$\varphi_{0.5SAR} = \frac{\lambda}{L_{SAR}} \rightarrow \Delta_{SAR} = 2r \sin\left(\frac{\varphi_{0.5SAR}}{2}\right) \approx r \cdot \varphi_{0.5SAR} \approx \frac{r \cdot \lambda \cdot L_A}{r \cdot \lambda} \approx L_A$$

# SAR/SAFT

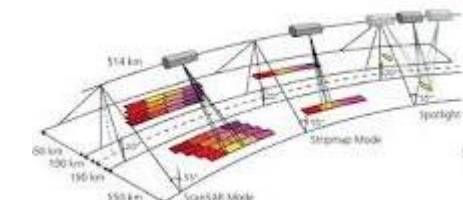
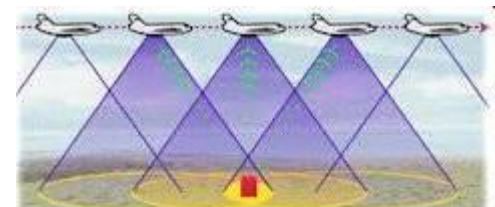
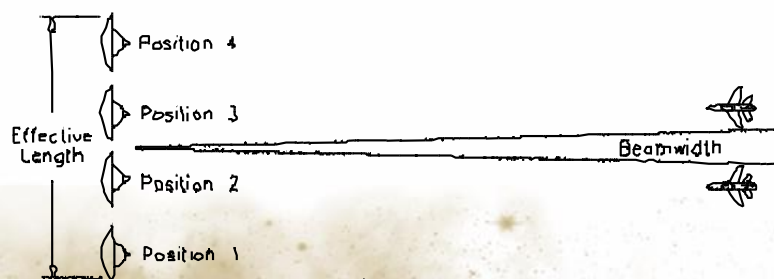
1922

ktu

Synthetic aperture radar: SAR



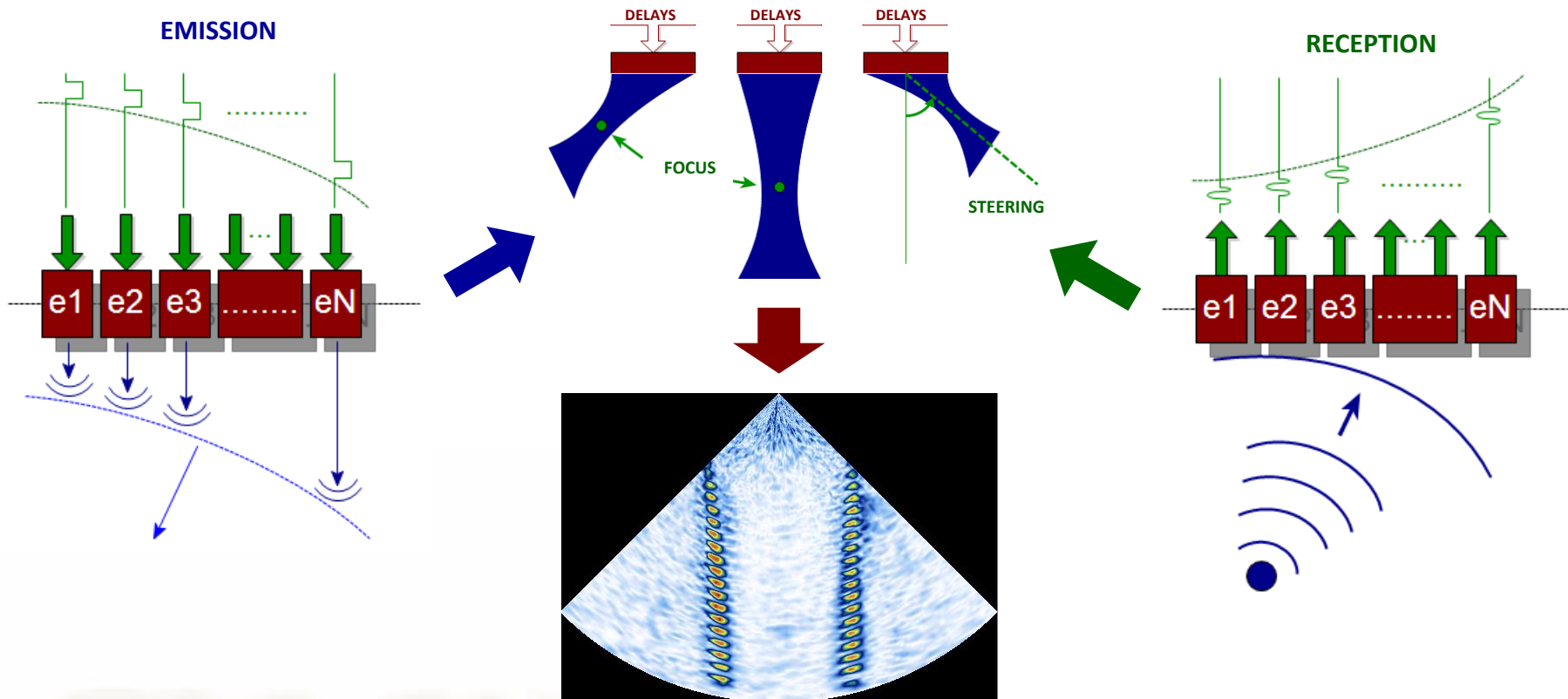
a. Small real antenna, targets not resolved



$$\varphi_{0.5 \text{ SAR}} = \frac{\lambda}{L_{\text{SAR}}}$$

# Beam steering

USING AN ARRAY OF TRANSDUCERS, THE ACOUSTIC BEAM CAN BE ELECTRONICALLY STEERED AND FOCUSED

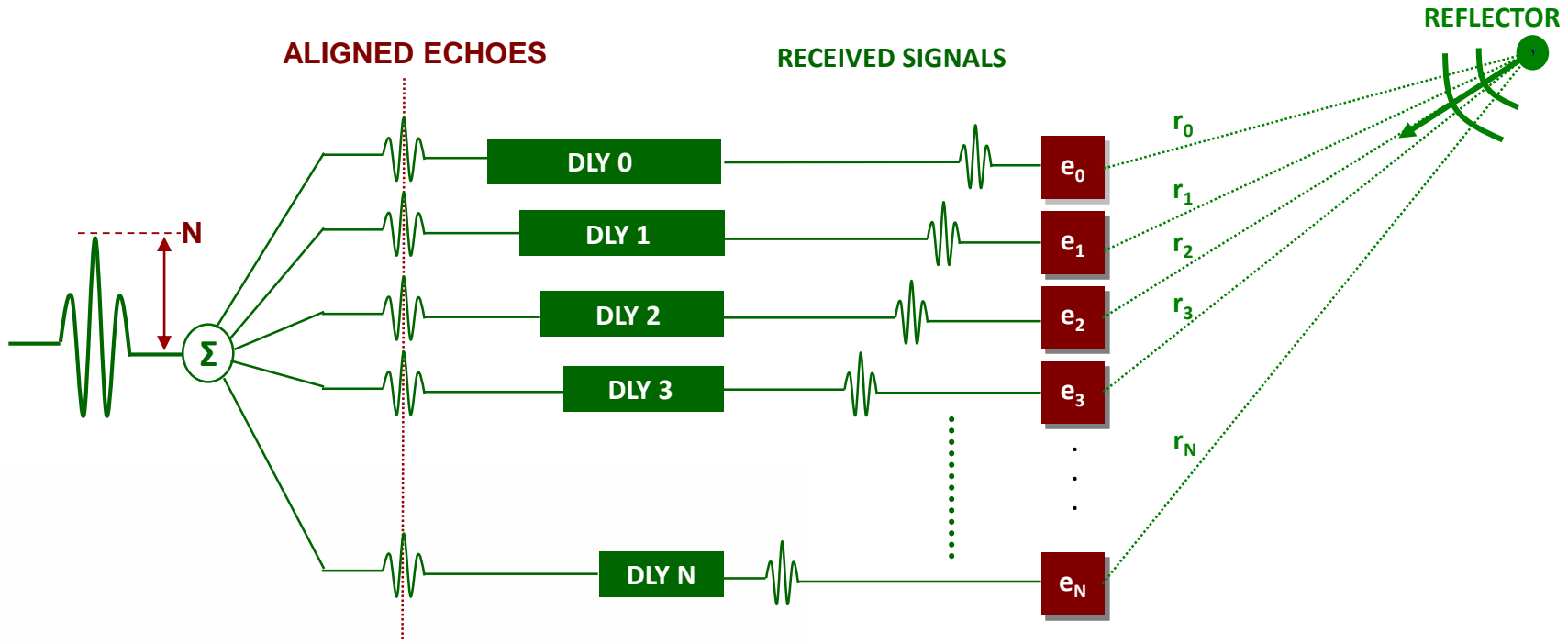


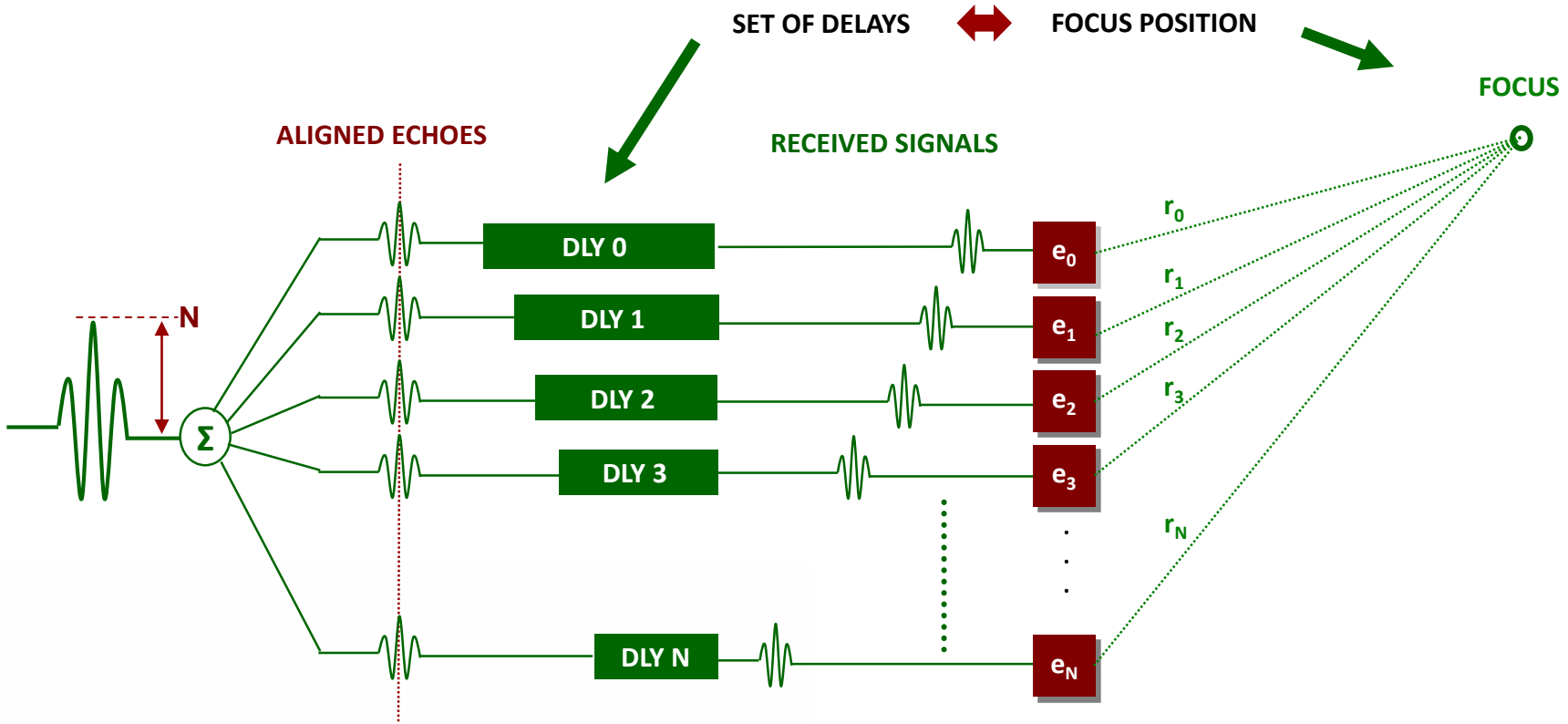
IMAGES OF THE VOLUME CAN BE OBTAINED AT HIGH FRAME RATES,  
HIGH RESOLUTION AND WITHOUT MECHANICAL MOVEMENT

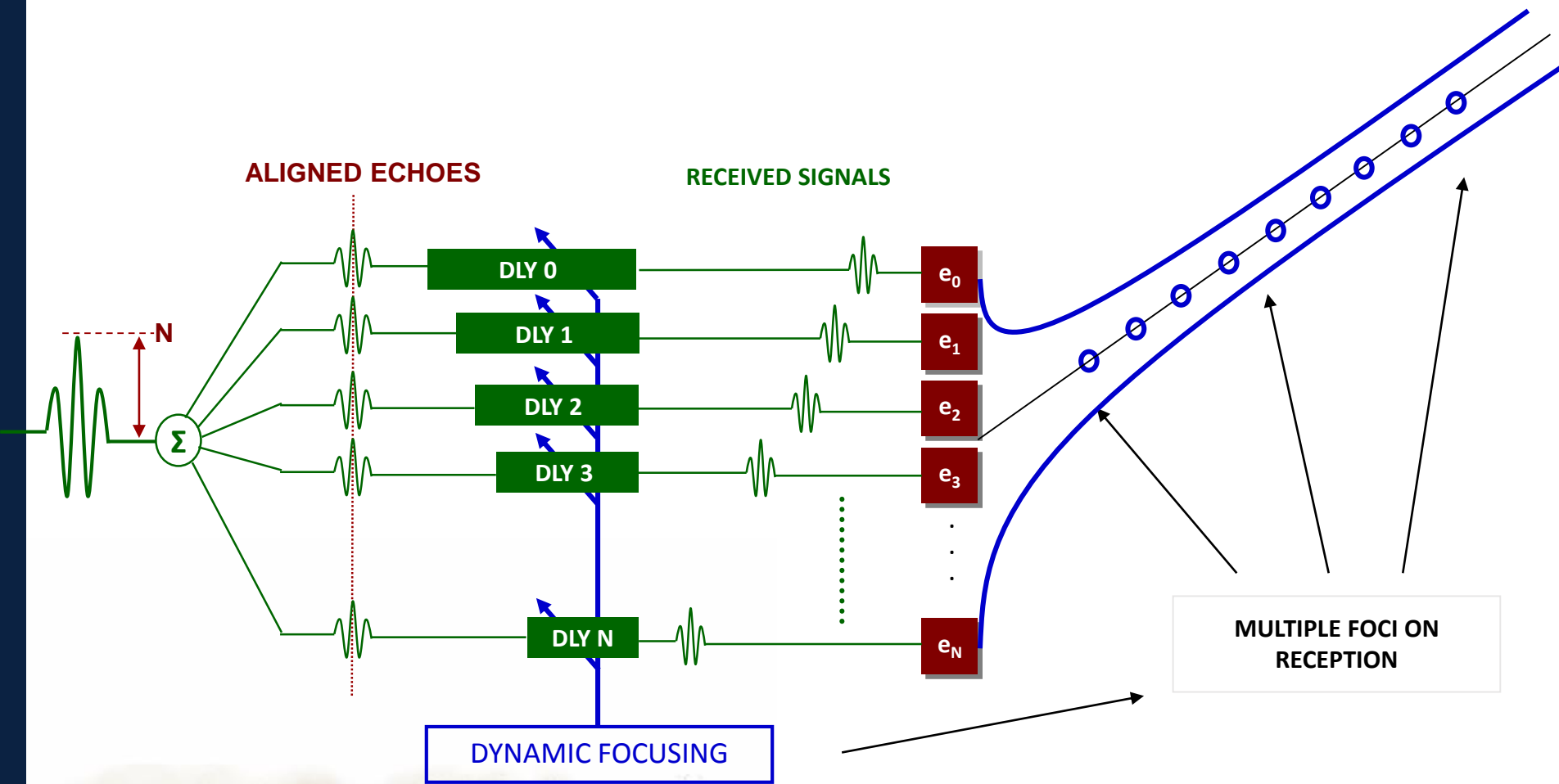
# SAFT

SAFT: Synthetic aperture focusing technique

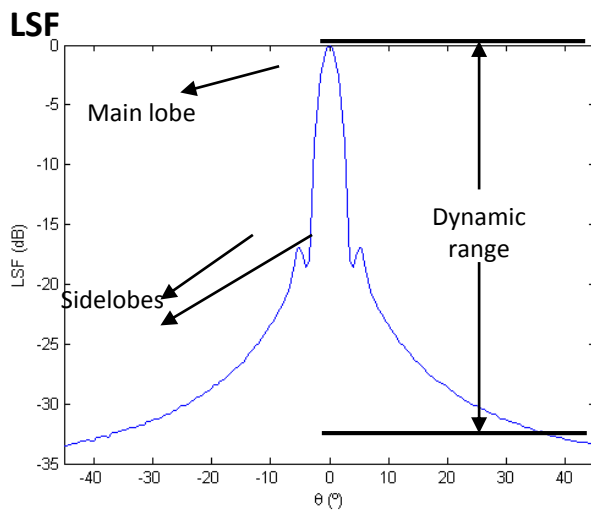
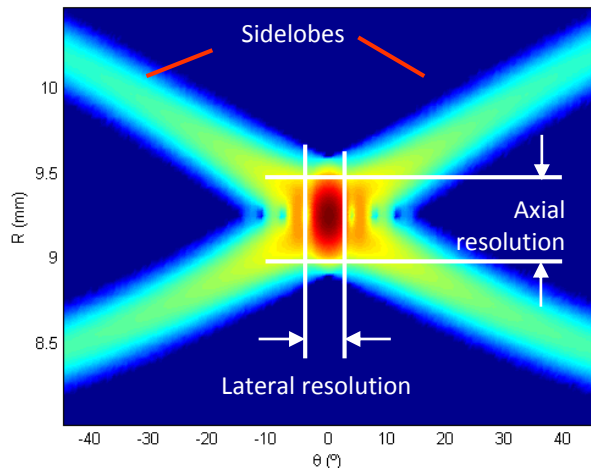
**BEAMFORMING:** PROCESS OF COMBINING THE RECEIVED SIGNALS TO FORM AN IMAGE



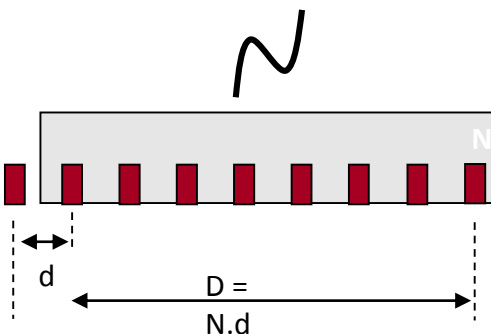




## Point Spread Function



## Line Spread Function



- **RESOLUTION**

- AXIAL :  $\uparrow$  FREQUENCY & BANDWIDTH
- LATERAL :  $\uparrow$  APERTURE SIZE ( $D$ )

- **CONTRAST**

- SIDELOBE LEVEL:  $\downarrow$  APODIZATION

- **DYNAMIC RANGE**

- DYNAMIC RANGE:  $\uparrow$  NUMBER OF ELEMENTS

**THE ARRAY CHARACTERISTICS LIMIT THE RESOLUTION AND DYNAMIC RANGE OF THE DELAY AND SUM BEAMFORMERS**

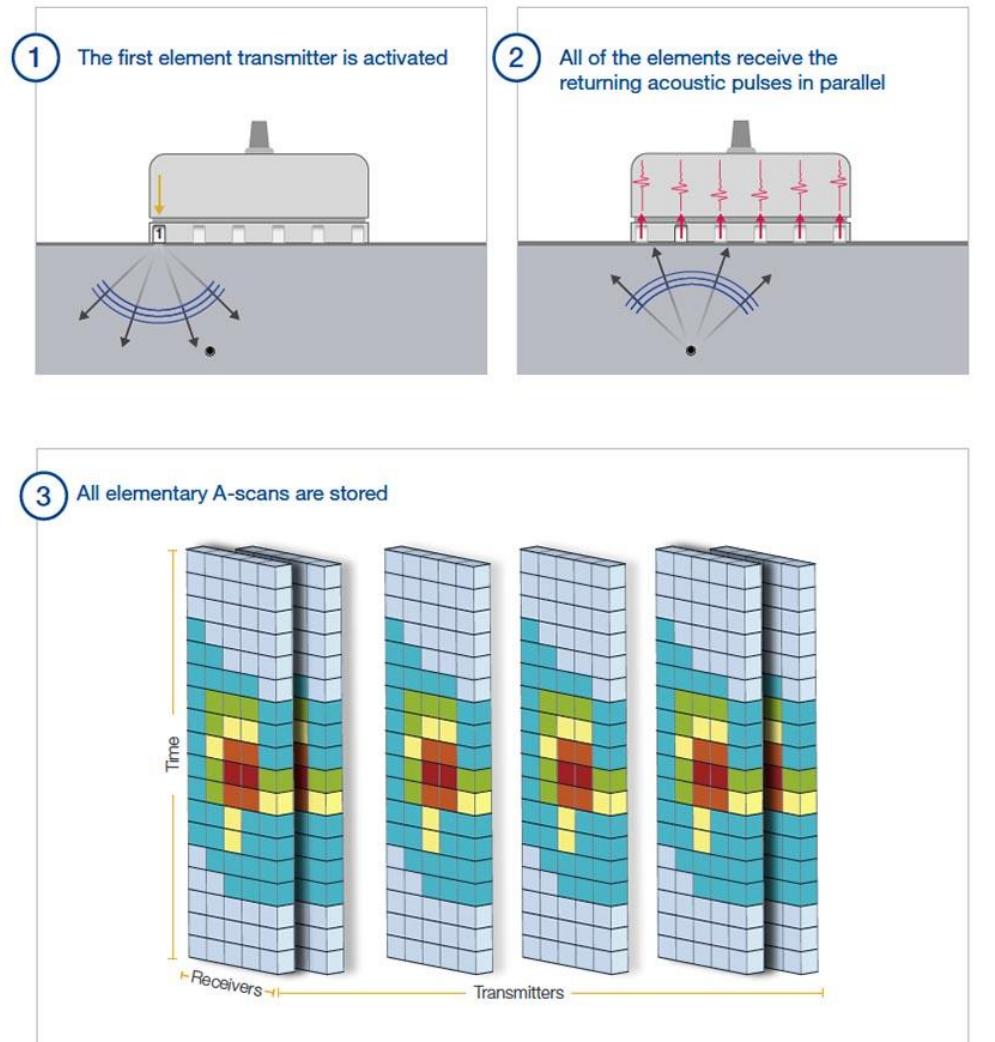
# SAFT->TFM/FMC

Total focusing method (TFM)=

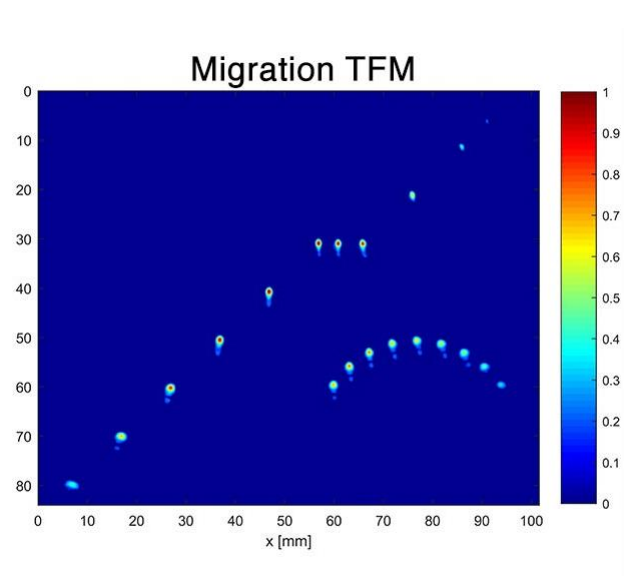
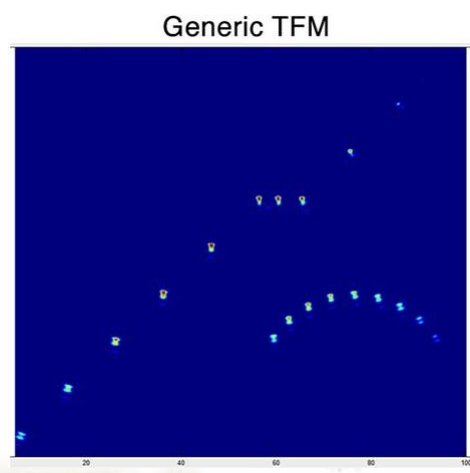
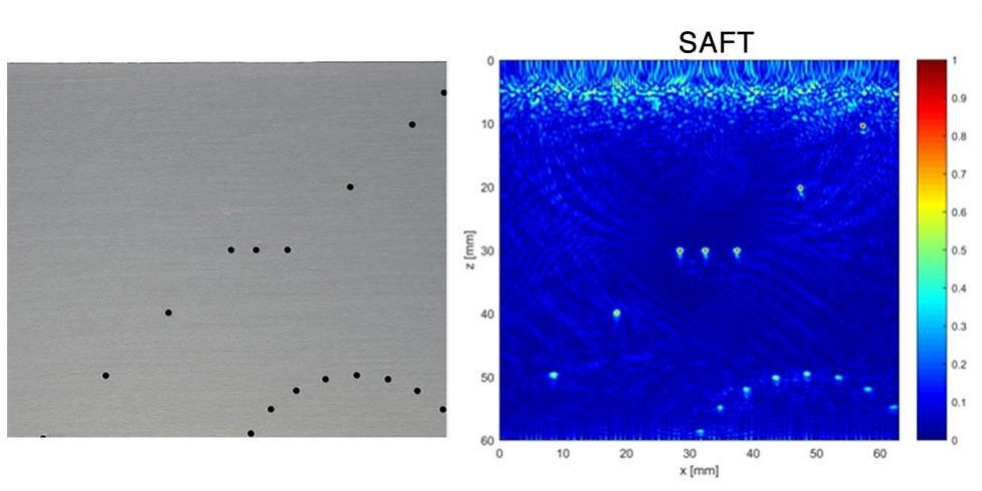
=All focusing method

Full matrix capture (FMC)=

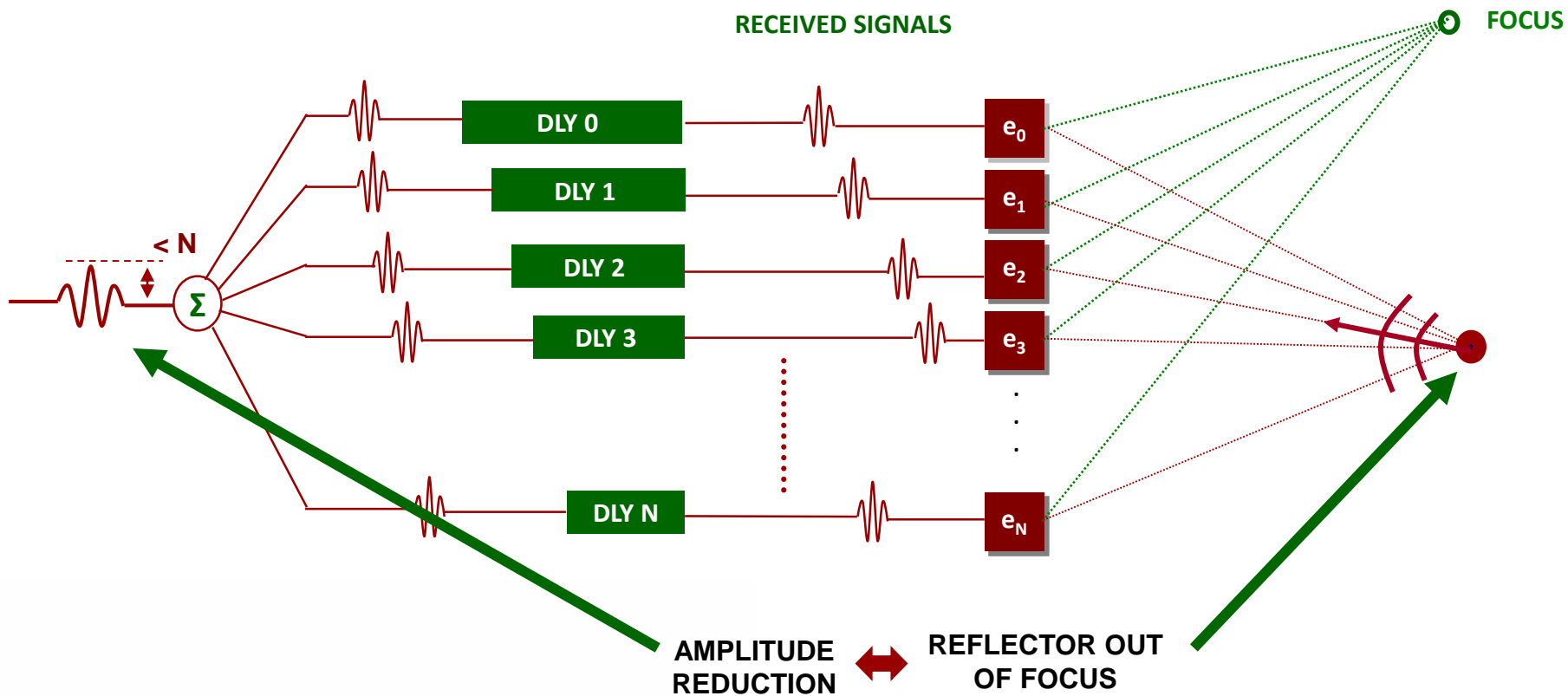
=one transmit+all capture...next transmit  
etc.



# SAFT vs. TFM/FMC



# SAFT/TFM + PCI



J. Camacho, C. Fritsch, J. Fernández-Cruza, M. Parrilla "Phase Coherence Imaging: Principles, applications and current developments" ICU 2019

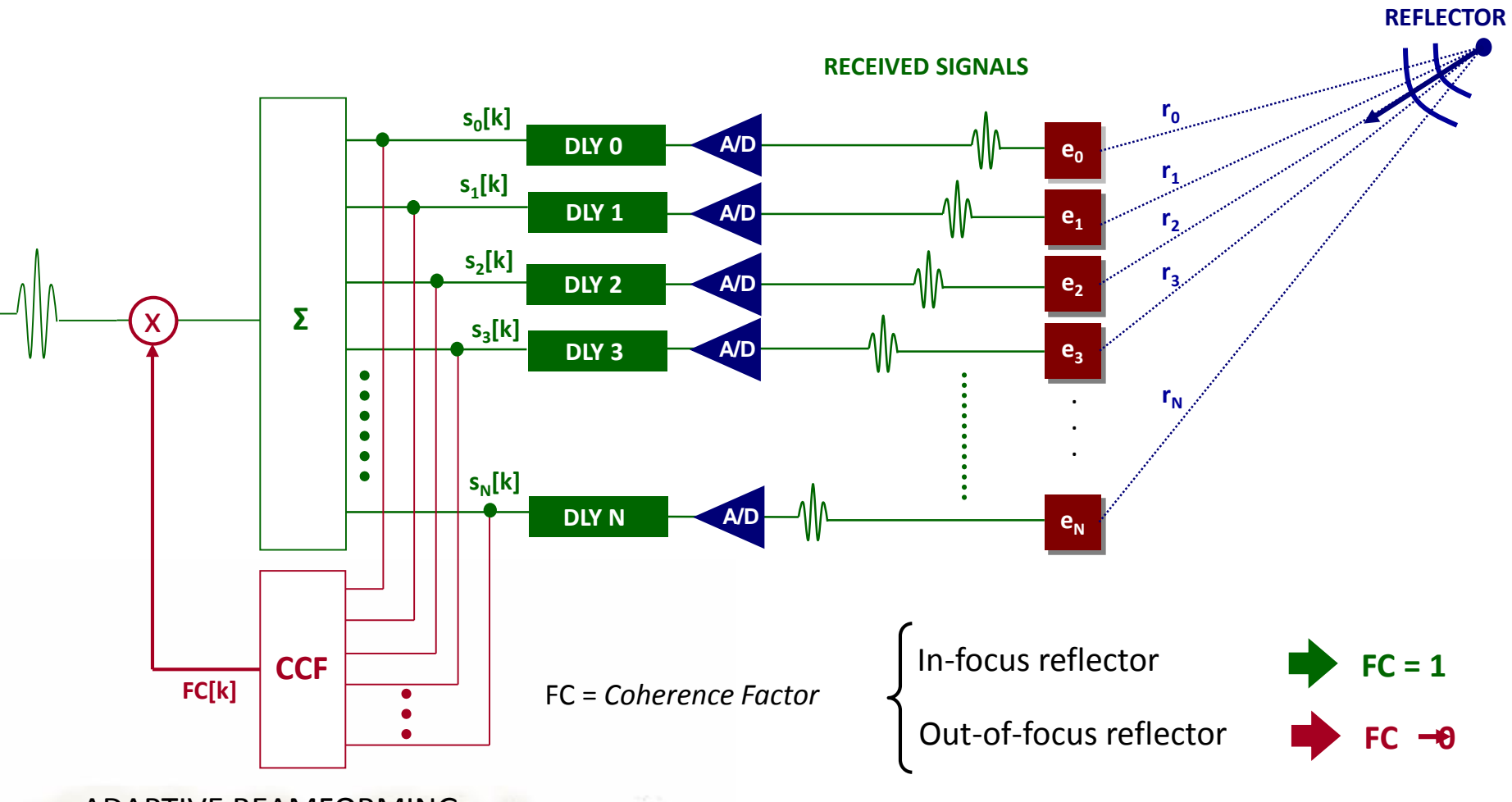
PJ.F. Cruza, J. Camacho, C. Fritsch "Plane-wave phase-coherence imaging for NDE" 2017

J. Brizuela et al. "Improving elevation resolution in phased-array inspections for NDT" 2019

J. F. Cruza et al. "A new beamforming method and hardware architecture for real time two way dynamic depth focusing" 2019

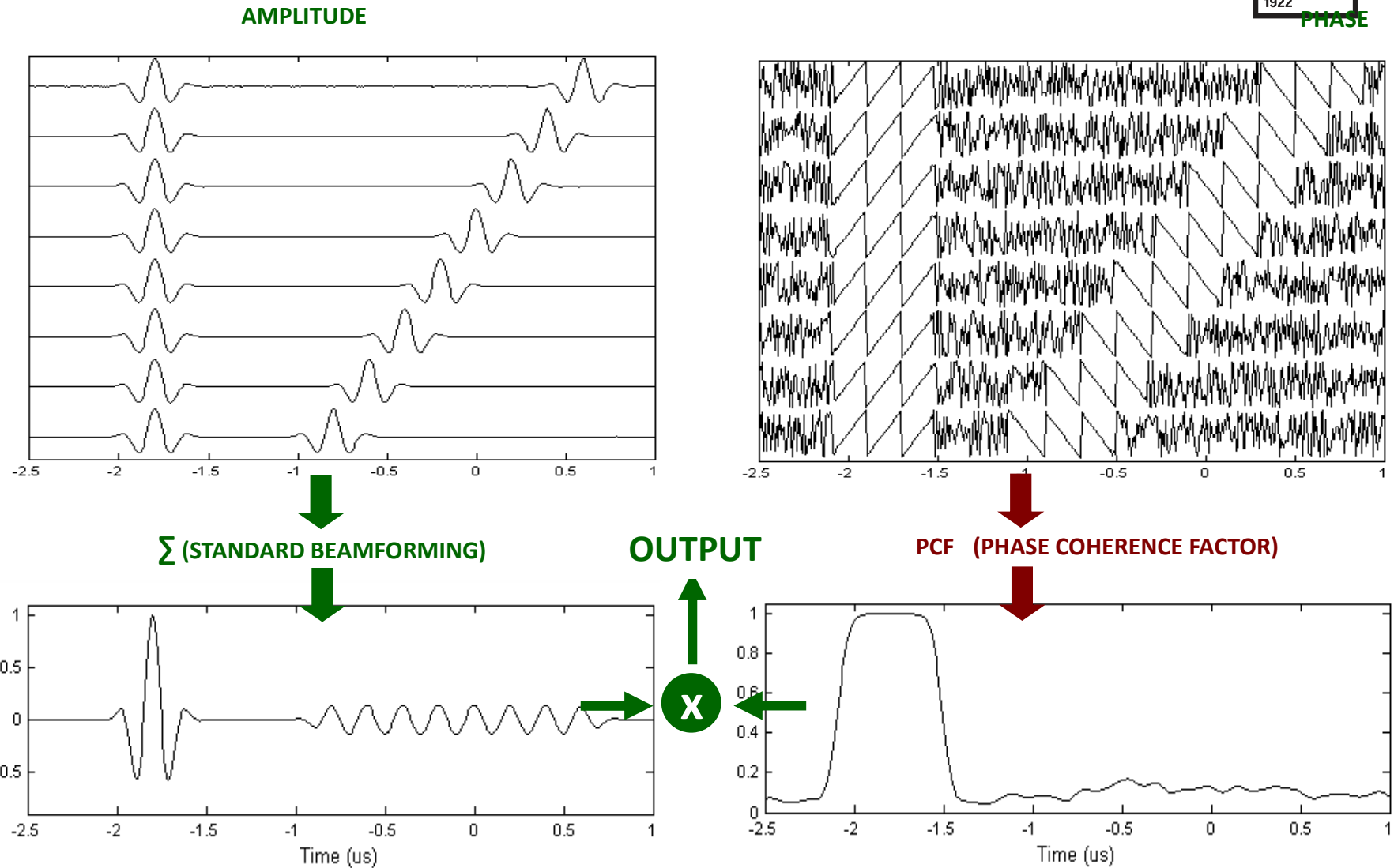
T. Robins, J.Camacho, O.Calderon Agudo, J.L. Herraiz, L. Guasch "Deep-Learning-Driven Full-Waveform Inversion for Ultrasound Breast Imaging" 2021

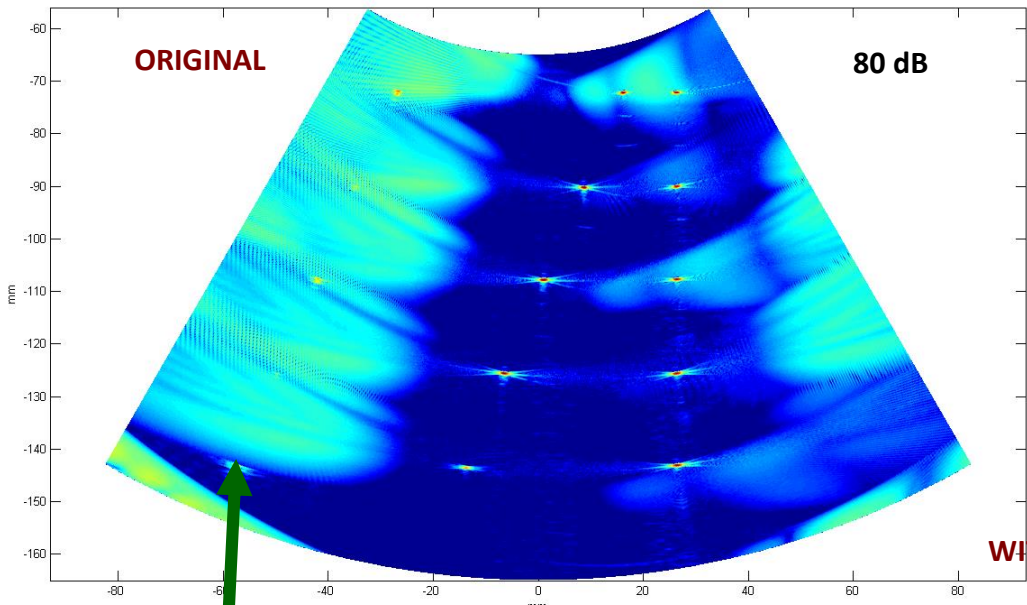
# PCI: COHERENCE FACTOR MASK



ADAPTIVE BEAMFORMING

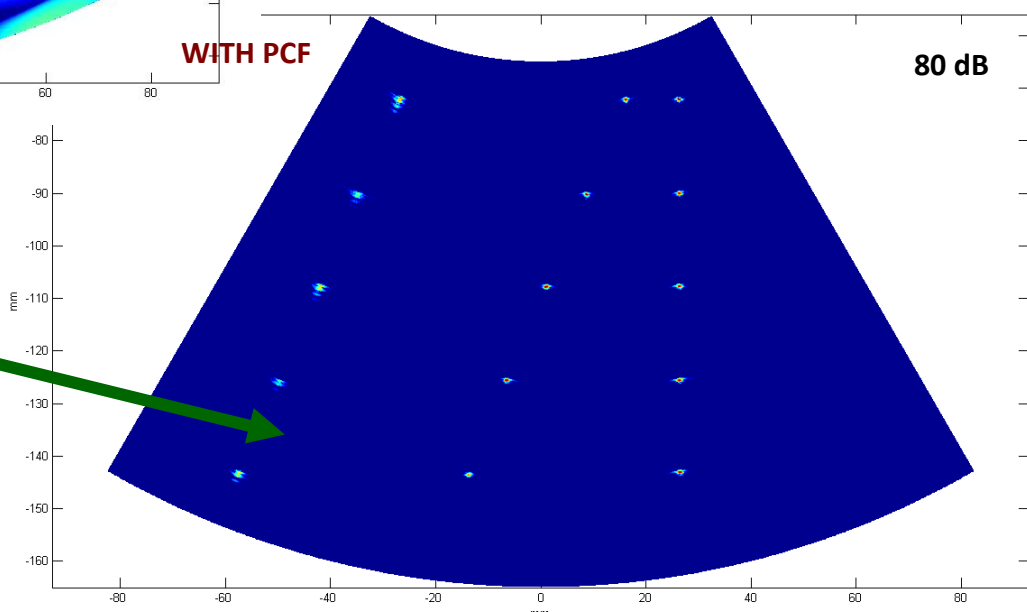
# PCI: coherence factor mask





WIRE PHANTOM IN WATER  
ARRAY: 5 MHz, 128 elements

$$d = 1.7 \lambda$$

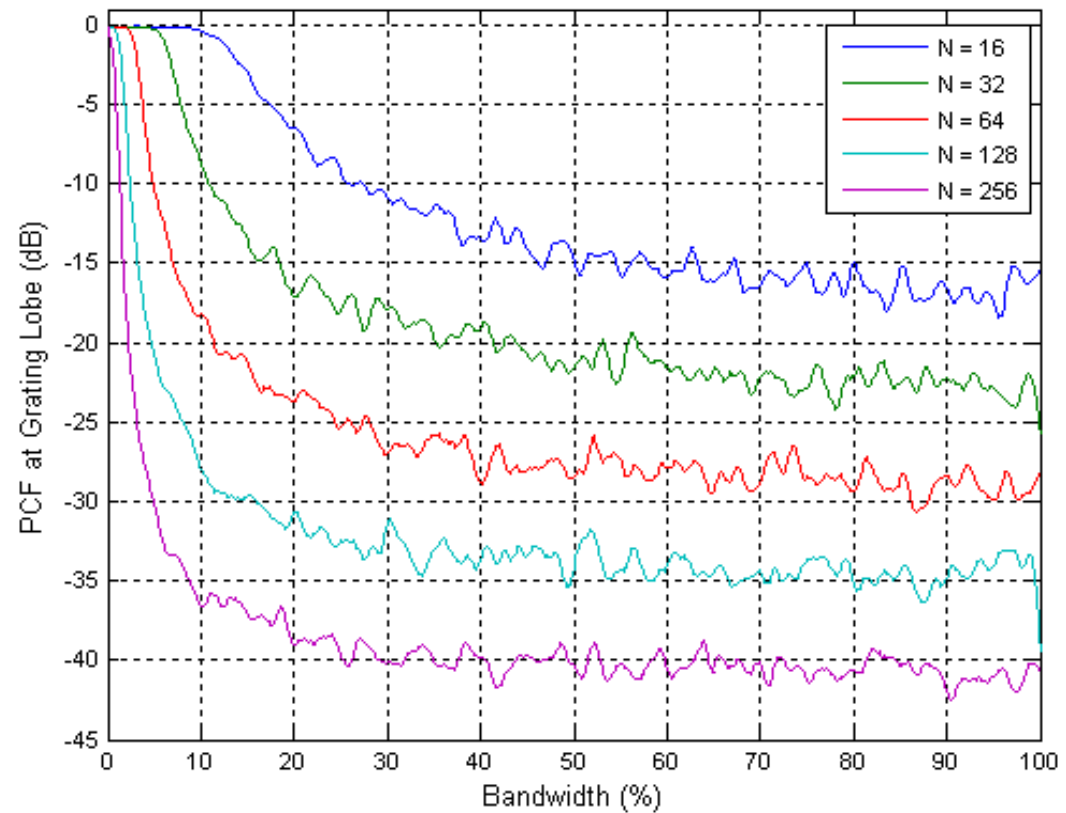


GRATING LOBE SUPPRESSION

# PCI: performance factors

PCF PERFORMANCE INCREASES WITH:

- ✓ SIGNAL BANDWIDTH
- ✓ NUMBER OF ELEMENTS



**END**



**Thank you for your attention**